كلية الهندسة- جامعة القاهرة
قسم هندسة القوى الميكانيكية
معمل التحكم الأوتوماتيكى

ACC Virtual Labs
Automatic Control Circuits &Virtual Labs for Mechanical Power Systems
معمل التحكم الاتوماتيكى و المعامل الإفتراضية لأنظمة القوى الميكانيكية

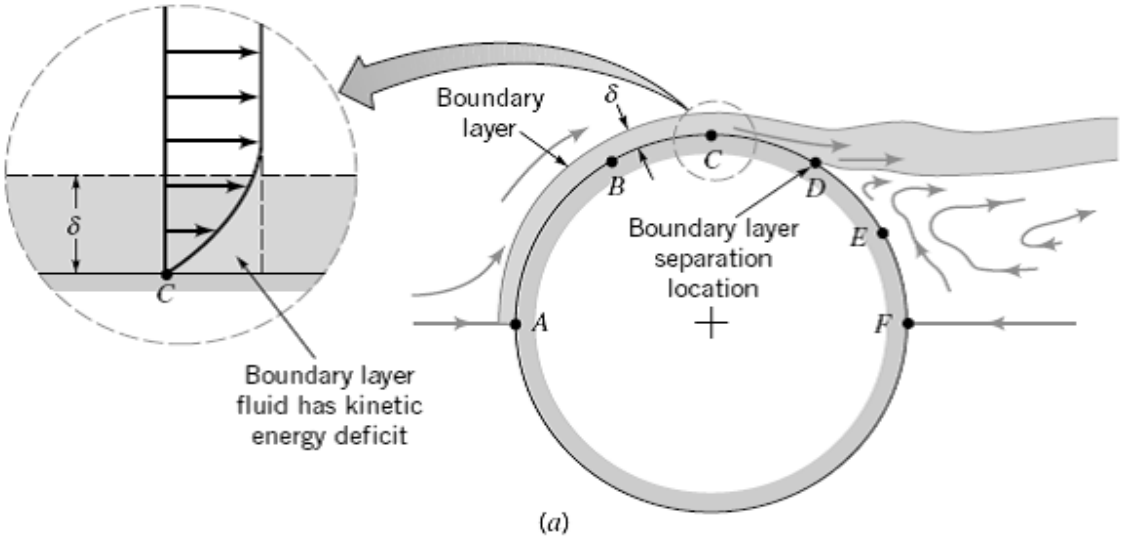

Notes on the course

Fluid Mechanics (3) - MEP 303A

For THRID YEAR MECHANICS (POWER)

Part (4)

Differential Analysis of Boundary Layer

Compiled and Edited by

Dr. Mohsen Soliman

2017/2018

Table of Contents of Part (4)

Part (4)*

Differential Analysis of Boundary Layer

(Lift and Drag of Flow Over Immersed Bodies)

In this part we consider various aspects of the viscous effects in the boundary layer region and the relationship between the boundary layer and the flow over bodies that are immersed in a real (i.e., viscous) fluid. Examples of such immersed bodies include the flow over air around airplanes, automobiles, and falling snow flakes, or the flow of water around submarines and fish. In these situations the object is completely surrounded by the fluid and the flows are termed external flows. External flows involving air are often termed aerodynamics in response to the important external flows produced when an object such as an airplane flies through the atmosphere. Although this field of external flows is extremely important, there are many other examples that are of equal importance. We should note that the boundary layer region and the large viscous effects exists also in many internal flows. Examples include the entrance length of the flow in pipes or ducts and the near wall flow in a diffuser where in both cases the viscous effects in boundary layer flow is dominant.

We study the boundary layer flow to calculate all the forces generated because of the viscous effects at the wall. The fluid force (lift and drag) on surface vehicles (cars, trucks, bicycles) has become a very important topic. By correctly designing cars and trucks, it has become possible to greatly decrease the fuel consumption and improve the handling characteristics of the vehicle. Similar efforts have resulted in improved ships, whether they are surface vessels (i.e., surrounded by two fluids, air and water) or submersible vessels (i.e., surrounded only by water). Other applications of external flows involve objects that are not completely surrounded by fluid, although they are placed in some external-type flow. For example, the proper design of a building (whether it is your house or a tall skyscraper) must include consideration of the various wind effects involved.

As with the other areas of fluid mechanics, two approaches (i.e., theoretical and experimental) are used to obtain information on fluid forces developed by external flows. Theoretical (i.e., analytical and numerical) techniques can provide much of the needed information about such flows. However, because of the complexities of both the governing equations and geometry of the objects involved, the amount of information obtained from purely theoretical methods is limited. With current and anticipated advancements in the area of computational fluid mechanics, it is likely that computer prediction of forces and complicated flow patterns will become readily available.

Much of the information about external flows comes from experiments carried out, for the most part, on scale models of the actual objects. Such testing includes the obvious wind tunnel testing of model airplanes, buildings, and even entire cities. In some instances the actual device, not a model, is tested in the wind tunnels. Figure 4.1 shows tests of vehicles in wind tunnels. Better performance of cars, bikes, skiers, and numerous other objects has resulted from testing in wind tunnels. The use of water tunnels and towing tanks also provides useful information about the flow around ships and other objects.

In this part, we first consider the general characteristics of external flow past immersed objects before we make detailed differential analysis of the flow in the boundary layer region. We investigate the qualitative aspects of such external flows and learn how to determine the various forces on objects surrounded by a moving fluid.

---

* Ref.:(1) Bruce R. Munson, Donald F. Young, Theodore H. Okiishi "Fundamental of Fluid Mechanics" 4th ed., John Wiley & Sons, Inc., 2002.
(2) Frank M. White "Fluid Mechanics", 4th ed. McGraw Hill, 2002.

4.1 General External Flow Characteristics

A body immersed in a moving fluid experiences a resultant force due to the interaction between the body and the fluid surrounding it. In some instances (such as an airplane flying through still air) the fluid far from the body is stationary and the body moves through the fluid with velocity U. In other instances (such as the wind blowing past a building) the body is stationary and the fluid flows past the body with velocity U. In any case, we can fix the coordinate system in the body and treat the situation as fluid flowing past a stationary body

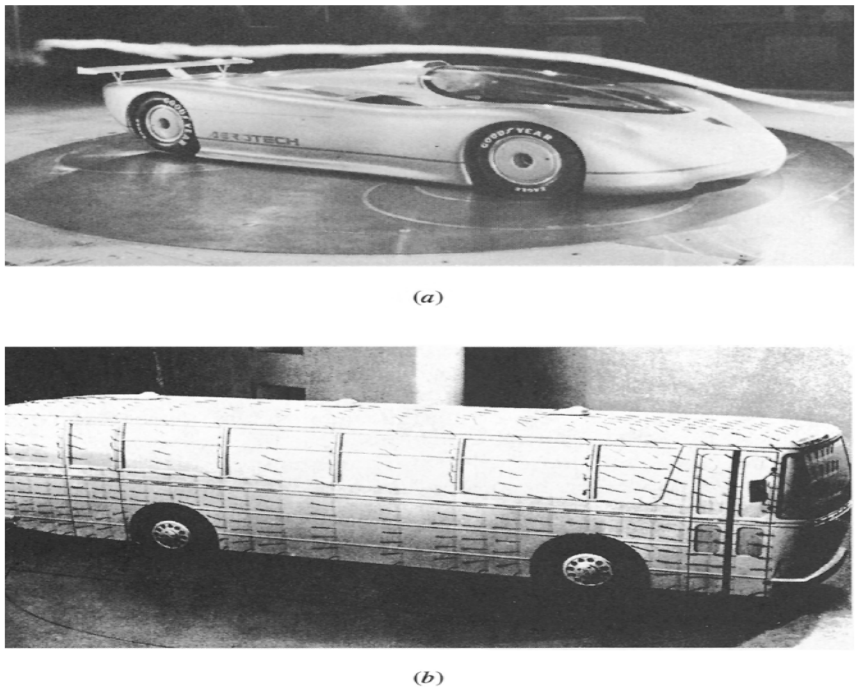

■ FIGURE 4.1
(*a*) Flow past a full-sized streamlined vehicle in the GM aerodynamics laboratory wind tunnel, an 18-ft by 34-ft test section facility driven by a 4000-hp, 43-ft-diameter fan. (Photograph courtesy of General Motors Corporation.) (*b*) Surface flow on a model vehicle as indicated by tufts attached to the surface. (Reprinted with permission from Society of Automotive Engineers, Ref. 28.)

with velocity U, the *upstream velocity*. For the purposes of this book, we will assume that the upstream velocity is constant in both time and location. That is, there is a uniform, constant velocity fluid flowing past the object. In actual situations this is often not true. For example, the wind blowing past a smokestack is nearly always turbulent and gusty (unsteady) and probably not of uniform velocity from the top to the bottom of the stack. Usually the unsteadiness and nonuniformity are of minor importance.

Even with a steady, uniform upstream flow, the flow in the vicinity of an object may be unsteady. Examples of this type of behavior include the flutter that is sometimes found in the flow past airfoils (wings), the regular oscillation of telephone wires that "sing" in a wind, and the irregular turbulent fluctuations in the wake regions behind bodies.

The structure of an external flow and the ease with which the flow can be described and analyzed often depend on the nature of the body in the flow. Three general categories of bodies are shown in Fig. 4.2 . They include (a) two-dimensional objects (infinitely long and of constant cross-sectional size and shape), (b) axisymmetric bodies (formed by rotating their cross-sectional shape about the axis of symmetry), and (c) three-dimensional bodies that may or may not possess a line or plane of symmetry. In practice there can be no truly two-dimensional bodies—nothing extends to infinity. However, many objects are sufficiently long so that the end effects are negligibly small.

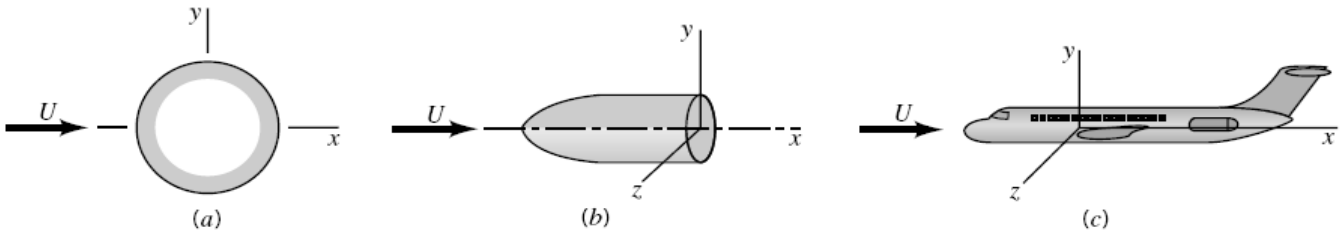

■ FIGURE 4.2 **Flow classification: (*a*) two-dimensional, (*b*) axisymmetric, (*c*) three-dimensional.**

Another classification of body shape can be made depending on whether the body is streamlined or blunt. The flow characteristics depend strongly on the amount of streamlining present. In general, *streamlined bodies* (i.e., airfoils, racing cars, etc.) have little effect on the surrounding fluid, compared with the effect that *blunt bodies* (i.e., parachutes, buildings, etc.) have on the fluid. Usually, but not always, it is easier to force a streamlined body through a fluid than it is to force a similar-sized blunt body at the same velocity. There are important exceptions to this basic rule.

4.1.1 Lift and Drag Concepts

When any body moves through a fluid, an interaction between the body and the fluid occurs; this effect can be described in terms of the forces at the fluid–body interface. This can be described in terms of the stresses—wall shear stresses, τ_w, due to viscous effects and normal stresses due to the pressure, p. Typical shear stress and pressure distributions are shown in Figs.4.3 *a* and4.3 *b*. Both τ_w and p vary in magnitude and direction along the surface.

It is often useful to know the detailed distribution of shear stress and pressure over the surface of the body, although such information is difficult to obtain. Many times, however, only the integrated or resultant effects of these distributions are needed. The resultant force in the direction of the upstream velocity is termed the *drag*, $\mathcal{D}$, and the resultant force normal to the upstream velocity is termed the *lift*, $\mathcal{L}$, as is indicated in Fig.4.3 *c*. For some

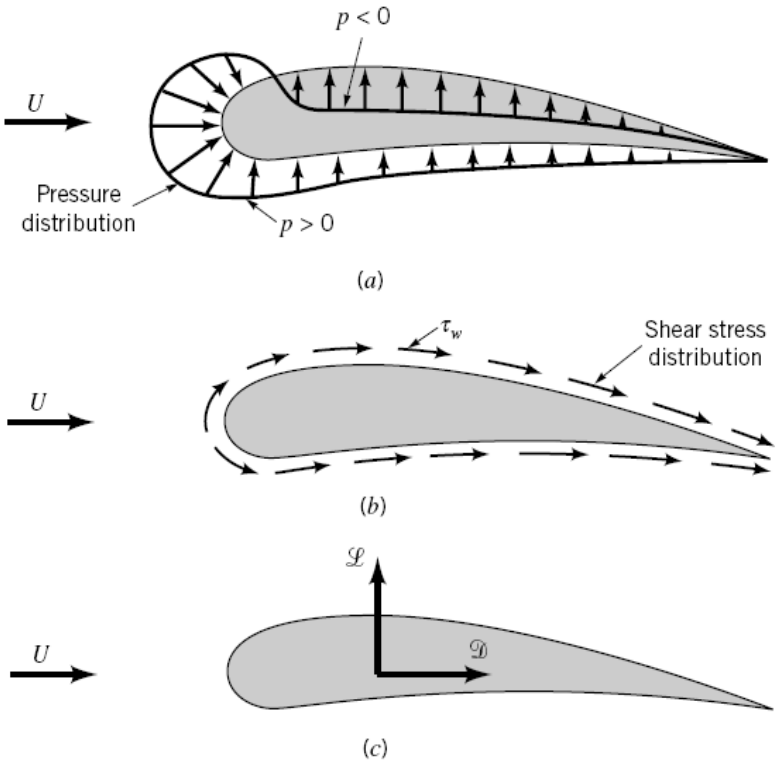

■ FIGURE 4.3 **Forces from the surrounding fluid on a two-dimensional object: (*a*) pressure force, (*b*) viscous force, (*c*) resultant force (lift and drag).**

three-dimensional bodies there may also be a side force that is perpendicular to the plane containing $\mathcal{D}$ and $\mathcal{L}$.

The resultant of the shear stress and pressure distributions can be obtained by integrating the effect of these two quantities on the body surface as is indicated in Fig. 4.4 . The x and y components of the fluid force on the small area element dA are

$$dF_x = (p\,dA)\cos\theta + (\tau_w\,dA)\sin\theta$$

and

$$dF_y = -(p\,dA)\sin\theta + (\tau_w\,dA)\cos\theta$$

Thus, the net x and y components of the force on the object are

$$\mathcal{D} = \int dF_x = \int p\cos\theta\,dA + \int \tau_w \sin\theta\,dA \tag{4.1}$$

and

$$\mathcal{L} = \int dF_y = -\int p\sin\theta\,dA + \int \tau_w \cos\theta\,dA \tag{4.2}$$

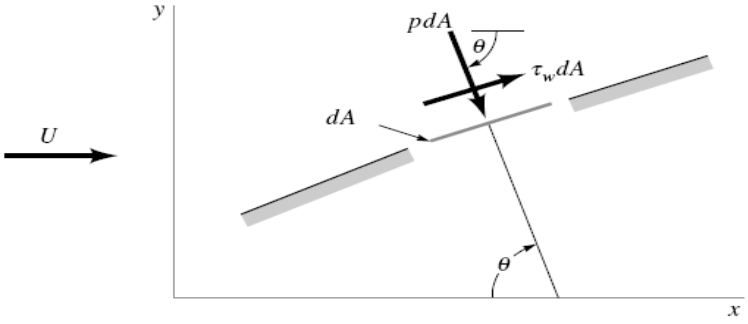

■ FIGURE 4.4 **Pressure and shear forces on a small element of the surface of a body.**

Of course, to carry out the integrations and determine the lift and drag, we must know the body shape (i.e., θ as a function of location along the body) and the distribution of τ_w and p along the surface. These distributions are often extremely difficult to obtain, either experimentally or theoretically. The pressure distribution can be obtained experimentally without too much difficulty by use of a series of static pressure taps along the body surface. On the other hand, it is usually quite difficult to measure the wall shear stress distribution.

It is seen that both the shear stress and pressure force contribute to the lift and drag, since for an arbitrary body θ is neither zero nor 90° along the entire body. The exception is a flat plate aligned either parallel to the upstream flow ($\theta = 90°$) or normal to the upstream flow ($\theta = 0$) as is discussed in Example 4.1.

Example 4.1:

Air at standard conditions flows past a flat plate as is indicated in Fig. E4.1. In case (a) the plate is parallel to the upstream flow, and in case (b) it is perpendicular to the upstream flow. If the pressure and shear stress distributions on the surface are as indicated (obtained either by experiment or theory), determine the lift and drag on the plate.

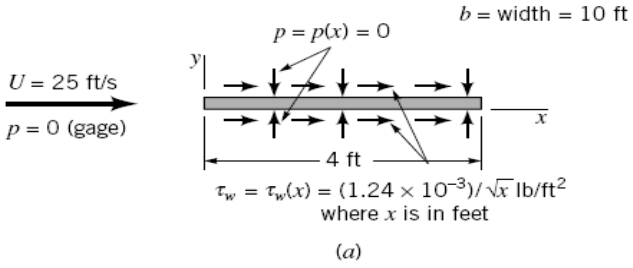

■ FIGURE E4.1

Solution

For either orientation of the plate, the lift and drag are obtained from Eqs. 4.1 and 4.2 . With the plate parallel to the upstream flow we have $\theta = 90°$ on the top surface and $\theta = 270°$ on the bottom surface so that the lift and drag are given by

$$\mathscr{L} = -\int_{\text{top}} p\, dA + \int_{\text{bottom}} p\, dA = 0$$

and

$$\mathscr{D} = \int_{\text{top}} \tau_w\, dA + \int_{\text{bottom}} \tau_w\, dA = 2\int_{\text{top}} \tau_w\, dA \qquad (1)$$

where we have used the fact that because of symmetry the shear stress distribution is the same on the top and the bottom surfaces, as is the pressure also [whether we use gage ($p = 0$) or absolute ($p = p_{\text{atm}}$) pressure]. There is no lift generated—the plate does not know up from

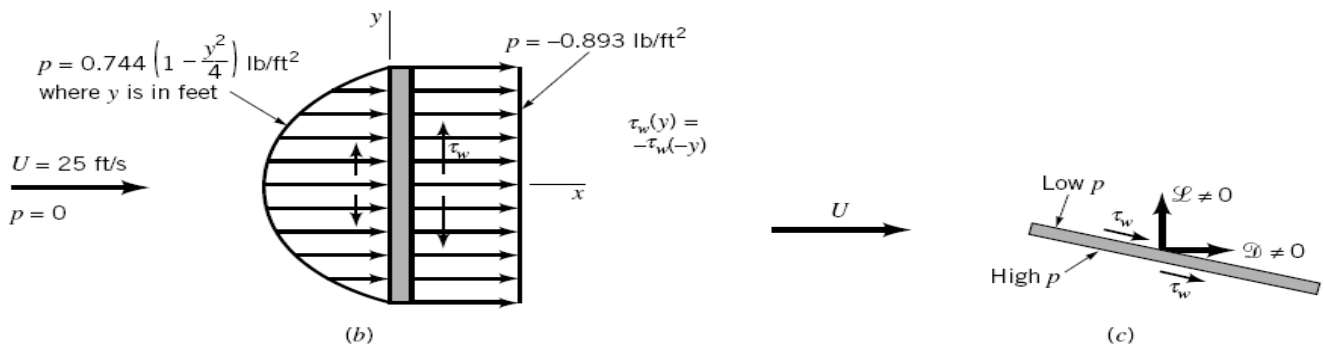

■ FIGURE E4.1 ***(Continued)***

down. With the given shear stress distribution, Eq. 1 gives

$$\mathcal{D} = 2\int_{x=0}^{4\text{ ft}} \left(\frac{1.24 \times 10^{-3}}{x^{1/2}}\text{lb/ft}^2\right)(10\text{ ft})\,dx$$

or

$$\mathcal{D} = 0.0992\text{ lb} \qquad \textbf{(Ans)}$$

With the plate perpendicular to the upstream flow, we have $\theta = 0°$ on the front and $\theta = 180°$ on the back. Thus, from Eqs. 4.1 and 4.2

$$\mathcal{L} = \int_{\text{front}} \tau_w\,dA - \int_{\text{back}} \tau_w\,dA = 0$$

and

$$\mathcal{D} = \int_{\text{front}} p\,dA - \int_{\text{back}} p\,dA$$

Again there is no lift because the pressure forces act parallel to the upstream flow (in the direction of $\mathcal{D}$ not $\mathcal{L}$) and the shear stress is symmetrical about the center of the plate. With the given relatively large pressure on the front of the plate (the center of the plate is a stagnation point) and the negative pressure (less than the upstream pressure) on the back of the plate, we obtain the following drag

$$\mathcal{D} = \int_{y=-2}^{2\text{ ft}} \left[0.744\left(1 - \frac{y^2}{4}\right)\text{lb/ft}^2 - (-0.893)\text{ lb/ft}^2\right](10\text{ ft})\,dy$$

or

$$\mathcal{D} = 55.6\text{ lb} \qquad \textbf{(Ans)}$$

Clearly there are two mechanisms responsible for the drag. On the ultimately streamlined body (a zero thickness flat plate parallel to the flow) the drag is entirely due to the shear stress at the surface and, in this example, is relatively small. For the ultimately blunted body (a flat plate normal to the upstream flow) the drag is entirely due to the pressure difference between the front and back portions of the object and, in this example, is relatively large.

If the flat plate were oriented at an arbitrary angle relative to the upstream flow as indicated in Fig. E 4.1*c*, there would be both a lift and a drag, each of which would be dependent on both the shear stress and the pressure. Both the pressure and shear stress distributions would be different for the top and bottom surfaces.

Although Eqs. 4.1 and 4.2 are valid for any body, the difficulty in their use lies in obtaining the appropriate shear stress and pressure distributions on the body surface. Considerable effort has gone into determining these quantities, but because of the various complexities involved, such information is available only for certain simple situations.

Without detailed information concerning the shear stress and pressure distributions on a body, Eqs. 4.1 and 4.2 cannot be used. The widely used alternative is to define dimensionless lift and drag coefficients and determine their approximate values by means of either a simplified analysis, some numerical technique, or an appropriate experiment. The *lift coefficient*, C_L, and *drag coefficient*, C_D, are defined as

$$C_L = \frac{\mathcal{L}}{\frac{1}{2}\rho U^2 A}$$

and

$$C_D = \frac{\mathcal{D}}{\frac{1}{2}\rho U^2 A}$$

where A is a characteristic area of the object. Typically, A is taken to be the projected or *frontal area*—the projected area seen by a person looking toward the object from a direction parallel to the upstream velocity, U. It would be the area of the shadow of the object projected onto a screen normal to the upstream velocity as formed by a light shining along the upstream flow. In other situations A is taken to be the *planform area*—the projected area seen by an observer looking toward the object from a direction normal to the upstream velocity (i.e., from "above" it). Obviously, which characteristic area is used in the definition of the lift and drag coefficients must be clearly stated.

4.1.2 Characteristics of Flow Past an Object

External flows past objects encompass an extremely wide variety of fluid mechanics phenomena. Clearly the character of the flow field is a function of the shape of the body. Flows past relatively simple geometric shapes (i.e., a sphere or circular cylinder) are expected to have less complex flow fields than flows past a complex shape such as an airplane or a tree. However, even the simplest-shaped objects produce rather complex flows.

For a given-shaped object, the characteristics of the flow depend very strongly on various parameters such as size, orientation, speed, and fluid properties. As is discussed in second year , according to dimensional analysis arguments, the character of the flow should depend on the various dimensionless parameters involved. For typical external flows the most important of these parameters are the Reynolds number, $\mathrm{Re} = \rho U\ell/\mu = U\ell/\nu$, the Mach number, $\mathrm{Ma} = U/c$, and for flows with a free surface (i.e., flows with an interface between two fluids, such as the flow past a surface ship), the Froude number, $\mathrm{Fr} = U/\sqrt{g\ell}$. (Recall that ℓ is some characteristic length of the object and c is the speed of sound.)

For the present, we consider how the external flow and its associated lift and drag vary as a function of Reynolds number. Recall that the Reynolds number represents the ratio of inertial effects to viscous effects. In the absence of all viscous effects ($\mu = 0$), the Reynolds number is infinite. On the other hand, in the absence of all inertial effects (negligible mass or $\rho = 0$), the Reynolds number is zero. Clearly, any actual flow will have a Reynolds number between (but not including) these two extremes. The nature of the flow past a body depends strongly on whether $\mathrm{Re} \gg 1$ or $\mathrm{Re} \ll 1$.

Most external flows with which we are familiar are associated with moderately sized objects with a characteristic length on the order of $0.01\ \mathrm{m} < \ell < 10\ \mathrm{m}$. In addition, typical upstream velocities are on the order of $0.01\ \mathrm{m/s} < U < 100\ \mathrm{m/s}$ and the fluids involved are typically water or air. The resulting Reynolds number range for such flows is approximately $10 < \mathrm{Re} < 10^9$. As a rule of thumb, flows with $\mathrm{Re} > 100$ are dominated by inertial effects, whereas flows with $\mathrm{Re} < 1$ are dominated by viscous effects. Hence, most familiar external flows are dominated by inertia.

On the other hand, there are many external flows in which the Reynolds number is considerably less than 1, indicating in some sense that viscous forces are more important than inertial forces. The gradual settling of small particles of dirt in a lake or stream is governed by low Reynolds number flow principles because of the small diameter of the particles and their small settling speed. Similarly, the Reynolds number for objects moving through large viscosity oils is small because μ is large. The general differences between small and large Reynolds number flow past streamlined and blunt objects can be illustrated by considering flows past two objects—one a flat plate parallel to the upstream velocity and the other a circular cylinder.

Flows past three flat plates of length ℓ with $\mathrm{Re} = \rho U\ell/\mu = 0.1$, 10, and 10^7 are shown in Fig.4.5 . If the Reynolds number is small, the viscous effects are relatively strong and the plate affects the uniform upstream flow far ahead, above, below, and behind the plate. To reach that portion of the flow field where the velocity has been altered by less than 1% of its undisturbed value (i.e., $U - u < 0.01\ U$) we must travel relatively far from the plate. In low Reynolds number flows the viscous effects are felt far from the object in all directions.

As the Reynolds number is increased (by increasing U, for example), the region in which viscous effects are important becomes smaller in all directions except downstream, as is shown in Fig. 4.5*b*. One does not need to travel very far ahead, above, or below the plate to reach areas in which the viscous effects of the plate are not felt. The streamlines are displaced from their original uniform upstream conditions, but the displacement is not as great as for the $\mathrm{Re} = 0.1$ situation shown in Fig. 4.5*a*.

If the Reynolds number is large (but not infinite), the flow is dominated by inertial effects and the viscous effects are negligible everywhere except in a region very close to the plate and in the relatively thin *wake region* behind the plate, as shown in Fig. 4.5 *c*. Since the fluid viscosity is not zero ($\text{Re} < \infty$), it follows that the fluid must stick to the solid surface (the no-slip boundary condition). There is a thin *boundary layer* region of thickness $\delta = \delta(x) \ll \ell$ (i.e., thin relative to the length of the plate) next to the plate in which the fluid velocity changes from the upstream value of $u = U$ to zero velocity on the plate. The thickness of this layer increases in the direction of flow, starting from zero at the forward or leading edge of the plate. The flow within the boundary layer may be laminar or turbulent, depending on various parameters involved.

The streamlines of the flow outside of the boundary layer are nearly parallel to the plate. As we will see in the next section, the slight displacement of the external streamlines that are outside of the boundary layer is due to the thickening of the boundary layer in the direction of flow. The existence of the plate has very little effect on the streamlines outside of the boundary layer—either ahead, above, or below the plate. On the other hand, the wake region is due entirely to the viscous interaction between the fluid and the plate.

One of the great advancements in fluid mechanics occurred in 1904 as a result of the insight of **Ludwig Prandtl** (1875–1953), a German physicist and aerodynamicist. He con-

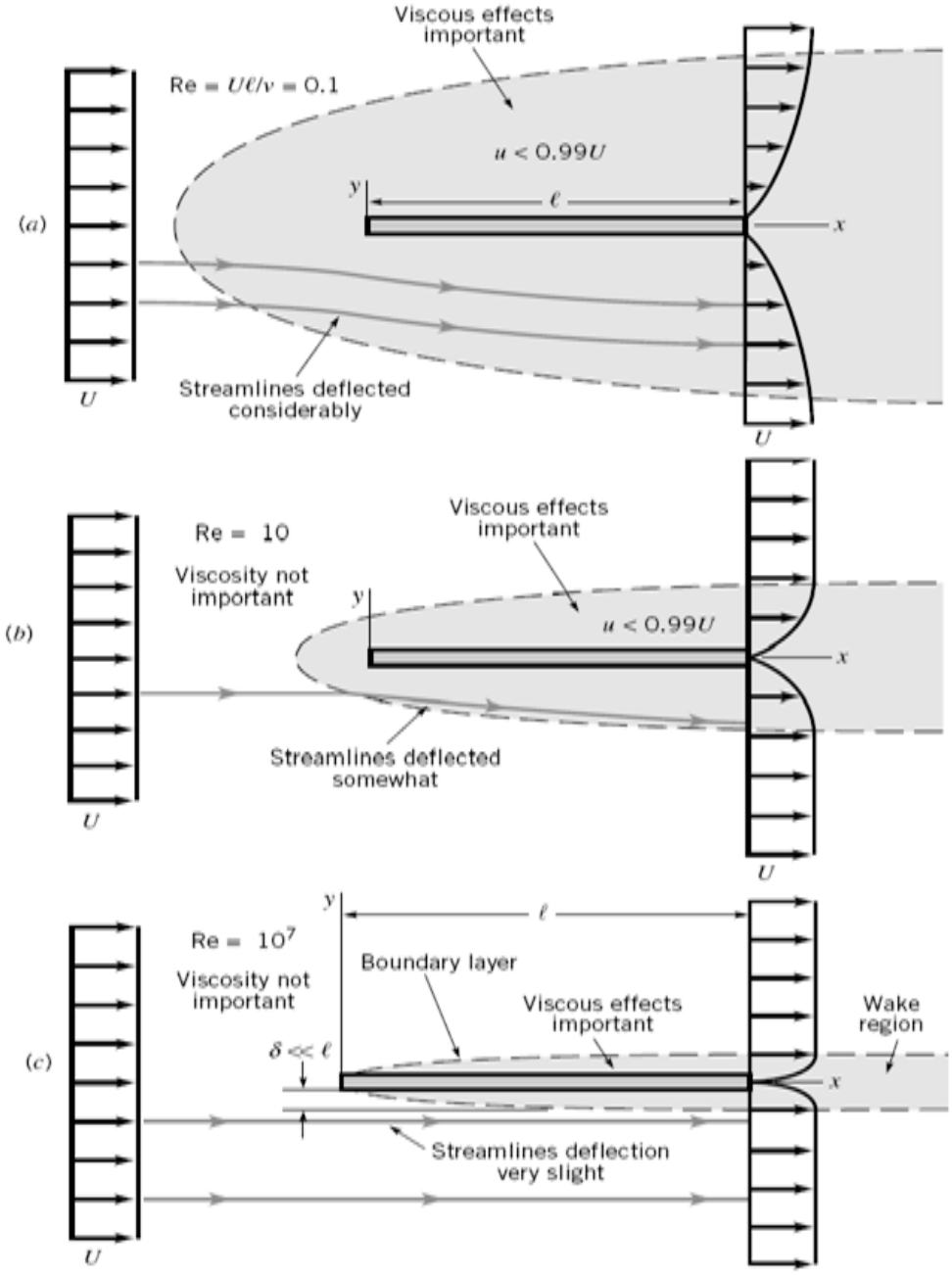

■ **FIGURE 4.5**
Character of the steady, viscous flow past a flat plate parallel to the upstream velocity: (*a*) low Reynolds number flow, (*b*) moderate Reynolds number flow, (*c*) large Reynolds number flow.

ceived of the idea of the boundary layer—a thin region on the surface of a body in which viscous effects are very important and outside of which the fluid behaves essentially as if it were inviscid. Clearly the actual fluid viscosity is the same throughout; only the relative importance of the viscous effects (due to the velocity gradients) is different within or outside of the boundary layer. As is discussed in the next section, by using such a hypothesis it is possible to simplify the analysis of large Reynolds number flows, thereby allowing solution to external flow problems that are otherwise still unsolvable.

As with the flow past the flat plate described above, the flow past a blunt object (such as a circular cylinder) also varies with Reynolds number. In general, the larger the Reynolds number, the smaller the region of the flow field in which viscous effects are important. For objects that are not sufficiently streamlined, however, an additional characteristic of the flow is observed. This is termed *flow separation* and is illustrated in Fig. 4.6.

Low Reynolds number flow ($\mathrm{Re} = UD/\nu < 1$) past a circular cylinder is characterized by the fact that the presence of the cylinder and the accompanying viscous effects are felt throughout a relatively large portion of the flow field. As is indicated in Fig. 4.6*a*, for $\mathrm{Re} = UD/\nu = 0.1$, the viscous effects are important several diameters in any direction from the cylinder. A somewhat surprising characteristic of this flow is that the streamlines are essentially symmetric about the center of the cylinder—the streamline pattern is the same in front of the cylinder as it is behind the cylinder.

As the Reynolds number is increased, the region ahead of the cylinder in which viscous effects are important becomes smaller, with the viscous region extending only a short distance ahead of the cylinder. The viscous effects are convected downstream and the flow loses its symmetry. Another characteristic of external flows becomes important—the flow separates from the body at the *separation location* as indicated in Fig. 4.6 *b*. With the increase in Reynolds number, the fluid inertia becomes more important and at some location on the body, denoted the separation location, the fluid's inertia is such that it cannot follow the curved path around to the rear of the body. The result is a separation bubble behind the cylinder in which some of the fluid is actually flowing upstream, against the direction of the upstream flow.

At still larger Reynolds numbers, the area affected by the viscous forces is forced farther downstream until it involves only a thin ($\delta \ll D$) boundary layer on the front portion of

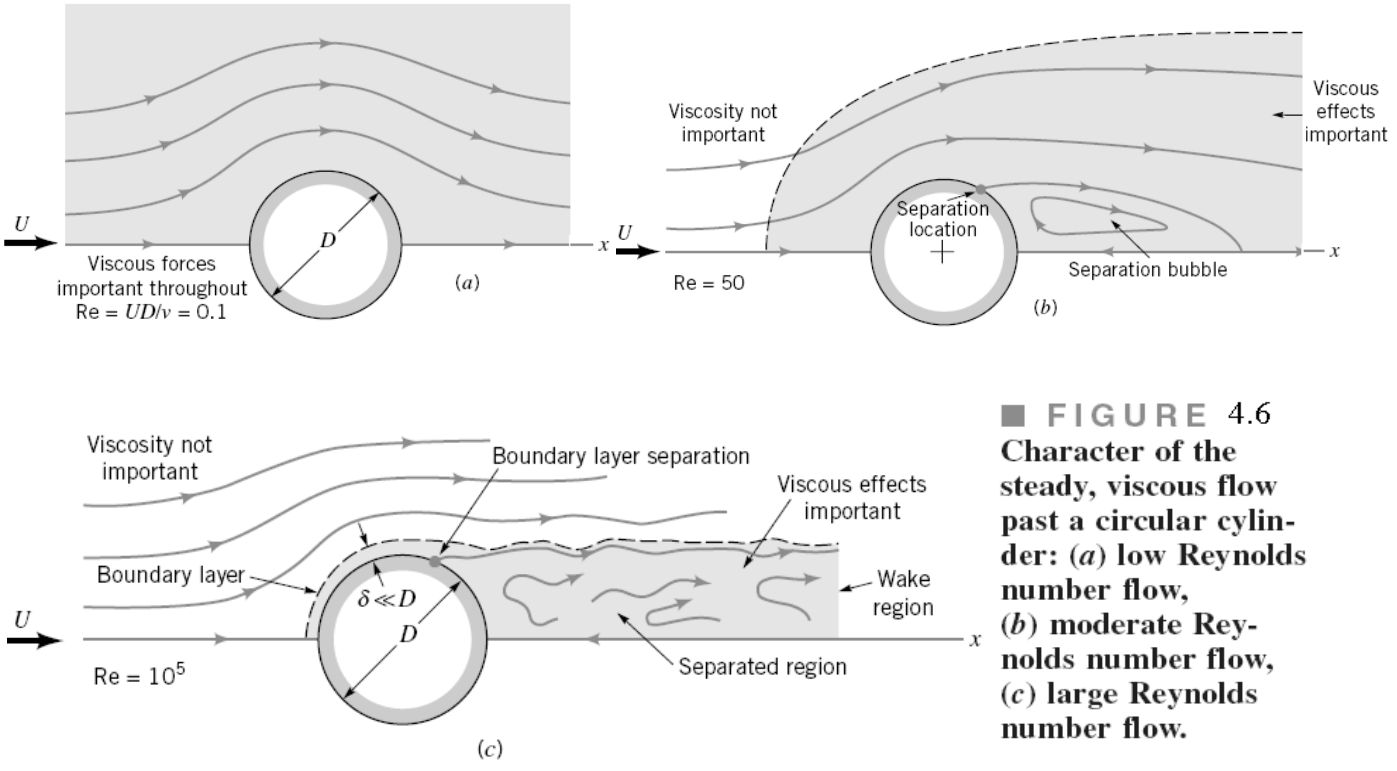

■ **FIGURE 4.6**
Character of the steady, viscous flow past a circular cylinder: (*a*) low Reynolds number flow, (*b*) moderate Reynolds number flow, (*c*) large Reynolds number flow.

the cylinder and an irregular, unsteady (perhaps turbulent) wake region that extends far downstream of the cylinder. The fluid in the region outside of the boundary layer and wake region flows as if it were inviscid. Of course, the fluid viscosity is the same throughout the entire flow field. Whether viscous effects are important or not depends on which region of the flow field we consider. The velocity gradients within the boundary layer and wake regions are much larger than those in the remainder of the flow field. Since the shear stress (i.e., viscous effect) is the product of the fluid viscosity and the velocity gradient, it follows that viscous effects are confined to the boundary layer and wake regions.

The characteristics described in Figs. 4.5 and 4.6 for flow past a flat plate and a circular cylinder are typical of flows past streamlined and blunt bodies, respectively. The nature of the flow depends strongly on the Reynolds number. (See Ref. 31 for many examples illustrating this behavior.) Most familiar flows are similar to the large Reynolds number flows depicted in Figs. 4.5 *c* and 4.6 *c*, rather than the low Reynolds number flow situations. In the remainder of this chapter we will investigate more thoroughly these ideas and determine how to calculate the forces on immersed bodies.

Example 4.2:

It is desired to determine the various characteristics of flow past a car. The following tests could be carried out: (a) $U = 20$ mm/s flow of glycerin past a scale model that is 34-mm tall, 100-mm long and 40-mm wide, (b) $U = 20$ mm/s air flow past the scale model, or (c) $U = 25$ m/s air flow past the actual car, which is 1.7-m tall, 5-m long, and 2-m wide. Would the flow characteristics for these three situations be similar? Explain.

Solution

The characteristics of flow past an object depend on the Reynolds number. For this instance we could pick the characteristic length to be the height, h, width, b, or length, ℓ, of the car to obtain three possible Reynolds numbers, $\mathrm{Re}_h = Uh/\nu$, $\mathrm{Re}_b = Ub/\nu$, and $\mathrm{Re}_\ell = U\ell/\nu$. These numbers will be different because of the different values of h, b, and ℓ. Once we arbitrarily decide on the length we wish to use as the characteristic length, we must stick with it for all calculations when using comparisons between model and prototype.

With the values of kinematic viscosity for air and glycerin obtained as $\nu_{\text{air}} = 1.46 \times 10^{-5}$ m^2/s and $\nu_{\text{glycerin}} = 1.19 \times 10^{-3}$ m^2/s, we obtain the following Reynolds numbers for the flows described.

Reynolds Number	(a) Model in Glycerin	(b) Model in Air	(c) Car in Air
Re_h	0.571	46.6	2.91×10^6
Re_b	0.672	54.8	3.42×10^6
Re_ℓ	1.68	137.0	8.56×10^6

Clearly, the Reynolds numbers for the three flows are quite different (regardless of which characteristic length we choose). Based on the previous discussion concerning flow past a flat plate or flow past a circular cylinder, we would expect that the flow past the actual car would behave in some way similar to the flows shown in Figs. 4.5 *c* or 4.6 *c*. That is, we would expect some type of boundary layer characteristic in which viscous effects would be confined to relatively thin layers near the surface of the car and the wake region behind it. Whether the car would act more like a flat plate or a cylinder would depend on the amount of streamlining incorporated into the car's design.

Because of the small Reynolds number involved, the flow past the model car in glycerin would be dominated by viscous effects, in some way reminiscent of the flows depicted in Figs. 4.5*a* or 4.6 *a*. Similarly, with the moderate Reynolds number involved for the air flow past the model, a flow with characteristics similar to those indicated in Figs. 4.5*b* and 4.6 *b* would be expected. Viscous effects would be important—not as important as with the glycerin flow, but more important than with the full-sized car.

It would not be a wise decision to expect the flow past the full-sized car to be similar to the flow past either of the models. The same conclusions result regardless of whether we use Re_h, Re_b, or Re_ℓ. As is indicated in second year, the flows past the model car and the full-sized prototype will not be similar unless the Reynolds numbers for the model and prototype are the same. It is not always an easy task to ensure this condition. One (expensive) solution is to test full-sized prototypes in very large wind tunnels (see Fig. 4.1).

4.2 Boundary Layer Characteristics

As was discussed in the previous section, it is often possible to treat flow past an object as a combination of viscous flow in the boundary layer and inviscid flow elsewhere. If the Reynolds number is large enough, viscous effects are important only in the boundary layer regions near the object (and in the wake region behind the object). The boundary layer is needed to allow for the no-slip boundary condition that requires the fluid to cling to any solid surface that it flows past. Outside of the boundary layer the velocity gradients normal to the flow are relatively small, and the fluid acts as if it were inviscid, even though the viscosity is not zero. A necessary condition for this structure of the flow is that the Reynolds number be large.

4.2.1 Boundary Layer Structure and Thickness on a Flat Plate

There can be a wide variety in the size of a boundary layer and the structure of the flow within it. Part of this variation is due to the shape of the object on which the boundary layer forms. In this section we consider the simplest situation, one in which the boundary layer is formed on an infinitely long flat plate along which flows a viscous, incompressible fluid as is shown in Fig.4.7 . If the surface were curved (i.e., a circular cylinder or an airfoil), the boundary layer structure would be more complex. Such flows are discussed in Section 4.2.6 .

If the Reynolds number is sufficiently large, only the fluid in a relatively thin boundary layer on the plate will feel the effect of the plate. That is, except in the region next to the plate the flow velocity will be essentially $\mathbf{V} = U\hat{\mathbf{i}}$, the upstream velocity. For the infinitely long flat plate extending from $x = 0$ to $x = \infty$, it is not obvious how to define the

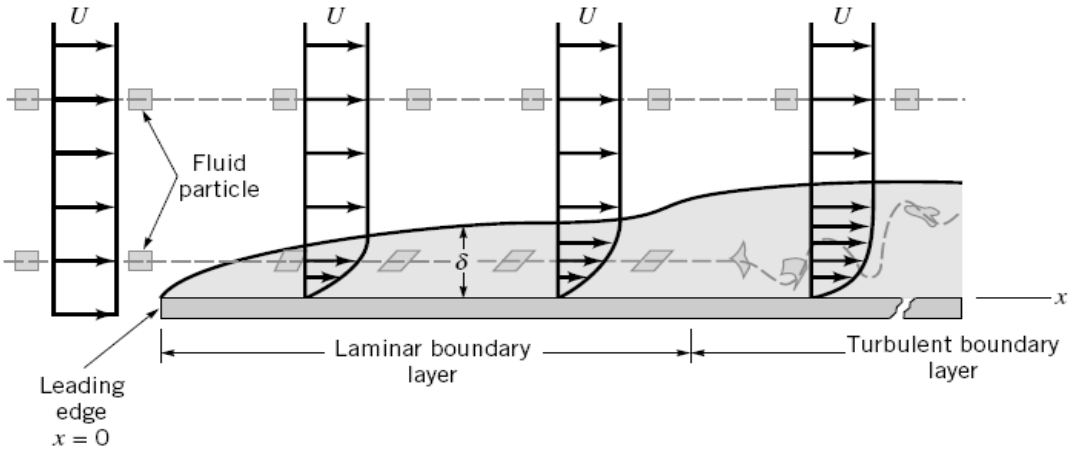

■ FIGURE 4.7
Distortion of a fluid particle as it flows within the boundary layer.

Reynolds number because there is no characteristic length. The plate has no thickness and is not of finite length!

For a finite length plate, it is clear that the plate length, ℓ, can be used as the characteristic length. For an infinitely long plate we use x, the coordinate distance along the plate from the leading edge, as the characteristic length and define the Reynolds number as

$Re_x = Ux/\nu$. Thus, for any fluid or upstream velocity the Reynolds number will be sufficiently large for boundary layer type flow (i.e., Fig. 4.5*c*) if the plate is long enough. Physically, this means that the flow situations illustrated in Fig. 4.5 could be thought of as occurring on the same plate, but should be viewed by looking at longer portions of the plate as we step away from the plate to see the flows in Fig. 4.5*a*, 4.5*b*, and 4.5*c*, respectively.

If the plate is sufficiently long, the Reynolds number $Re = U\ell/\nu$ is sufficiently large so that the flow takes on its boundary layer character (except very near the leading edge). The details of the flow field near the leading edge are lost to our eyes because we are standing so far from the plate that we cannot make out these details. On this scale (Fig. 9.5*c*) the plate has negligible effect on the fluid ahead of the plate. The presence of the plate is felt only in the relatively thin boundary layer and wake regions. As previously noted, Prandtl in 1904 was the first to hypothesize such a concept. It has become one of the major turning points in fluid mechanics analysis.

A better appreciation of the structure of the boundary layer flow can be obtained by considering what happens to a fluid particle that flows into the boundary layer. As is indicated in Fig. 4.7 , a small rectangular particle retains its original shape as it flows in the uniform flow outside of the boundary layer. Once it enters the boundary layer, the particle begins to distort because of the velocity gradient within the boundary layer—the top of the particle has a larger speed than its bottom. The fluid particles do not rotate as they flow along outside the boundary layer, but they begin to rotate once they pass through the fictitious boundary layer surface and enter the world of viscous flow. The flow is said to be irrotational outside the boundary layer and rotational within the boundary layer. (In terms of the kinematics of fluid particles as is discussed in part1 sec1.1, the flow outside the boundary layer has zero vorticity, and the flow within the boundary layer has nonzero vorticity.)

At some distance downstream from the leading edge, the boundary layer flow becomes turbulent and the fluid particles become greatly distorted because of the random, irregular nature of the turbulence. One of the distinguishing features of turbulent flow is the occurrence of irregular mixing of fluid parcels that range in size from the smallest fluid particles up to those comparable in size with the object of interest. For laminar flow, mixing occurs only on the molecular scale. This molecular scale is orders of magnitude smaller in size than typical size scales for turbulent flow mixing. The transition from laminar to turbulent flow occurs at a critical value of the Reynolds number, Re_{xcr}, on the order of 2×10^5 to 3×10^6, depending on the roughness of the surface and the amount of turbulence in the upstream flow, as is discussed in **Section** 4.2.4 .

The purpose of the boundary layer on the plate is to allow the fluid to change its velocity from the upstream value of U to zero on the plate. Thus, $\mathbf{V} = 0$ at $y = 0$ and $\mathbf{V} \approx U\hat{\mathbf{i}}$ at $y = \delta$, with the velocity profile, $u = u(x, y)$ bridging the boundary layer thickness. In actuality (both mathematically and physically), there is no sharp "edge" to the boundary layer. That is, $u \to U$ as we get farther from the plate; it is not precisely $u = U$ at $y = \delta$. We define the *boundary layer thickness*, δ, as that distance from the plate at which the fluid velocity is within some arbitrary value of the upstream velocity. Typically, as indicated in Fig. 4.8*a*,

$$\delta = y \quad \text{where} \quad u = 0.99\,U$$

To remove this arbitrariness (i.e., what is so special about 99%; why not 98%?), the following definitions are introduced. Shown in Fig. 4.8 *b* are two velocity profiles for flow past a flat plate—one if there were no viscosity (a uniform profile) and the other if there are viscosity and zero slip at the wall (the boundary layer profile). Because of the velocity deficit, $U - u$, within the boundary layer, the flowrate across section b–b is less than that across section a–a. However, if we displace the plate at section a–a by an appropriate amount δ^*, the *boundary layer displacement thickness*, the flowrates across each section will be identical. This is true if

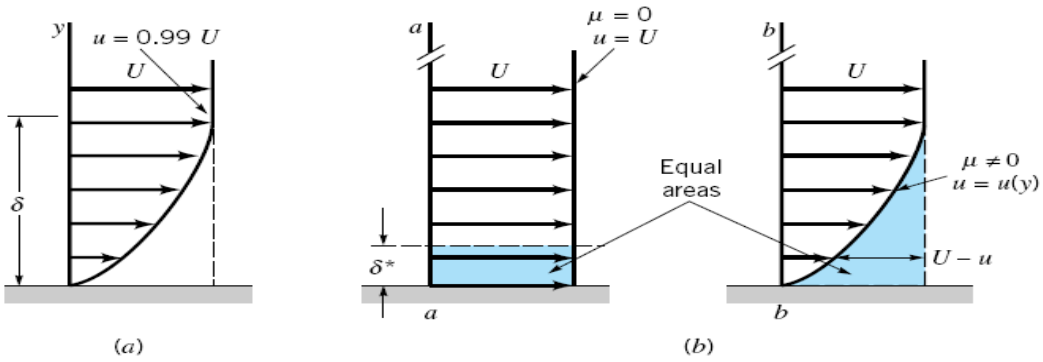

■ FIGURE 4.8
Boundary layer thickness: (*a*) standard boundary layer thickness, (*b*) boundary layer displacement thickness.

$$\delta^* b U = \int_0^\infty (U - u) b \, dy$$

where b is the plate width. Thus,

$$\delta^* = \int_0^\infty \left(1 - \frac{u}{U}\right) dy \tag{4.3}$$

The displacement thickness represents the amount that the thickness of the body must be increased so that the fictitious uniform inviscid flow has the same mass flowrate properties as the actual viscous flow. It represents the outward displacement of the streamlines caused by the viscous effects on the plate. This idea allows us to simulate the presence that the boundary layer has on the flow outside of the boundary layer by adding the displacement thickness to the actual wall and treating the flow over the thickened body as an inviscid flow. The displacement thickness concept is illustrated in Example 4.3.

Example 4.3:

Air flowing into a 2-ft-square duct with a uniform velocity of 10 ft/s forms a boundary layer on the walls as shown in Fig. E4.3. The fluid within the core region (outside the boundary layers) flows as if it were inviscid. From advanced calculations it is determined that for this flow the boundary layer displacement thickness is given by

$$\delta^* = 0.0070(x)^{1/2} \tag{1}$$

where δ^* and x are in feet. Determine the velocity $U = U(x)$ of the air within the duct but outside of the boundary layer.

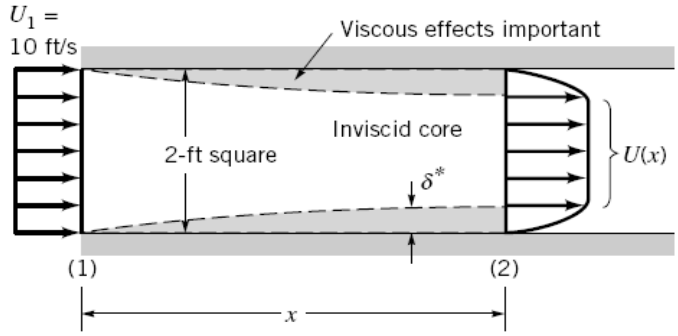

■ FIGURE E4.3

Solution

If we assume incompressible flow (a reasonable assumption because of the low velocities involved), it follows that the volume flowrate across any section of the duct is equal to that at the entrance (i.e., $Q_1 = Q_2$). That is,

$$U_1 A_1 = 10 \text{ ft/s } (2 \text{ ft})^2 = 40 \text{ ft}^3/\text{s} = \int_{(2)} u \, dA$$

According to the definition of the displacement thickness, δ^*, the flowrate across section (2) is the same as that for a uniform flow with velocity U through a duct whose walls have been moved inward by δ^*. That is,

$$40 \text{ ft}^3/\text{s} = \int_{(2)} u \, dA = U(2 \text{ ft} - 2\delta^*)^2 \tag{2}$$

By combining Eqs. 1 and 2 we obtain

$$40 \text{ ft}^3/\text{s} = 4U(1 - 0.0070x^{1/2})^2$$

or

$$U = \frac{10}{(1 - 0.0070x^{1/2})^2} \text{ ft/s} \qquad \text{(Ans)}$$

Note that U increases in the downstream direction. For example, $U = 11.6$ ft/s at $x = 100$ ft. The viscous effects that cause the fluid to stick to the walls of the duct reduce the effective size of the duct, thereby (from conservation of mass principles) causing the fluid to accelerate. The pressure drop necessary to do this can be obtained by using the Bernoulli equation (part 3) along the inviscid streamlines from section (1) to (2). (Recall that this equation is not valid for viscous flows within the boundary layer. It is, however, valid for the inviscid flow outside the boundary layer.) Thus,

$$p_1 + \tfrac{1}{2}\rho U_1^2 = p + \tfrac{1}{2}\rho U^2$$

Hence, with $\rho = 2.38 \times 10^{-3}$ slugs/ft^3 and $p_1 = 0$ we obtain

$$p = \frac{1}{2}\rho\,(U_1^2 - U^2)$$

$$= \frac{1}{2}(2.38 \times 10^{-3}\ \text{slugs/ft}^3)\left[(10\ \text{ft/s})^2 - \frac{10^2}{(1 - 0.0079x^{1/2})^4}\,\text{ft}^2/\text{s}^2\right]$$

or

$$p = 0.119\left[1 - \frac{1}{(1 - 0.0070x^{1/2})^4}\right]\text{lb/ft}^2$$

For example, $p = -0.0401$ lb/ft^2 at $x = 100$ ft.

If it were desired to maintain a constant velocity along the centerline of this entrance region of the duct, the walls could be displaced outward by an amount equal to the boundary layer displacement thickness, δ^*.

Another boundary layer thickness definition, the *boundary layer momentum thickness*, Θ, is often used when determining the drag on an object. Again because of the velocity deficit, $U - u$, in the boundary layer, the momentum flux across section b–b in Fig. 4.8 is less than that across section a–a. This deficit in momentum flux for the actual boundary layer flow is given by

$$\int \rho u(U - u)\,dA = \rho b\int_0^\infty u(U - u)\,dy$$

which by definition is the momentum flux in a layer of uniform speed U and thickness Θ. That is,

$$\rho b U^2\Theta = \rho b\int_0^\infty u(U - u)\,dy$$

or

$$\Theta = \int_0^\infty \frac{u}{U}\left(1 - \frac{u}{U}\right)dy \tag{4.4}$$

All three boundary layer thickness definitions, δ, δ^*, and Θ, are of use in boundary layer analyses.

The boundary layer concept is based on the fact that the boundary layer is thin. For the flat plate flow this means that at any location x along the plate, $\delta \ll x$. Similarly, $\delta^* \ll x$ and $\Theta \ll x$. Again, this is true if we do not get too close to the leading edge of the plate (i.e., not closer than $\text{Re}_x = Ux/\nu = 1000$ or so).

The structure and properties of the boundary layer flow depend on whether the flow is laminar or turbulent. As is illustrated in Fig. 4.9 and discussed in Sections 4.2.2 through 4.2.5 , both the boundary layer thickness and the wall shear stress are different in these two regimes.

4.2.2 Prandtl/Blasius Boundary Layer Solution

In theory, the details of viscous, incompressible flow past any object can be obtained by solving the governing Navier-Stokes equations discussed in Parts 1 and 2 . For steady, two-dimensional laminar flows with negligible gravitational effects, these equations

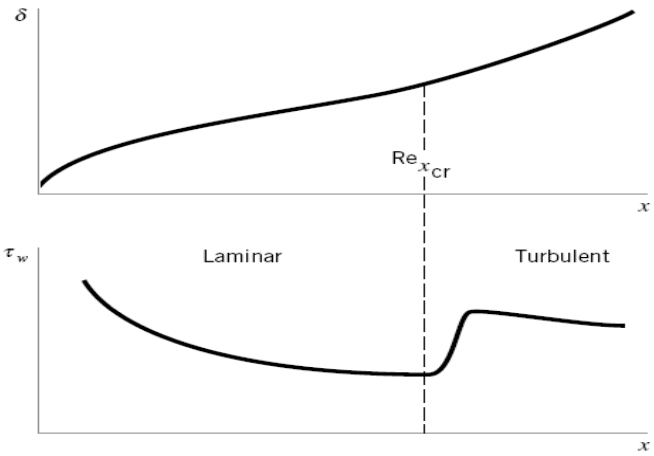

■ FIGURE 4.9 **Typical characteristics of boundary layer thickness and wall shear stress for laminar and turbulent boundary layers.**

reduce to the following:

$$u\frac{\partial u}{\partial x} + v\frac{\partial u}{\partial y} = -\frac{1}{\rho}\frac{\partial p}{\partial x} + \nu\left(\frac{\partial^2 u}{\partial x^2} + \frac{\partial^2 u}{\partial y^2}\right) \tag{4.5}$$

$$u\frac{\partial v}{\partial x} + v\frac{\partial v}{\partial y} = -\frac{1}{\rho}\frac{\partial p}{\partial y} + \nu\left(\frac{\partial^2 v}{\partial x^2} + \frac{\partial^2 v}{\partial y^2}\right) \tag{4.6}$$

which express Newton's second law. In addition, the conservation of mass equation, for incompressible flow is

$$\frac{\partial u}{\partial x} + \frac{\partial v}{\partial y} = 0 \tag{4.7}$$

The appropriate boundary conditions are that the fluid velocity far from the body is the upstream velocity and that the fluid sticks to the solid body surfaces. Although the mathematical problem is well-posed, no one has obtained an analytical solution to these equations for flow past any shaped body! Currently much work is being done to obtain numerical solutions to these governing equations for many flow geometries.

By using boundary layer concepts introduced in the previous sections, Prandtl was able to impose certain approximations (valid for large Reynolds number flows), and thereby to simplify the governing equations. In 1908, **H. Blasius** (1883–1970), one of Prandtl's students, was able to solve these simplified equations for the boundary layer flow past a flat plate parallel to the flow. A brief outline of this technique and the results are presented below. Additional details may be found in the literature (Refs. 1, 2, 3).

Since the boundary layer is thin, it is expected that the component of velocity normal to the plate is much smaller than that parallel to the plate and that the rate of change of any parameter across the boundary layer should be much greater than that along the flow direction. That is,

$$v \ll u \quad \text{and} \quad \frac{\partial}{\partial x} \ll \frac{\partial}{\partial y}$$

Physically, the flow is primarily parallel to the plate and any fluid property is convected downstream much more quickly than it is diffused across the streamlines.

With these assumptions it can be shown that the governing equations (Eqs. 4.5, 4.6, and 4.7) reduce to the following boundary layer equations:

$$\frac{\partial u}{\partial x} + \frac{\partial v}{\partial y} = 0 \tag{4.8}$$

$$u\frac{\partial u}{\partial x} + v\frac{\partial u}{\partial y} = \nu\frac{\partial^2 u}{\partial y^2} \tag{4.9}$$

Although both these boundary layer equations and the original Navier–Stokes equations are nonlinear partial differential equations, there are considerable differences between them. For one, the y momentum equation has been eliminated, leaving only the original, unaltered continuity equation and a modified x momentum equation. One of the variables, the pressure, has been eliminated, leaving only the x and y components of velocity as unknowns. For boundary layer flow over a flat plate the pressure is constant throughout the fluid. The flow represents a balance between viscous and inertial effects, with pressure playing no role.

Note: For a curved wall, x can represent the arc length along the wall and y can be everywhere normal to x with negligible change in the boundary-layer equations as long as the radius of curvature of the wall is large compared with the boundary-layer thickness

More detailed analysis of the 2-D Boundary Layer equations:

In 1904 Prandtl correctly deduced that a shear layer must be very thin if the Reynolds number is large, so that the following approximations apply:

Velocities: $v \ll u$

Rates of change: $\frac{\partial u}{\partial x} \ll \frac{\partial u}{\partial y} \qquad \frac{\partial v}{\partial x} \ll \frac{\partial v}{\partial y}$

Our discussion of displacement thickness in the previous section was intended to justify these assumptions.

Applying these approximations to Eq. (4.6) results in a powerful simplification

$$\frac{\partial p}{\partial y} \approx 0 \qquad \text{or} \qquad p \approx p(x) \text{ only}$$

In other words, the y-momentum equation can be neglected entirely, and the pressure varies only *along* the boundary layer, not through it. The pressure-gradient term in Eq. (4.5) is assumed to be known in advance from Bernoulli's equation applied to the outer inviscid flow

$$\frac{\partial p}{\partial x} = \frac{dp}{dx} = -\rho U \frac{dU}{dx}$$

Presumably we have already made the inviscid analysis and know the distribution of $U(x)$ along the wall from frectionless flow analysis given in part (3).

Meanwhile, one term in Eq. (4.5) is negligible due to

$$\frac{\partial^2 u}{\partial x^2} \ll \frac{\partial^2 u}{\partial y^2}$$

However, neither term in the continuity relation (4.7) can be neglected—another warning that continuity is always a vital part of any fluid-flow analysis.

The net result is that the three full equations of motion are reduced to Prandtl's two boundary-layer equations

Continuity: $$\frac{\partial u}{\partial x} + \frac{\partial v}{\partial y} = 0$$

Momentum along wall: $$u \frac{\partial u}{\partial x} + v \frac{\partial u}{\partial y} \approx U \frac{dU}{dx} + \frac{1}{\rho} \frac{\partial \tau}{\partial y}$$

where $$\tau = \begin{cases} \mu \dfrac{\partial u}{\partial y} & \text{laminar flow} \\ \mu \dfrac{\partial u}{\partial y} - \rho \overline{u'v'} & \text{turbulent flow} \end{cases}$$

These are to be solved for $u(x, y)$ and $v(x, y)$, with $U(x)$ assumed to be a known function from the outer inviscid-flow analysis. There are boundary conditions on u and on v:

At $y = 0$ (wall): $u = v = 0$ (no slip)

At $y = \delta(x)$ (outer stream): $u = U(x)$ (patching) also $\frac{\partial u}{\partial y} = 0$ at the outer edge

At y = 0 (wall) : the shear stress is maximum $\frac{\partial \tau}{\partial y} = 0$

Unlike the Navier-Stokes equations , which are mathematically elliptic and must be solved simultaneously over the entire flow field, the boundary-layer equations are mathematically parabolic and are solved by beginning at the leading edge and marching downstream as far as you like, stopping at the separation point or earlier if you prefer.

The boundary conditions for the governing boundary layer equations are that the fluid sticks to the plate

$$u = v = 0 \quad \text{on} \quad y = 0 \tag{4.10}$$

and that outside of the boundary layer the flow is the uniform upstream flow $u = U$. That is,

$$u \to U \quad \text{as} \quad y \to \infty \tag{4.11}$$

Mathematically, the upstream velocity is approached asymptotically as one moves away from the plate. Physically, the flow velocity is within 1% of the upstream velocity at a distance of δ from the plate.

In mathematical terms, the Navier–Stokes equations (Eqs. 4.5 , 4.6) and the continuity equation (Eq. 4.7) are elliptic equations, whereas the equations for boundary layer flow (Eqs. 4.8 and 4.9) are parabolic equations. The nature of the solutions to these two sets of equations, therefore, is different. Physically, this fact translates to the idea that what happens downstream of a given location in a boundary layer cannot affect what happens upstream of that point. That is, whether the plate shown in Fig. 4.5*c* ends with length ℓ or is extended to length 2ℓ, the flow within the first segment of length ℓ will be the same. In addition, the presence of the plate has no effect on the flow ahead of the plate.

In general, the solutions of nonlinear partial differential equations (such as the boundary layer equations, Eqs. 4.8 and 4.9) are extremely difficult to obtain. However, by applying a clever coordinate transformation and change of variables, Blasius reduced the partial differential equations to an ordinary differential equation that he was able to solve. A brief description of this process is given below. Additional details can be found in standard books dealing with boundary layer flow (Refs. 1, 2).

It can be argued that in dimensionless form the boundary layer velocity profiles on a flat plate should be similar regardless of the location along the plate. That is,

$$\frac{u}{U} = g\left(\frac{y}{\delta}\right)$$

where $g(y/\delta)$ is an unknown function to be determined. In addition, by applying an order of magnitude analysis of the forces acting on fluid within the boundary layer, it can be shown that the boundary layer thickness grows as the square root of x and inversely proportional to the square root of U. That is,

$$\delta \sim \left(\frac{\nu x}{U}\right)^{1/2}$$

Such a conclusion results from a balance between viscous and inertial forces within the boundary layer and from the fact that the velocity varies much more rapidly in the direction across the boundary layer than along it.

Thus, we introduce the dimensionless *similarity variable* $\eta = (U/\nu x)^{1/2} y$ and the stream function $\psi = (\nu\, x\, U)^{1/2} f(\eta)$, where $f = f(\eta)$ is an unknown function. Recall from part (3) that the velocity components for two-dimensional flow are given in terms of the stream function as $u = \partial\psi/\partial y$ and $v = -\partial\psi/\partial x$, which for this flow become

$$u = U f'(\eta) \tag{4.12}$$

and

$$v = \left(\frac{\nu U}{4x}\right)^{1/2} (\eta f' - f) \tag{4.13}$$

with the notation $(\ )' = d/d\eta$. We substitute Eqs. 4.12 and 4.13 into the governing equations, Eqs. 4.8 and 4.9, to obtain (after considerable manipulation) the following nonlinear,

third-order ordinary differential equation:

$$2f''' + ff'' = 0 \tag{4.14a}$$

The boundary conditions given in Eqs. 9.10 and 9.11 can be written as

$$f = f' = 0 \text{ at } \eta = 0 \quad \text{and} \quad f' \to 1 \text{ as } \eta \to \infty \tag{4.14b}$$

The original partial differential equation and boundary conditions have been reduced to an ordinary differential equation by use of the similarity variable η. The two independent variables, x and y, were combined into the similarity variable in a fashion that reduced the partial differential equation (and boundary conditions) to an ordinary differential equation. This type of reduction is not generally possible. For example, this method does not work on the full Navier-Stokes equations, although it does on the boundary layer equations (Eqs. 4.8 and 4.9).

Although there is no known analytical solution to Eq. 4.14 , it is relatively easy to integrate this equation on a computer. The dimensionless boundary layer profile, $u/U = f'(\eta)$, obtained by numerical solution of Eq. 4.14 (termed the Blasius solution), is sketched in Fig. 4.10*a* and is tabulated in Table 4.1. The velocity profiles at different x locations are similar in that there is only one curve necessary to describe the velocity at any point in the boundary layer. Because the similarity variable η contains both x and y, it is seen from Fig. 4.10 *b* that the actual velocity profiles are a function of both x and y. The profile at location x_1 is the same as that at x_2 except that the y coordinate is stretched by a factor of $(x_2/x_1)^{1/2}$.

From the solution it is found that $u/U \approx 0.99$ when $\eta = 5.0$. Thus,

$$\delta = 5\sqrt{\frac{\nu x}{U}} \tag{4.15}$$

or

$$\frac{\delta}{x} = \frac{5}{\sqrt{\text{Re}_x}}$$

where $\text{Re}_x = Ux/\nu$. It can also be shown that the displacement and momentum thicknesses are given by

$$\frac{\delta^*}{x} = \frac{1.721}{\sqrt{\text{Re}_x}} \tag{4.16}$$

and

$$\frac{\Theta}{x} = \frac{0.664}{\sqrt{\text{Re}_x}} \tag{4.17}$$

As postulated, the boundary layer is thin provided that Re_x is large (i.e., $\delta/x \to 0$ as $\text{Re}_x \to \infty$).

With the velocity profile known, it is an easy matter to determine the wall shear stress, $\tau_w = \mu(\partial u/\partial y)_{y=0}$, where the velocity gradient is evaluated at the plate. The value of $\partial u/\partial y$ at $y = 0$ can be obtained from the Blasius solution to give

$$\tau_w = 0.332U^{3/2}\sqrt{\frac{\rho\mu}{x}} \tag{4.18}$$

Note that the shear stress decreases with increasing x because of the increasing thickness of the boundary layer—the velocity gradient at the wall decreases with increasing x. Also, τ_w varies as $U^{3/2}$, not as U as it does for fully developed laminar pipe flow. These variations are discussed in Section 4.2.3 .

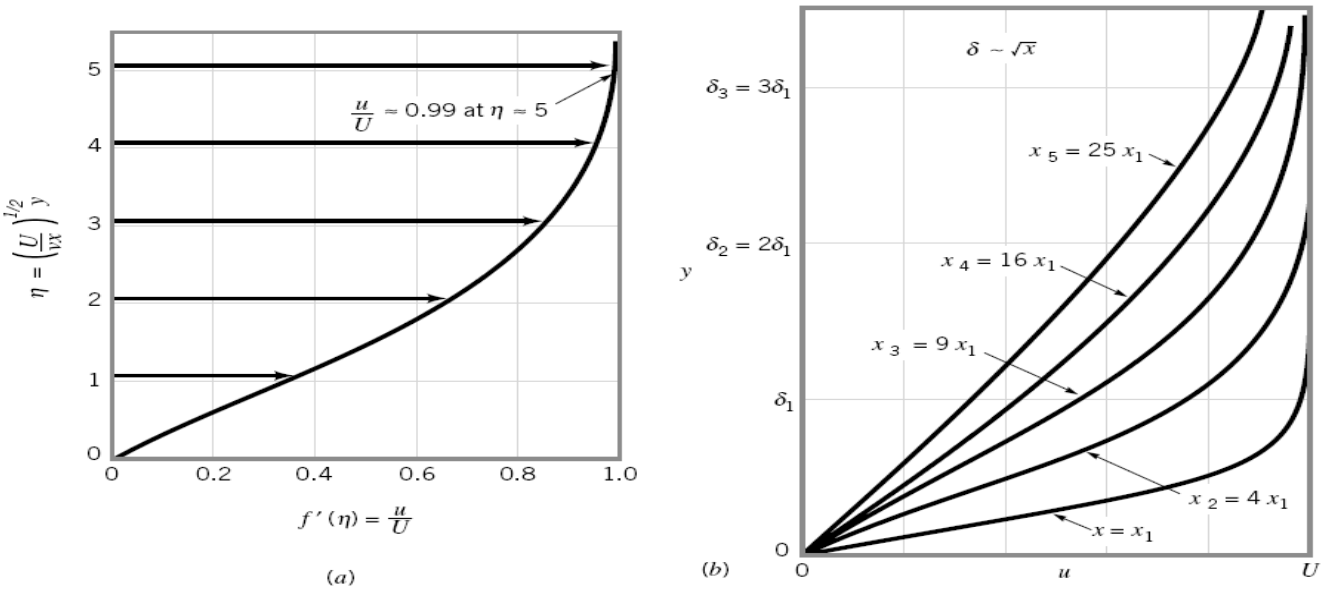

■ **FIGURE** 4.10 **Blasius boundary layer profile: (*a*) boundary layer profile in dimensionless form using the similarity variable η, (*b*) similar boundary layer profiles at different locations along the flat plate.**

Table 4.1 Blasius Velocity Profile for laminar flow on a flat plate

$y[U/(\nu x)]^{1/2}$	u/U	$y[U/(\nu x)]^{1/2}$	u/U
0.0	0.0	2.8	0.81152
0.2	0.06641	3.0	0.84605
0.4	0.13277	3.2	0.87609
0.6	0.19894	3.4	0.90177
0.8	0.26471	3.6	0.92333
1.0	0.32979	3.8	0.94112
1.2	0.39378	4.0	0.95552
1.4	0.45627	4.2	0.96696
1.6	0.51676	4.4	0.97587
1.8	0.57477	4.6	0.98269
2.0	0.62977	4.8	0.98779
2.2	0.68132	5.0	0.99155
2.4	0.72899	∞	1.00000
2.6	0.77246		

Since δ is so ill defined, the momentum thickness, being definite, is often used to correlate data taken for a variety of boundary layers under differing conditions. The ratio of displacement to momentum thickness, called the dimensionless-profile *shape factor,* is also useful in integral theories. For laminar flat-plate flow

$$H = \frac{\delta^*}{\theta} = \frac{1.721}{0.664} = 2.59$$

A large shape factor then implies that boundary-layer separation is about to occur.

Example (A) :

A sharp flat plate with $L = 1$ m and $b = 3$ m is immersed parallel to a stream of velocity 2 m/s. Find the drag on one side of the plate, and at the trailing edge find the thicknesses δ, δ^*, and θ for (*a*) air, $\rho = 1.23$ kg/m^3 and $\nu = 1.46 \times 10^{-5}$ m^2/s, and (*b*) water, $\rho = 1000$ kg/m^3 and $\nu = 1.02 \times 10^{-6}$ m^2/s.

Solution

Part (a)

The airflow Reynolds number is

$$\frac{VL}{\nu} = \frac{(2.0 \text{ m/s})(1.0 \text{ m})}{1.46 \times 10^{-5} \text{ m}^2/\text{s}} = 137{,}000$$

Since this is less than 3×10^6, we assume that the boundary layer is laminar.

the drag coefficient is $$C_D = \frac{1.328}{(137{,}000)^{1/2}} = 0.00359$$

Thus the drag on one side in the airflow is

$$D = C_D \tfrac{1}{2}\rho U^2 bL = 0.00359(\tfrac{1}{2})(1.23)(2.0)^2(3.0)(1.0) = 0.0265 \text{ N} \quad \textit{Ans. (a)}$$

The boundary-layer thickness at the end of the plate is

$$\frac{\delta}{L} = \frac{5.0}{\text{Re}_L^{1/2}} = \frac{5.0}{(137{,}000)^{1/2}} = 0.0135$$

or $$\delta = 0.0135(1.0) = 0.0135 \text{ m} = 13.5 \text{ mm} \quad \textit{Ans. (a)}$$

We find the other two thicknesses simply by ratios:

$$\delta^* = \frac{1.721}{5.0}\,\delta = 4.65 \text{ mm} \qquad \theta = \frac{\delta^*}{2.59} = 1.79 \text{ mm} \quad \textit{Ans. (a)}$$

Notice that no conversion factors are needed with SI units.

Part (b)

The water Reynolds number is $$\text{Re}_L = \frac{2.0(1.0)}{1.02 \times 10^{-6}} = 1.96 \times 10^6$$

This is rather close to the critical value of 3×10^6, so that a rough surface or noisy free stream might trigger transition to turbulence; but let us assume that the flow is laminar. The water drag coefficient is

$$C_D = \frac{1.328}{(1.96 \times 10^6)^{1/2}} = 0.000949$$

and $$D = 0.000949(\tfrac{1}{2})(1000)(2.0)^2(3.0)(1.0) = 5.70 \text{ N} \quad \textit{Ans. (b)}$$

The drag is 215 times more for water in spite of the higher Reynolds number and lower drag coefficient because water is 57 times more viscous and 813 times denser than air. From Eq. , in laminar flow, it should have $(57)^{1/2}(813)^{1/2} = 7.53(28.5) = 215$ times more drag.

The boundary-layer thickness is given by

$$\frac{\delta}{L} = \frac{5.0}{(1.96 \times 10^6)^{1/2}} = 0.00357$$

or $$\delta = 0.00357(1000 \text{ mm}) = 3.57 \text{ mm} \quad \textit{Ans. (b)}$$

By scaling down we have

$$\delta^* = \frac{1.721}{5.0}\,\delta = 1.23 \text{ mm} \qquad \theta = \frac{\delta^*}{2.59} = 0.48 \text{ mm} \quad \textit{Ans. (b)}$$

The water layer is 3.8 times thinner than the air layer, which reflects the square root of the 14.3 ratio of air to water kinematic viscosity.

4.2.3 Momentum-Integral Boundary Layer Equation for a Flat Plate

One of the important aspects of boundary layer theory is the determination of the drag caused by shear forces on a body. As was discussed in the previous section, such results can be obtained from the governing differential equations for laminar boundary layer flow. Since these solutions are extremely difficult to obtain, it is of interest to have an alternative approximate method. The momentum integral method described in this section provides such an alternative.

We consider the uniform flow past a flat plate and the fixed control volume as shown in Fig. 4.11. In agreement with advanced theory and experiment, we assume that the pressure is constant throughout the flow field. The flow entering the control volume at the leading edge of the plate [section (1)] is uniform, while the velocity of the flow exiting the control volume [section (2)] varies from the upstream velocity at the edge of the boundary layer to zero velocity on the plate.

The fluid adjacent to the plate makes up the lower portion of the control surface. The upper surface coincides with the streamline just outside the edge of the boundary layer at section (2). It need not (in fact, does not) coincide with the edge of the boundary layer except at section (2). If we apply the x component of the momentum equation to the steady flow of fluid within this control volume we obtain

$$\sum F_x = \rho \int_{(1)} u\mathbf{V} \cdot \hat{\mathbf{n}}\, dA + \rho \int_{(2)} u\mathbf{V} \cdot \hat{\mathbf{n}}\, dA$$

where for a plate of width b

$$\sum F_x = -\mathcal{D} = -\int_{\text{plate}} \tau_w \, dA = -b \int_{\text{plate}} \tau_w \, dx \tag{4.19}$$

and $\mathcal{D}$ is the drag that the plate exerts on the fluid. Note that the net force caused by the uniform pressure distribution does not contribute to this flow. Since the plate is solid and the upper surface of the control volume is a streamline, there is no flow through these areas. Thus,

$$-\mathcal{D} = \rho \int_{(1)} U(-U) \, dA + \rho \int_{(2)} u^2 \, dA$$

or

$$\mathcal{D} = \rho U^2 bh - \rho b \int_0^{\delta} u^2 \, dy \tag{4.20}$$

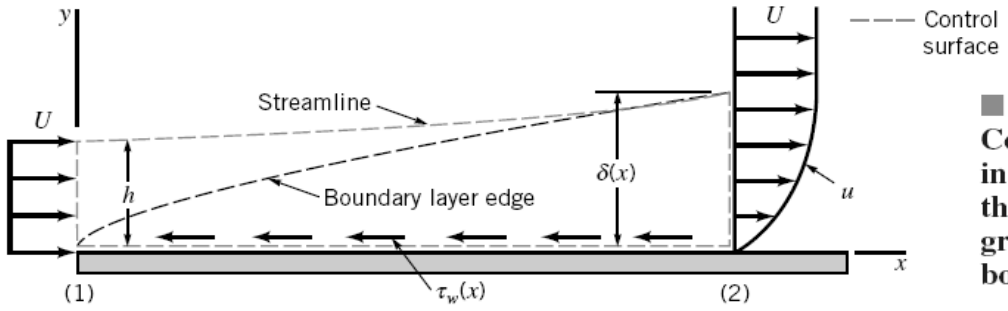

■ **FIGURE 4.11**
Control volume used in the derivation of the momentum integral equation for boundary layer flow.

Although the height h is not known, it is known that for conservation of mass the flowrate through section (1) must equal that through section (2), or

$$Uh = \int_0^{\delta} u \, dy$$

which can be written as

$$\rho U^2 bh = \rho b \int_0^{\delta} Uu \, dy \tag{4.21}$$

Thus, by combining Eqs. 4.20 and 4.21 we obtain the drag in terms of the deficit of momentum flux across the outlet of the control volume as

$$\mathcal{D} = \rho b \int_0^{\delta} u(U - u) \, dy \tag{4.22}$$

If the flow were inviscid, the drag would be zero, since we would have $u \equiv U$ and the right-hand side of Eq. 4.22 would be zero. (This is consistent with the fact that $\tau_w = 0$ if $\mu = 0$.) Equation 4.22 points out the important fact that boundary layer flow on a flat plate is governed by a balance between shear drag (the left-hand side of Eq. 4.22) and a decrease in the momentum of the fluid (the right-hand side of Eq. 4.22). As x increases, δ increases and the drag increases. The thickening of the boundary layer is necessary to overcome the drag of the viscous shear stress on the plate. This is contrary to horizontal fully developed pipe flow in which the momentum of the fluid remains constant and the shear force is overcome by the pressure gradient along the pipe.

The development of Eq. 4.22 and its use was first put forth in 1921 by **T. von Karman** (1881–1963), a Hungarian/German aerodynamicist. By comparing Eqs. 4.22 and 4.9 we see that the drag can be written in terms of the momentum thickness, Θ, as

$$\mathcal{D} = \rho b U^2 \Theta \tag{4.23}$$

Note that this equation is valid for laminar or turbulent flows.

The shear stress distribution can be obtained from Eq. 4.23 by differentiating both sides with respect to x to obtain

$$\frac{d\mathcal{D}}{dx} = \rho b U^2 \frac{d\Theta}{dx} \tag{4.24}$$

The increase in drag per length of the plate, $d\mathcal{D}/dx$, occurs at the expense of an increase of the momentum boundary layer thickness, which represents a decrease in the momentum of the fluid.

Since $d\mathcal{D} = \tau_w b \, dx$ (see Eq. 4.19) it follows that

$$\frac{d\mathcal{D}}{dx} = b\tau_w \tag{4.25}$$

Hence, by combining Eqs. 4.24 and 4.25 we obtain the *momentum integral equation* for the boundary layer flow on a flat plate

$$\tau_w = \rho U^2 \frac{d\Theta}{dx} \tag{4.26}$$

The usefulness of this relationship lies in the ability to obtain approximate boundary layer results easily by using rather crude assumptions. For example, if we knew the detailed velocity profile in the boundary layer (i.e., the Blasius solution discussed in the previous section), we could evaluate either the right-hand side of Eq. 4.23 to obtain the drag, or the right-hand side of Eq. 4.26 to obtain the shear stress. Fortunately, even a rather crude guess at the velocity profile will allow us to obtain reasonable drag and shear stress results from Eq. 4.26 . This method is illustrated in Example 4.4.

Example 4.4:

Consider the laminar flow of an incompressible fluid past a flat plate at $y = 0$. The boundary layer velocity profile is approximated as $u = Uy/\delta$ for $0 \le y \le \delta$ and $u = U$ for $y > \delta$, as is shown in Fig. E4.4. Determine the shear stress by using the momentum integral equation. Compare these results with the Blasius results given by Eq. 4.18 .

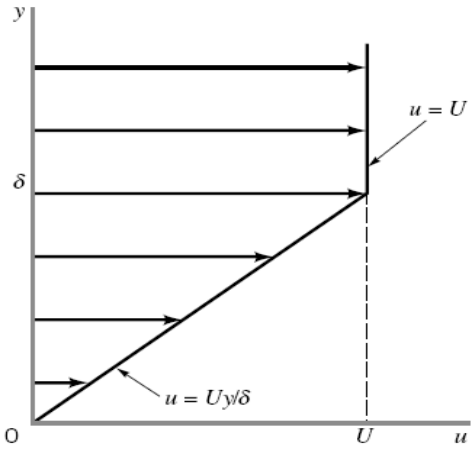

■ FIGURE E 4.4

Solution

From Eq. 4.26 the shear stress is given by

$$\tau_w = \rho U^2 \frac{d\Theta}{dx} \tag{1}$$

while for laminar flow we know that $\tau_w = \mu(\partial u/\partial y)_{y=0}$. For the assumed profile we have

$$\tau_w = \mu \frac{U}{\delta} \tag{2}$$

and from Eq. 4.4

$$\Theta = \int_0^\infty \frac{u}{U}\left(1 - \frac{u}{U}\right)dy = \int_0^\delta \frac{u}{U}\left(1 - \frac{u}{U}\right)dy = \int_0^\delta \left(\frac{y}{\delta}\right)\left(1 - \frac{y}{\delta}\right)dy$$

or

$$\Theta = \frac{\delta}{6} \tag{3}$$

Note that as yet we do not know the value of δ (but suspect that it should be a function of x).

By combining Eqs. 1, 2, and 3 we obtain the following differential equation for δ:

$$\frac{\mu U}{\delta} = \frac{\rho U^2}{6}\frac{d\delta}{dx}$$

or

$$\delta\, d\delta = \frac{6\mu}{\rho U} dx$$

This can be integrated from the leading edge of the plate, $x = 0$ (where $\delta = 0$) to an arbitrary location x where the boundary layer thickness is δ. The result is

$$\frac{\delta^2}{2} = \frac{6\mu}{\rho U} x$$

or

$$\delta = 3.46\sqrt{\frac{\nu x}{U}} \tag{4}$$

Note that this approximate result (i.e., the velocity profile is not actually the simple straight line we assumed) compares favorably with the (much more laborious to obtain) Blasius result given by Eq. 4.15 .

The wall shear stress can also be obtained by combining Eqs. 1, 3, and 4 to give

$$\tau_w = 0.289 U^{3/2} \sqrt{\frac{\rho\mu}{x}} \qquad \text{(Ans)}$$

Again this approximate result is close (within 13%) to the Blasius value of τ_w given by Eq. 4.18 .

As is illustrated in Example 4.4 , the momentum integral equation, Eq. 4.26 , can be used along with an assumed velocity profile to obtain reasonable, approximate boundary layer results. The accuracy of these results depends on how closely the shape of the assumed velocity profile approximates the actual profile.

Thus, we consider a general velocity profile $\dfrac{u}{U} = g(Y) \quad \text{for} \quad 0 \le Y \le 1$

and $\dfrac{u}{U} = 1 \quad \text{for} \quad Y > 1$

where the dimensionless coordinate $Y = y/\delta$ varies from 0 to 1 across the boundary layer. The dimensionless function $g(Y)$ can be any shape we choose, although it should be a reasonable approximation to the boundary layer profile. In particular, it should certainly satisfy the boundary conditions $u = 0$ at $y = 0$ and $u = U$ at $y = \delta$. That is,

$$g(0) = 0 \quad \text{and} \quad g(1) = 1$$

The linear function $g(Y) = Y$ used in Example 4.4 is one such possible profile. Other conditions, such as $dg/dY = 0$ at $Y = 1$ (i.e., $\partial u/\partial y = 0$ at $y = \delta$), could also be incorporated into the function $g(Y)$ to more closely approximate the actual profile.

For a given $g(Y)$, the drag can be determined from Eq. 4.22 as

$$\mathcal{D} = \rho b \int_0^\delta u(U - u)\, dy = \rho b U^2 \delta \int_0^1 g(Y)[1 - g(Y)]\, dY$$

or

$$\mathcal{D} = \rho b U^2 \delta C_1 \qquad (4.27)$$

where the dimensionless constant C_1 has the value

$$C_1 = \int_0^1 g(Y)[1 - g(Y)]\, dY$$

Also, the wall shear stress can be written as

$$\tau_w = \mu \left.\frac{\partial u}{\partial y}\right|_{y=0} = \left.\frac{\mu U}{\delta}\frac{dg}{dY}\right|_{Y=0} = \frac{\mu U}{\delta} C_2 \qquad (4.28)$$

where the dimensionless constant C_2 has the value $C_2 = \left.\dfrac{dg}{dY}\right|_{Y=0}$

By combining Eqs. 4.25 , 4.27 , and 4.28 we obtain $\delta\, d\delta = \dfrac{\mu C_2}{\rho U C_1} dx$

which can be integrated from $\delta = 0$ at $x = 0$ to give $\delta = \sqrt{\dfrac{2\nu C_2 x}{U C_1}}$

or

$$\frac{\delta}{x} = \frac{\sqrt{2C_2/C_1}}{\sqrt{\mathrm{Re}_x}} \qquad (4.29)$$

By substituting this expression back into Eqs. 4.28 we obtain

$$\tau_w = \sqrt{\frac{C_1 C_2}{2}}\, U^{3/2} \sqrt{\frac{\rho\mu}{x}} \qquad (4.30)$$

To use Eqs. 4.29 and 4.30 we must determine the values of C_1 and C_2. Several assumed velocity profiles and the resulting values of δ are given in Fig. 4.12 and Table 4.2 . The more closely the assumed shape approximates the acutal (i.e., Blasius) profile, the more accurate the final results. For any assumed profile shape, the functional dependence of δ and τ_w on the physical parameters ρ, μ, U, and x is the same. Only the constants are different. That is, $\delta \sim (\mu x/\rho U)^{1/2}$ or $\delta \mathrm{Re}_x^{1/2}/x =$ constant, and $\tau_w \sim (\rho\mu U^3/x)^{1/2}$, where $\mathrm{Re}_x = \rho U x/\mu$.

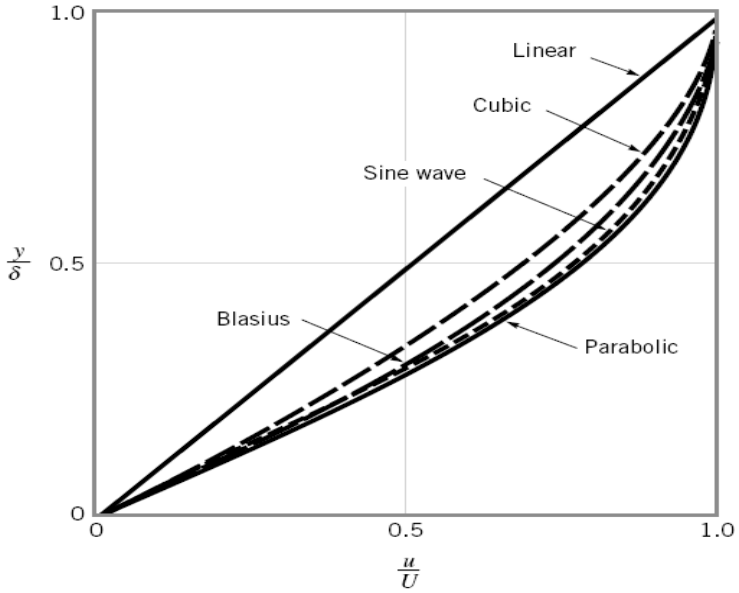

■ **FIGURE 4.12** **Typical approximate boundary layer profiles used in the momentum integral equation.**

It is often convenient to use the dimensionless *local friction coefficient*, c_f, defined as

$$c_f = \frac{\tau_w}{\frac{1}{2}\rho U^2} \tag{4.31}$$

to express the wall shear stress. From Eq. 4.30 we obtain the approximate value

$$c_f = \sqrt{2C_1C_2}\sqrt{\frac{\mu}{\rho Ux}} = \frac{\sqrt{2C_1C_2}}{\sqrt{\mathrm{Re}_x}}$$

while the Blasius solution result is given by

$$c_f = \frac{0.664}{\sqrt{\mathrm{Re}_x}} \tag{4.32}$$

These results are also indicated in Table 4.2 .

■ **TABLE 4.2**

Flat Plate Momentum-Integral Results for Various Assumed Laminar Flow Velocity Profiles

Profile Character	$\delta\mathrm{Re}_x^{1/2}/x$	$c_f\mathrm{Re}_x^{1/2}$	$C_{Df}\mathrm{Re}_\ell^{1/2}$
a. Blasius solution	5.00	0.664	1.328
b. Linear $u/U = y/\delta$	3.46	0.578	1.156
c. Parabolic $u/U = 2y/\delta - (y/\delta)^2$	5.48	0.730	1.460
d. Cubic $u/U = 3(y/\delta)/2 - (y/\delta)^3/2$	4.64	0.646	1.292
e. Sine wave $u/U = \sin[\pi(y/\delta)/2]$	4.79	0.655	1.310

For a flat plate of length ℓ and width b, the net friction drag, $\mathscr{D}_f$, can be expressed in terms of the *friction drag coefficient*, C_{Df}, as

$$C_{Df} = \frac{\mathscr{D}_f}{\frac{1}{2}\rho U^2 b\ell} = \frac{b\int_0^\ell \tau_w\,dx}{\frac{1}{2}\rho U^2 b\ell}$$

or

$$C_{Df} = \frac{1}{\ell}\int_0^\ell c_f\,dx \tag{4.33}$$

We use the above approximate value of $c_f = (2C_1C_2\mu/\rho Ux)^{1/2}$ to obtain

$$C_{Df} = \frac{\sqrt{8C_1C_2}}{\sqrt{\mathrm{Re}_\ell}}$$

where $\mathrm{Re}_\ell = U\ell/\nu$ is the Reynolds number based on the plate length. The corresponding value obtained from the Blasius solution (Eq. 4.32) gives

$$C_{Df} = \frac{1.328}{\sqrt{\mathrm{Re}_\ell}}$$

These results are also indicated in Table 4.2 .

The momentum-integral boundary layer method provides a relatively simple technique to obtain useful boundary layer results. As is discussed in Sections 4.2.5 and 4.2.6, this technique can be extended to boundary layer flows on curved surfaces (where the pressure and fluid velocity at the edge of the boundary layer are not constant) and to turbulent flows.

4.2.4 Transition from Laminar to Turbulent Flow

The analytical results given in Table 4.2 are restricted to laminar boundary layer flows along a flat plate with zero pressure gradient. They agree quite well with experimental results up to the point where the boundary layer flow becomes turbulent, which will occur for any free stream velocity and any fluid provided the plate is long enough. This is true because the parameter that governs the transition to turbulent flow is the Reynolds number—in this case the Reynolds number based on the distance from the leading edge of the plate, $Re_x = Ux/\nu$.

The value of the Reynolds number at the transition location is a rather complex function of various parameters involved, including the roughness of the surface, the curvature of the surface (e.g., a flat plate or a sphere), and some measure of the disturbances in the flow outside the boundary layer. On a flat plate with a sharp leading edge in a typical air stream, the transition takes place at a distance x from the leading edge given by $Re_{xcr} = 2 \times 10^5$ to 3×10^6. Unless otherwise stated, we will use $Re_{xcr} = 5 \times 10^5$ in our calculations.

The actual transition from laminar to turbulent boundary layer flow may occur over a region of the plate, not at a specific single location. This occurs, in part, because of the spottiness of the transition. Typically, the transition begins at random locations on the plate in the vicinity of $Re_x = Re_{xcr}$. These spots grow rapidly as they are convected downstream until the entire width of the plate is covered with turbulent flow. The photo shown in Fig. 4.13 illustrates this transition process.

The complex process of transition from laminar to turbulent flow involves the instability of the flow field. Small disturbances imposed on the boundary layer flow (i.e., from a vibration of the plate, a roughness of the surface, or a "wiggle" in the flow past the plate) will either grow (instability) or decay (stability), depending on where the disturbance is introduced into the flow. If these disturbances occur at a location with $Re_x < Re_{xcr}$ they will

■ FIGURE 4.13
Turbulent spots and the transition from laminar to turbulent boundary layer flow on a flat plate. Flow from left to right. (Photograph courtesy of B. Cantwell, Stanford University.)

die out, and the boundary layer will return to laminar flow at that location. Disturbances imposed at a location with $Re_x > Re_{xcr}$ will grow and transform the boundary layer flow downstream of this location into turbulence. The study of the initiation, growth, and structure of these turbulent bursts or spots is an active area of fluid mechanics research.

Transition from laminar to turbulent flow also involves a noticeable change in the shape of the boundary layer velocity profile. Typical profiles obtained in the neighborhood of the transition location are indicated in Fig. 4.14. The turbulent profiles are flatter, have a larger velocity gradient at the wall, and produce a larger boundary layer thickness than do the laminar profiles.

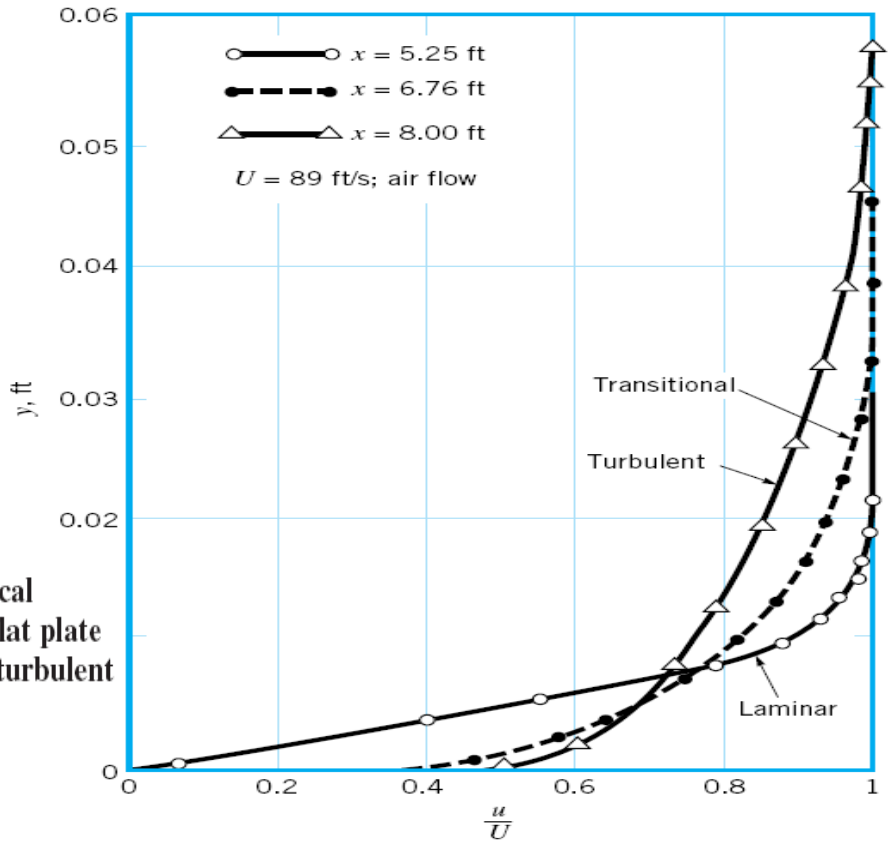

■ **FIGURE** 4.14 **Typical boundary layer profiles on a flat plate for laminar, transitional, and turbulent flow (Ref. 1).**

Example 4.5:

A fluid flows steadily past a flat plate with a velocity of $U = 10$ ft/s. At approximately what location will the boundary layer become turbulent, and how thick is the boundary layer at that point if the fluid is (a) water at 60 °F, (b) standard air, or (c) glycerin at 68 °F?

Solution

For any fluid, the laminar boundary layer thickness is found from Eq. 4.15 as $\delta = 5\sqrt{\frac{\nu x}{U}}$

The boundary layer remains laminar up to $x_{cr} = \frac{\nu \mathrm{Re}_{xcr}}{U}$

Thus, if we assume $\mathrm{Re}_{xcr} = 5 \times 10^5$ we obtain $x_{cr} = \frac{5 \times 10^5}{10 \text{ ft/s}} \nu = 5 \times 10^4 \, \nu$

and

$$\delta_{cr} \equiv \delta|_{x=x_{cr}} = 5\left[\frac{\nu}{10}(5 \times 10^4 \, \nu)\right]^{1/2} = 354 \, \nu$$

where ν is in ft^2/s and x_{cr} and δ_{cr} are in feet. The values of the kinematic viscosity obtained from Tables are listed in Table E4.5 along with the corresponding x_{cr} and δ_{cr}.

■ **TABLE** E4.5

Fluid	ν(ft^2/s)	x_{cr}(ft)	δ_{cr}(ft)
a. Water	1.21×10^{-5}	0.605	0.00428
b. Air	1.57×10^{-4}	7.85	0.0556
c. Glycerin	1.28×10^{-2}	640.0	4.53

Ans

Laminar flow can be maintained on a longer portion of the plate if the viscosity is increased. However, the boundary layer flow eventually becomes turbulent, provided the plate is long enough. Similarly, the boundary layer thickness is greater if the viscosity is increased.

4.2.5 .a Turbulent Boundary Layer Flow

The structure of turbulent boundary layer flow is very complex, random, and irregular. It shares many of the characteristics described for turbulent pipe flow in part (2) . In particular, the velocity at any given location in the flow is unsteady in a random fashion. The flow can be thought of as a jumbled mix of interwined eddies (or swirls) of different sizes (diameters and angular velocities). The various fluid quantities involved (i.e., mass, momentum, energy) are convected downstream in the free-stream direction as in a laminar boundary layer. For turbulent flow they are also convected across the boundary layer (in the direction perpendicular to the plate) by the random transport of finite-sized fluid particles associated with the turbulent eddies. There is considerable mixing involved with these finite-sized eddies—considerably more than is associated with the mixing found in laminar flow where it is confined to the molecular scale. Although there is considerable random motion of fluid particles perpendicular to the plate, there is very little net transfer of mass across the boundary layer—the largest flowrate by far is parallel to the plate.

There is, however, a considerable net transfer of x component of momentum perpendicular to the plate because of the random motion of the particles. Fluid particles moving toward the plate (in the negative y direction) have some of their excess momentum (they come from areas of higher velocity) removed by the plate. Conversely, particles moving away from the plate (in the positive y direction) gain momentum from the fluid (they come from areas of lower velocity). The net result is that the plate acts as a momentum sink, continually extracting momentum from the fluid. For laminar flows, such cross-stream transfer of these properties takes place solely on the molecular scale. For turbulent flow the randomness is associated with fluid particle mixing. Consequently, the shear force for turbulent boundary layer flow is considerably greater than it is for laminar boundary layer flow .

There are no "exact" solutions for turbulent boundary layer flow. As is discussed in Section 4.2.2, it is possible to solve the Prandtl boundary layer equations for laminar flow past a flat plate to obtain the Blasius solution (which is "exact" within the framework of the assumptions involved in the boundary layer equations). Since there is no precise expression for the shear stress in turbulent flow (see part (2)), solutions are not available for turbulent flow. However, considerable headway has been made in obtaining numerical (computer) solutions for turbulent flow by using approximate shear stress relationships. Also, progress is being made in the area of direct, full numerical integration of the basic governing equations, the Navier-Stokes equations.

Approximate turbulent boundary layer results can also be obtained by use of the momentum integral equation, Eq. 4.26 , which is valid for either laminar or turbulent flow. What is needed for the use of this equation are reasonable approximations to the velocity profile $u = U\,g(Y)$, where $Y = y/\delta$ and u is the time-averaged velocity (the overbar notation, $\overline{u}$, of part (2) has been dropped for convenience) and a functional relationship describing the wall shear stress. For laminar flow the wall shear stress was used as $\tau_w = \mu(\partial u/\partial y)_{y=0}$. In theory, such a technique should work for turbulent boundary layers also. However, as is discussed in part (2) , the details of the velocity gradient at the wall are not well understood for turbulent flow. Thus, it is necessary to use some empirical relationship for the wall shear stress. This is illustrated in Example 4.6 .

> Consider turbulent flow of an incompressible fluid past a flat plate. The boundary layer velocity profile is assumed to be $u/U = (y/\delta)^{1/7} = Y^{1/7}$ for $Y = y/\delta \le 1$ and $u = U$ for $Y > 1$ as shown in Fig. E4.6. This is a reasonable approximation of experimentally observed profiles, except very near the plate where this formula gives $\partial u/\partial y = \infty$ at $y = 0$. Note the differences between the assumed turbulent profile and the laminar profile.

Also assume that the shear stress agrees with the experimentally determined formula:

$$\tau_w = 0.0225\rho U^2 \left(\frac{\nu}{U\delta}\right)^{1/4} \tag{1}$$

Determine the boundary layer thicknesses δ, δ^*, and Θ and the wall shear stress, τ_w, as a function of x. Determine the friction drag coefficient, C_{Df}.

Solution

Whether the flow is laminar or turbulent, it is true that the drag force is accounted for by a reduction in the momentum of the fluid flowing past the plate. The shear is obtained from

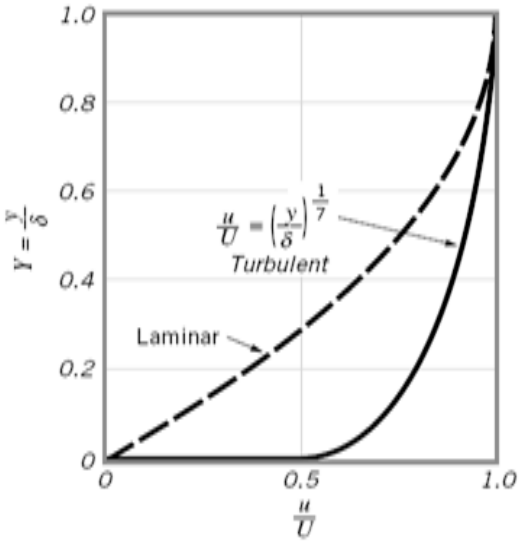

FIGURE E4.6

Eq. 4.26 in terms of the rate at which the momentum boundary layer thickness, Θ, increases with distance along the plate as

$$\tau_w = \rho U^2 \frac{d\Theta}{dx}$$

For the assumed velocity profile, the boundary layer momentum thickness is obtained from Eq. 4.9 as

$$\Theta = \int_0^\infty \frac{u}{U}\left(1 - \frac{u}{U}\right)dy = \delta \int_0^1 \frac{u}{U}\left(1 - \frac{u}{U}\right)dY$$

or by integration

$$\Theta = \delta \int_0^1 Y^{1/7}\left(1 - Y^{1/7}\right)dY = \frac{7}{72}\delta \tag{2}$$

where δ is an unknown function of x. By combining the assumed shear force dependence (Eq. 1) with Eq. 2, we obtain the following differential equation for δ:

$$0.0225\rho U^2 \left(\frac{\nu}{U\delta}\right)^{1/4} = \frac{7}{72}\rho U^2 \frac{d\delta}{dx}$$

or

$$\delta^{1/4}\, d\delta = 0.231 \left(\frac{\nu}{U}\right)^{1/4} dx$$

This can be integrated from $\delta = 0$ at $x = 0$ to obtain

$$\delta = 0.370 \left(\frac{\nu}{U}\right)^{1/5} x^{4/5} \tag{3}$$

or in dimensionless form

$$\frac{\delta}{x} = \frac{0.370}{\mathrm{Re}_x^{1/5}} \qquad \text{(Ans)}$$

Strictly speaking, the boundary layer near the leading edge of the plate is laminar, not turbulent, and the precise boundary condition should be the matching of the initial turbulent boundary layer thickness (at the transition location) with the thickness of the laminar boundary layer at that point. In practice, however, the laminar boundary layer often exists over a relatively short portion of the plate, and the error associated with starting the turbulent boundary layer with $\delta = 0$ at $x = 0$ can be negligible.

The displacement thickness, δ^*, and the momentum thickness, Θ, can be obtained from Eqs. 4.3 and 4.4 by integrating as follows:

$$\delta^* = \int_0^\infty \left(1 - \frac{u}{U}\right) dy = \delta \int_0^1 \left(1 - \frac{u}{U}\right) dY$$

$$= \delta \int_0^1 (1 - Y^{1/7})\, dY = \frac{\delta}{8}$$

Thus, by combining this with Eq. 3 we obtain

$$\delta^* = 0.0463 \left(\frac{\nu}{U}\right)^{1/5} x^{4/5} \qquad \text{(Ans)}$$

Similarly, from Eq. 2,

$$\Theta = \tfrac{7}{72}\,\delta = 0.0360 \left(\frac{\nu}{U}\right)^{1/5} x^{4/5} \qquad \textbf{(4)} \quad \text{(Ans)}$$

The functional dependence for δ, δ^*, and Θ is the same; only the constants of proportionality are different. Typically, $\Theta < \delta^* < \delta$.

By combining Eqs. 1 and 3, we obtain the following result for the wall shear stress

$$\tau_w = 0.0225\rho U^2 \left[\frac{\nu}{U(0.370)(\nu/U)^{1/5} x^{4/5}}\right]^{1/4} = \frac{0.0288\rho U^2}{\mathrm{Re}_x^{1/5}} \qquad \text{(Ans)}$$

This can be integrated over the length of the plate to obtain the friction drag on one side of the plate, $\mathscr{D}_f$, as

$$\mathscr{D}_f = \int_0^\ell b\tau_w\, dx = b(0.0288\rho U^2) \int_0^\ell \left(\frac{\nu}{Ux}\right)^{1/5} dx$$

or

$$\mathscr{D}_f = 0.0360\rho U^2 \frac{A}{\mathrm{Re}_\ell^{1/5}}$$

where $A = b\ell$ is the area of the plate. (This result can also be obtained by combining Eq. 4.23 and the expression for the momentum thickness given in Eq. 4.) The corresponding friction drag coefficient, C_{Df}, is

$$C_{Df} = \frac{\mathscr{D}_f}{\frac{1}{2}\rho U^2 A} = \frac{0.0720}{\mathrm{Re}_\ell^{1/5}} \qquad \text{(Ans)}$$

Note that for the turbulent boundary layer flow the boundary layer thickness increases with x as $\delta \sim x^{4/5}$ and the shear stress decreases as $\tau_w \sim x^{-1/5}$. For laminar flow these dependencies are $x^{1/2}$ and $x^{-1/2}$, respectively. The random character of the turbulent flow causes a different structure of the flow.

Obviously the results presented in this example are valid only in the range of validity of the original data—the assumed velocity profile and shear stress. This range covers smooth flat plates with $5 \times 10^5 < \mathrm{Re}_\ell < 10^7$.

In general, the drag coefficient for a flat plate of length ℓ is a function of the Reynolds number, Re_ℓ, and the relative roughness, ε/ℓ. The results of numerous experiments covering a wide range of the parameters of interest are shown in Fig. 4.15 . For laminar boundary layer flow the drag coefficient is a function of only the Reynolds number—surface roughness is not important. This is similar to laminar flow in a pipe. However, for turbulent flow, the surface roughness does affect the shear stress and, hence, the drag coefficient. This is similar to turbulent pipe flow in which the surface roughness may protrude into or through the viscous sublayer next to the wall and alter the flow in this thin, but very important, layer Values of the roughness, ε, for different materials can be obtained from part (2).

The drag coefficient diagram of Fig. 4.15 (boundary layer flow) shares many characteristics in common with the familiar Moody diagram (pipe flow) of part (2) , even though the mechanisms governing the flow are quite different. Fully developed horizontal pipe flow is governed by a balance between pressure forces and viscous forces. The fluid inertia remains constant throughout the flow. Boundary layer flow on a horizontal flat plate is governed by a balance between inertia effects and viscous forces. The pressure remains constant throughout the flow. (As is discussed in Section 4.2.6, for boundary layer flow on curved surfaces, the pressure is not constant.)

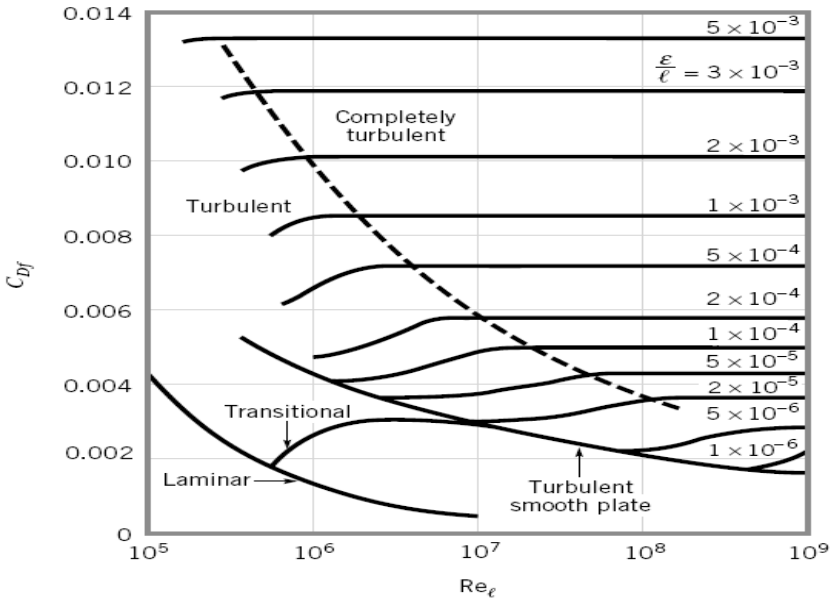

■ **FIGURE 4.15**
Friction drag coefficient for a flat plate parallel to the upstream flow (Ref. 18, with permission).

■ **TABLE 4.3**
Empirical Equations for the Flat Plate Drag Coefficient (Ref. 1)

Equation	Flow Conditions
$C_{Df} = 1.328/(\mathrm{Re}_\ell)^{0.5}$	Laminar flow
$C_{Df} = 0.455/(\log \mathrm{Re}_\ell)^{2.58} - 1700/\mathrm{Re}_\ell$	Transitional with $\mathrm{Re}_{xcr} = 5 \times 10^5$
$C_{Df} = 0.455/(\log \mathrm{Re}_\ell)^{2.58}$	Turbulent, smooth plate
$C_{Df} = [1.89 - 1.62 \log(\varepsilon/\ell)]^{-2.5}$	Completely turbulent

It is often convenient to have an equation for the drag coefficient as a function of the Reynolds number and relative roughness rather than the graphical representation given in Fig. 4.15. Although there is not one equation valid for the entire $\mathrm{Re}_\ell - \varepsilon/\ell$ range, the equations presented in Table 4.3 do work well for the conditions indicated.

Example 4.7:

The water ski shown in Fig. E4.7*a* moves through 70 °F water with a velocity U. Estimate the drag caused by the shear stress on the bottom of the ski for $0 < U < 30$ ft/s.

Solution

Clearly the ski is not a flat plate, and it is not aligned exactly parallel to the upstream flow. However, we can obtain a reasonable approximation to the shear force by using the flat plate results. That is, the friction drag, $\mathscr{D}_f$, caused by the shear stress on the bottom of the ski (the wall shear stress) can be determined as

$$\mathscr{D}_f = \tfrac{1}{2}\rho U^2 \ell b C_{Df}$$

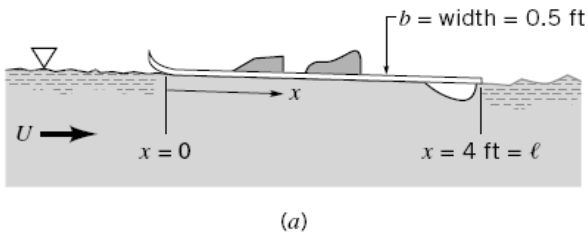

(*a*)

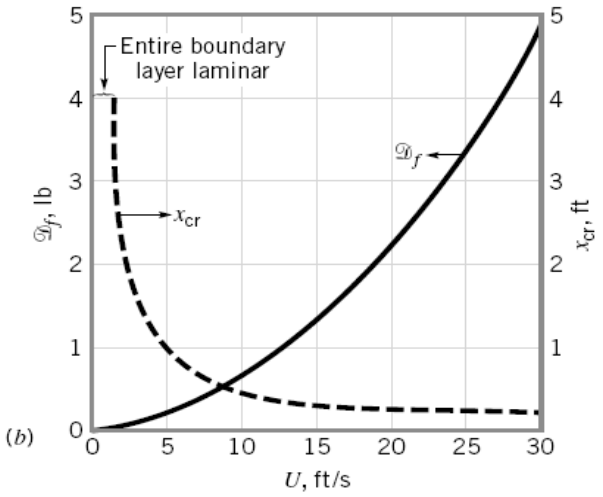

(*b*)

■ **FIGURE E 4.7**

With $A = \ell b = 4\text{ ft} \times 0.5\text{ ft} = 2\text{ ft}^2$, $\rho = 1.94\text{ slugs/ft}^3$, and $\mu = 2.04 \times 10^{-5}\text{ lb} \cdot \text{s/ft}^2$ we obtain

$$\mathcal{D}_f = \tfrac{1}{2}(1.94\text{ slugs/ft}^3)(2.0\text{ ft}^2)U^2 C_{Df} = 1.94\,U^2 C_{Df} \qquad (1)$$

where $\mathcal{D}_f$ and U are in pounds and ft/s, respectively.

The friction coefficient, C_{Df}, can be obtained from Fig. 4.15 or from the appropriate equations given in Table 4.3 . As we will see, for this problem, much of the flow lies within the transition regime where both the laminar and turbulent portions of the boundary layer flow occupy comparable lengths of the plate. We choose to use the values of C_{Df} from the table. For the given conditions we obtain

$$\text{Re}_\ell = \frac{\rho U \ell}{\mu} = \frac{(1.94\text{ slugs/ft}^3)(4\text{ ft})U}{2.04 \times 10^{-5}\text{ lb} \cdot \text{s/ft}^2} = 3.80 \times 10^5\,U$$

where U is in ft/s. With $U = 10$ ft/s, or $\text{Re}_\ell = 3.80 \times 10^6$, we obtain from Table 4.3 $C_{Df} = 0.455/(\log \text{Re}_\ell)^{2.58} - 1700/\text{Re}_\ell = 0.00308$. From Eq. 1 the corresponding drag is

$$\mathcal{D}_f = 1.94(10)^2(0.00308) = 0.598\text{ lb}$$

By covering the range of upstream velocities of interest we obtain the results shown in Fig. E4.7*b*.

If Re $\lesssim$ 1000, the results of boundary layer theory are not valid—inertia effects are not dominant enough and the boundary layer is not thin compared with the length of the plate. For our problem this corresponds to $U = 2.63 \times 10^{-3}$ ft/s. For all practical purposes U is greater than this value, and the flow past the ski is of the boundary layer type.

The approximate location of the transition from laminar to turbulent boundary layer flow as defined by $\text{Re}_{cr} = \rho U x_{cr}/\mu = 5 \times 10^5$ is indicated in Fig. E4.7*b*. Up to $U = 1.31$ ft/s the entire boundary layer is laminar. The fraction of the boundary layer that is laminar decreases as U increases until only the front 0.18 ft is laminar when $U = 30$ ft/s.

For anyone who has water skied, it is clear that it can require considerably more force to be pulled along at 30 ft/s than the 2×4.88 lb $= 9.76$ lb (two skis) indicated in Fig. E4.7*b*. As is discussed in Section 4.3 , the total drag on an object such as a water ski consists of more than just the friction drag. Other components, including pressure drag and wave-making drag, add considerably to the total resistance.

Example 4.8 :

A long, thin flat plate is placed parallel to a 20-ft/s stream of water at 20°C. At what distance x from the leading edge will the boundary-layer thickness be 1 in? Use any of these equations:

For Laminar flow: $\dfrac{\delta}{x} = \dfrac{5}{(Ux/\nu)^{1/2}}$ (1); For Turbulent flow: $\dfrac{\delta}{x} = \dfrac{0.16}{(Ux/\nu)^{1/7}}$ (2)

Solution

Since we do not know the Reynolds number, we must guess which of Eqs. (1) or (2) apply here.

for water, $\nu = 1.09 \times 10^{-5}\text{ ft}^2/\text{s}$; hence $\dfrac{U}{\nu} = \dfrac{20\text{ ft/s}}{1.09 \times 10^{-5}\text{ ft}^2/\text{s}} = 1.84 \times 10^6\text{ ft}^{-1}$

With $\delta = 1$ in $= \frac{1}{12}$ ft, try Eq. (1):

or $$x = \frac{\delta^2(U/\nu)}{5^2} = \frac{(\frac{1}{12}\text{ ft})^2(1.84 \times 10^6\text{ ft}^{-1})}{25} = 511\text{ ft}$$

Now we can test the Reynolds number to see whether the formula applied:

$$\text{Re}_x = \frac{Ux}{\nu} = \frac{(20\text{ ft/s})(511\text{ ft})}{1.09 \times 10^{-5}\text{ ft}^2/\text{s}} = 9.4 \times 10^8$$

This is impossible since the maximum Re_x for laminar flow past a flat plate is 3×10^6. So we

try again with Eq. (2)

$$\text{or} \qquad x = \left[\frac{\delta(U/\nu)^{1/7}}{0.16}\right]^{7/6} = \left[\frac{(\frac{1}{12}\text{ ft})(1.84 \times 10^6\text{ ft}^{-1})^{1/7}}{0.16}\right]^{7/6} = (4.09)^{7/6} = 5.17\text{ ft} \qquad \textit{Ans.}$$

Test $$\text{Re}_x = \frac{(20\text{ ft/s})(5.17\text{ ft})}{1.09 \times 10^{-5}\text{ ft}^2\text{/s}} = 9.5 \times 10^6$$

This is a perfectly proper turbulent-flow condition; hence we have found the correct position x on our second try.

Example 4.9 :

Are low-speed, small-scale air and water boundary layers really thin? Consider flow at $U = 1$ ft/s past a flat plate 1 ft long. Compute the boundary-layer thickness at the trailing edge for (*a*) air and (*b*) water at 20°C.

Solution

Part (a)

From Table, $\nu_{\text{air}} \approx 1.61$ E-4 ft^2/s. The trailing-edge Reynolds number thus is

$$\text{Re}_L = \frac{UL}{\nu} = \frac{(1\text{ ft/s})(1\text{ ft})}{1.61\text{ E-4 ft}^2\text{/s}} = 6200$$

Since this is less than 10^6, the flow is presumed laminar, and since it is greater than 2500, the boundary layer is reasonably thin. From exact solution, the predicted laminar thickness is

$$\frac{\delta}{x} \approx \frac{5.0}{\sqrt{6200}} = 0.0634$$

or, at $x = 1$ ft, $$\delta = 0.0634\text{ ft} \approx 0.76\text{ in} \qquad \textit{Ans. (a)}$$

Part (b)

From Table $\nu_{\text{water}} \approx 1.08$ E-5 ft^2/s. The trailing-edge Reynolds number is

$$\text{Re}_L = \frac{(1\text{ ft/s})(1\text{ ft})}{1.08\text{ E-5 ft}^2\text{/s}} \approx 92{,}600$$

This again satisfies the laminar and thinness conditions. The boundary-layer thickness is

$$\frac{\delta}{x} \approx \frac{5.0}{\sqrt{92{,}600}} = 0.0164$$

or, at $x = 1$ ft, $$\delta = 0.0164\text{ ft} \approx 0.20\text{ in} \qquad \textit{Ans. (b)}$$

Thus, even at such low velocities and short lengths, both airflows and water flows satisfy the boundary-layer approximations.

4.2.5.b Further Analysis of Turbulent Boundary Layer Flow :

There is no exact theory for turbulent flat-plate flow, although there are many elegant computer solutions of the boundary-layer equations using various empirical models for the turbulent eddy viscosity [9]. The most widely accepted result is simply an integal analysis similar to our study of the laminar-profile approximation Sec. (4.2.3).

We begin with Eq. (4.26), which is valid for laminar or turbulent flow. We write it here for convenient reference:

$$\tau_w(x) = \rho U^2 \frac{d\theta}{dx} \qquad (4.26)$$

From the definition of c_f, this can be rewritten as

$$c_f = 2\frac{d\theta}{dx} \qquad (4.34)$$

Now recall from Fig.4.14 that the turbulent profiles are nowhere near parabolic. From Fig.2.13 (part 2), we see that flat-plate flow is very nearly logarithmic, with a slight outer wake and a thin viscous sublayer. Therefore, just as in turbulent pipe flow, we assume that the logarithmic law (2.87) holds all the way across the boundary layer

$$\frac{u}{u^*} \approx \frac{1}{\kappa}\ln\frac{yu^*}{\nu} + B \qquad u^* = \left(\frac{\tau_w}{\rho}\right)^{1/2} \qquad (4.35)$$

with, as usual, $\kappa = 0.41$ and $B = 5.0$. At the outer edge of the boundary layer, $y = \delta$ and $u = U$, and Eq. (4.35) becomes

$$\frac{U}{u^*} = \frac{1}{\kappa} \ln \frac{\delta u^*}{\nu} + B \tag{4.36}$$

But the definition of the skin-friction coefficient, is such that the following identities hold:

$$\frac{U}{u^*} \equiv \left(\frac{2}{c_f}\right)^{1/2} \qquad \frac{\delta u^*}{\nu} \equiv \mathrm{Re}_\delta \left(\frac{c_f}{2}\right)^{1/2} \tag{4.37}$$

Therefore Eq. (4.36) is a *skin-friction law* for turbulent flat-plate flow

$$\left(\frac{2}{c_f}\right)^{1/2} \approx 2.44 \ln \left[\mathrm{Re}_\delta \left(\frac{c_f}{2}\right)^{1/2}\right] + 5.0 \tag{4.38}$$

It is a complicated law, but we can at least solve for a few values and list them:

Re_δ	10^4	10^5	10^6	10^7
c_f	0.00493	0.00315	0.00217	0.00158

Following a suggestion of Prandtl, we can forget the complex log friction law (4.38) and simply fit the numbers in the table to a power-law approximation

$$c_f \approx 0.02 \, \mathrm{Re}_\delta^{-1/6} \tag{4.39}$$

This we shall use as the left-hand side of Eq. (4.34). For the right-hand side, we need an estimate for $\theta(x)$ in terms of $\delta(x)$. If we use the logarithmic-law profile (4.35), we shall be up to our hips in logarithmic integrations for the momentum thickness. Instead we follow another suggestion of Prandtl, who pointed out that the turbulent profiles in Fig.4.14 can be approximated by a one-seventh-power law

$$\left(\frac{u}{U}\right)_{\text{turb}} \approx \left(\frac{y}{\delta}\right)^{1/7} \tag{4.40}$$

This is shown as a dashed line in Fig.4.14. It is an excellent fit to the low-Reynolds-number turbulent data, which were all that were available to Prandtl at the time. With this simple approximation, the momentum thickness can easily be evaluated:

$$\theta \approx \int_0^\delta \left(\frac{y}{\delta}\right)^{1/7} \left[1 - \left(\frac{y}{\delta}\right)^{1/7}\right] dy = \frac{7}{72} \delta \tag{4.41}$$

We accept this result and substitute Eqs. (4.39) and (4.41) into Kármán's momentum law (4.34)

$$c_f = 0.02 \, \mathrm{Re}_\delta^{-1/6} = 2 \frac{d}{dx}\left(\frac{7}{72} \delta\right)$$

or

$$\mathrm{Re}_\delta^{-1/6} = 9.72 \frac{d\delta}{dx} = 9.72 \frac{d(\mathrm{Re}\delta)}{d(\mathrm{Re}_x)} \tag{4.42}$$

Separate the variables and integrate, assuming $\delta = 0$ at $x = 0$:

$$\mathrm{Re}_\delta \approx 0.16 \, \mathrm{Re}_x^{6/7} \qquad \text{or} \qquad \frac{\delta}{x} \approx \frac{0.16}{\mathrm{Re}_x^{1/7}} \tag{4.43}$$

Thus the thickness of a turbulent boundary layer increases as $x^{6/7}$, far more rapidly than the laminar increase $x^{1/2}$. Equation (4.43) is the solution to the problem, because all other parameters are now available. For example, combining Eqs. (4.43) and (4.39), we obtain the friction variation

$$c_f \approx \frac{0.027}{\mathrm{Re}_x^{1/7}} \tag{4.44}$$

Writing this out in dimensional form, we have

$$\tau_{w,\text{turb}} \approx \frac{0.0135 \mu^{1/7} \rho^{6/7} U^{13/7}}{x^{1/7}} \tag{4.45}$$

Turbulent plate friction drops slowly with x, increases nearly as ρ and U^2, and is rather insensitive to viscosity.

We can evaluate the drag coefficient from Eq. (4.33)

$$C_D = \frac{0.031}{\mathrm{Re}_L^{1/7}} = \frac{7}{6} c_f(L) \tag{4.46}$$

Then C_D is only 16 percent greater than the trailing-edge skin friction [compare with for laminar flow where $C_D = 2\, C_f(L)$].

The displacement thickness can be estimated from the one-seventh-power law:

$$\delta^* \approx \int_0^\delta \left[1 - \left(\frac{y}{\delta}\right)^{1/7}\right] dy = \frac{1}{8}\,\delta \tag{4.47}$$

The turbulent flat-plate shape factor is approximately

$$H = \frac{\delta^*}{\theta} = \frac{\frac{1}{8}}{\frac{7}{72}} = 1.3 \tag{4.48}$$

These are the basic results of turbulent flat-plate theory.

Recall that for laminar flow, the drag cofficient $C_D = 1.328 / (\mathrm{Re}_L)^{0.5}$ for smooth wall

Figure 4.16 shows flat-plate drag coefficients for both laminar-and turbulent-flow conditions. The above smooth-wall relations and (4.46) are shown, along with the effect of wall roughness, which is quite strong. The proper roughness parameter here is x/ϵ or L/ϵ, by analogy with the pipe parameter ϵ/d. In the fully rough regime, C_D is independent of the Reynolds number, so that the drag varies exactly as U^2 and is inde-

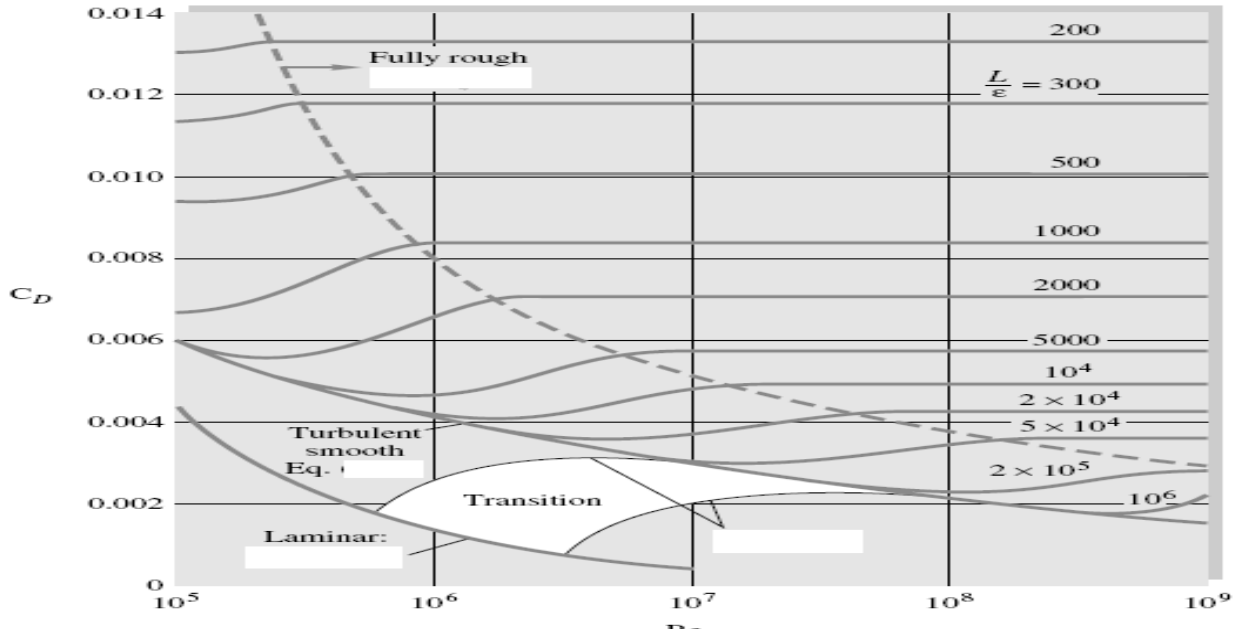

Fig.4.16 Drag coefficient of laminar and turbulent boundary layers on smooth and rough flat plates. This chart is the flat-plate analog of the Moody diagram **for pipe flow**

pendent of μ. Reference 2 presents a theory of rough flat-plate flow, and Ref. 1 gives a curve fit for skin friction and drag in the fully rough regime:

$$c_f \approx \left(2.87 + 1.58 \log \frac{x}{\epsilon}\right)^{-2.5} \tag{4.49a}$$

$$C_D \approx \left(1.89 + 1.62 \log \frac{L}{\epsilon}\right)^{-2.5} \tag{4.49b}$$

Equation (4.49b) is plotted to the right of the dashed line in Fig.4.16. The figure also shows the behavior of the drag coefficient in the transition region $5 \times 10^5 < \mathrm{Re}_L < 8 \times 10^7$, where the laminar drag at the leading edge is an appreciable fraction of the total drag. Schlichting [1] suggests the following curve fits for these transition drag curves depending upon the Reynolds number Re_{trans} where transition begins:

$$C_D \approx \begin{cases} \dfrac{0.031}{\mathrm{Re}_L^{1/7}} - \dfrac{1440}{\mathrm{Re}_L} & \mathrm{Re}_{\mathrm{trans}} = 5 \times 10^5 \quad (4.50a) \\ \dfrac{0.031}{\mathrm{Re}_L^{1/7}} - \dfrac{8700}{\mathrm{Re}_L} & \mathrm{Re}_{\mathrm{trans}} = 3 \times 10^6 \quad (4.50b) \end{cases}$$

Example 4.10 :

A hydrofoil 1.2 ft long and 6 ft wide is placed in a water flow of 40 ft/s, with $\rho = 1.99$ slugs/ft^3 and $\nu = 0.000011$ ft^2/s. (*a*) Estimate the boundary-layer thickness at the end of the plate. Estimate the friction drag for (*b*) turbulent smooth-wall flow from the leading edge, (*c*) laminar turbulent flow with $\mathrm{Re}_{\mathrm{trans}} = 5 \times 10^5$, and (*d*) turbulent rough-wall flow with $\epsilon = 0.0004$ ft.

Solution

Part (a)

The Reynolds number is $\mathrm{Re}_L = \dfrac{UL}{\nu} = \dfrac{(40 \text{ ft/s})(1.2 \text{ ft})}{0.000011 \text{ ft}^2/\text{s}} = 4.36 \times 10^6$

Thus the trailing-edge flow is certainly turbulent. The maximum boundary-layer thickness would occur for turbulent flow starting at the leading edge. From Eq. (4.43),

$$\frac{\delta(L)}{L} = \frac{0.16}{(4.36 \times 10^6)^{1/7}} = 0.018$$

or $$\delta = 0.018(1.2 \text{ ft}) = 0.0216 \text{ ft} \qquad \textit{Ans. (a)}$$

This is 7.5 times thicker than a fully laminar boundary layer at the same Reynolds number.

Part (b)

For fully turbulent smooth-wall flow, the drag coefficient on one side of the plate is, from Eq. (4.46),

$$C_D = \frac{0.031}{(4.36 \times 10^6)^{1/7}} = 0.00349$$

Then the drag on both sides of the foil is approximately

$$D = 2C_D(\tfrac{1}{2}\rho U^2)bL = 2(0.00349)(\tfrac{1}{2})(1.99)(40)^2(6.0)(1.2) = 80 \text{ lb}$$

Part (c)

With a laminar leading edge and $\mathrm{Re}_{\mathrm{trans}} = 5 \times 10^5$, Eq. (4.50*a*) applies:

$$C_D = 0.00349 - \frac{1440}{4.36 \times 10^6} = 0.00316$$

The drag can be recomputed for this lower drag coefficient:

$$D = 2C_D(\tfrac{1}{2}\rho U^2)bL = 72 \text{ lbf} \qquad \textit{Ans. (c)}$$

Part (d)

Finally, for the rough wall, we calculate $\dfrac{L}{\epsilon} = \dfrac{1.2 \text{ ft}}{0.0004 \text{ ft}} = 3000$

From Fig. 4.16 at $\mathrm{Re}_L = 4.36 \times 10^6$, this condition is just inside the fully rough regime. Equation (4.49*b*) applies:

$$C_D = (1.89 + 1.62 \log 3000)^{-2.5} = 0.00644$$

and the drag estimate is

$$D = 2C_D(\tfrac{1}{2}\rho U^2)bL = 148 \text{ lbf} \qquad \textit{Ans. (d)}$$

This small roughness nearly doubles the drag. It is probable that the total hydrofoil drag is still another factor of 2 larger because of trailing-edge flow-separation effects.

4.2.6 Effects of Pressure Gradient

The boundary layer discussions in the previous parts of Section 4.2 have dealt with flow along a flat plate in which the pressure is constant throughout the fluid. In general, when a fluid flows past an object other than a flat plate, the pressure field is not uniform. As shown in Fig. 4.6 , if the Reynolds number is large, relatively thin boundary layers will develop along the surfaces. Within these layers the component of the pressure gradient in the streamwise direction (i.e., along the body surface) is not zero, although the pressure gradient normal to the surface is negligibly small. That is, if we were to measure the pressure while moving across the boundary layer from the body to the boundary layer edge, we would find that the pressure is essentially constant. However, the pressure does vary in the direction along the body surface if the body is curved. The variation in the *free-stream velocity*, U_{fs}, the fluid velocity at the edge of the boundary layer, is the cause of the pressure gradient in the boundary layer. The characteristics of the entire flow (both within and outside of the boundary layer) are often highly dependent on the pressure gradient effects on the fluid within the boundary layer.

For a flat plate parallel to the upstream flow, the upstream velocity (that far ahead of the plate) and the free-stream velocity (that at the edge of the boundary layer) are equal—$U = U_{fs}$. This is a consequence of the negligible thickness of the plate. For bodies of nonzero thickness, these two velocities are different. This can be seen in the flow past a circular cylinder of diameter D. The upstream velocity and pressure are U and p_0, respectively. If the fluid were completely inviscid ($\mu = 0$), the Reynolds number would be infinite ($\text{Re} = \rho UD/\mu = \infty$) and the streamlines would be symmetrical, as are shown in Fig. 4.17*a*. The fluid velocity along the surface would vary from $U_{fs} = 0$ at the very front and rear of the cylinder (points A and F are stagnation points) to a maximum of $U_{fs} = 2U$ at the top and bottom of the cylinder (point C). The pressure on the surface of the cylinder would be symmetrical about the vertical midplane of the cylinder, reaching a maximum value of $p_0 + \rho U^2/2$ (the stagnation pressure) at both the front and back of the cylinder, and a minimum of $p_0 - 3\rho U^2/2$ at the top and bottom of the cylinder. The pressure and free-stream velocity distributions are shown in Figs. 4.17 *b* and 4.17 *c*. These characteristics can be obtained from potential flow analysis of Sections of part (3).

Because of the absence of viscosity (therefore, $\tau_w = 0$) and the symmetry of the pressure distribution for inviscid flow past a circular cylinder, it is clear that the drag on the cylinder is zero. Although it is not obvious, it can be shown that the drag is zero for any object that does not produce a lift (symmetrical or not) in an inviscid fluid (Ref. 4). Based on experimental evidence, however, we know that there must be a net drag. Clearly, since there is no purely inviscid fluid, the reason for the observed drag must lie on the shoulders of the viscous effects.

To test this hypothesis, we could conduct an experiment by measuring the drag on an object (such as a circular cylinder) in a series of fluids with decreasing values of viscosity. To our initial surprise we would find that no matter how small we make the viscosity (provided it is not precisely zero) we would measure a finite drag, essentially independent of the value of μ. As was noted in part (3) , this leads to what has been termed *d'Alembert's paradox*—the drag on an object in an inviscid fluid is zero, but the drag on an object in a fluid with vanishingly small (but nonzero) viscosity is not zero.

The reason for the above paradox can be described in terms of the effect of the pressure gradient on boundary layer flow. Consider large Reynolds number flow of a real (viscous) fluid past a circular cylinder. As was discussed in Section 4.1.2 , we expect the viscous effects to be confined to thin boundary layers near the surface. This allows the fluid to stick

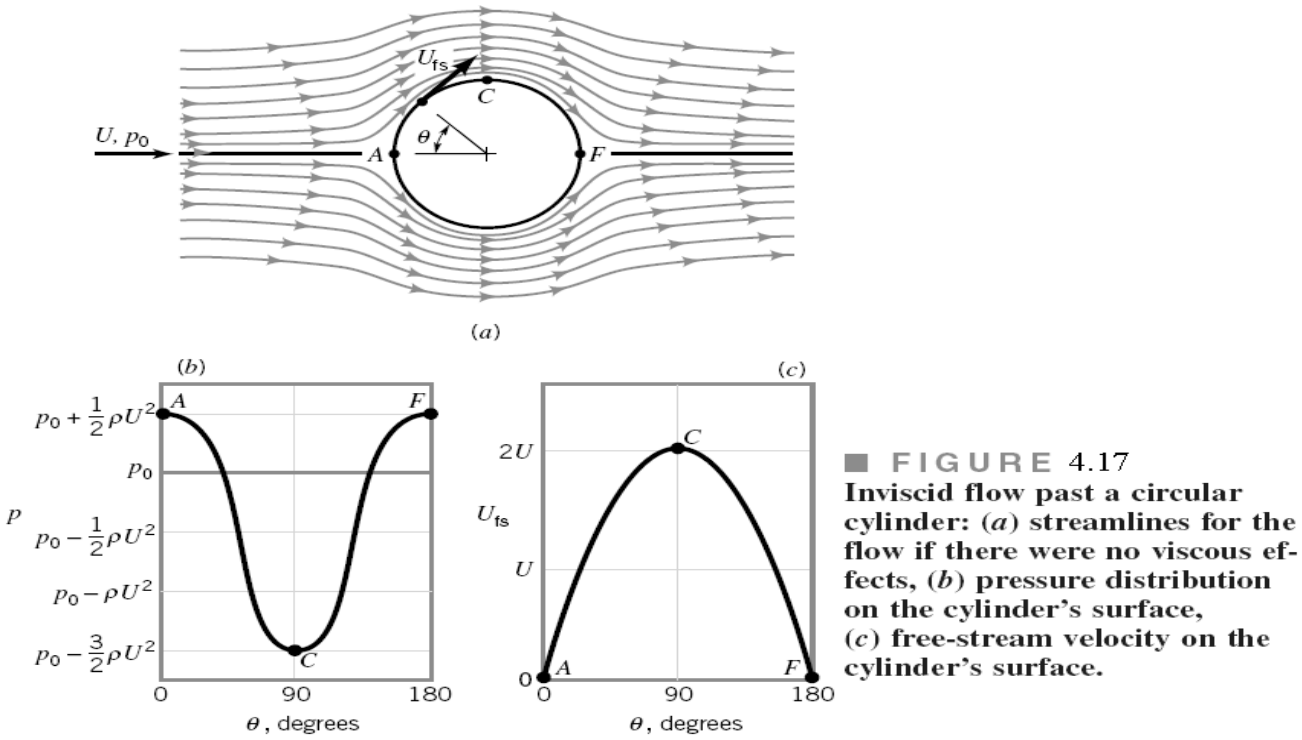

■ **FIGURE 4.17**
Inviscid flow past a circular cylinder: (*a*) streamlines for the flow if there were no viscous effects, (*b*) pressure distribution on the cylinder's surface, (*c*) free-stream velocity on the cylinder's surface.

($\mathbf{V} = 0$) to the surface—a necessary condition for any fluid, provided $\mu \neq 0$. The basic idea of boundary layer theory is that the boundary layer is thin enough so that it does not greatly disturb the flow outside the boundary layer. Based on this reasoning, for large Reynolds numbers the flow throughout most of the flow field would be expected to be as is indicated in Fig. 4.17 *a*, the inviscid flow field.

The pressure distribution indicated in Fig. 4.17*b* is imposed on the boundary layer flow along the surface of the cylinder. In fact, there is negligible pressure variation across the thin boundary layer so that the pressure within the boundary layer is that given by the inviscid flow field. This pressure distribution along the cylinder is such that the stationary fluid at the nose of the cylinder ($U_{fs} = 0$ at $\theta = 0$) is accelerated to its maximum velocity ($U_{fs} = 2U$ at $\theta = 90°$) and then is decelerated back to zero velocity at the rear of the cylinder ($U_{fs} = 0$ at $\theta = 180°$). This is accomplished by a balance between pressure and inertia effects; viscous effects are absent for the inviscid flow outside the boundary layer.

Physically, in the absence of viscous effects, a fluid particle traveling from the front to the back of the cylinder coasts down the "pressure hill" from $\theta = 0$ to $\theta = 90°$ (from point *A* to *C* in Fig. 4.17*b*) and then back up the hill to $\theta = 180°$ (from point *C* to *F*) without any loss of energy. There is an exchange between kinetic and pressure energy, but there are no energy losses. The same pressure distribution is imposed on the viscous fluid within the boundary layer. The decrease in pressure in the direction of flow along the front half of the cylinder is termed a *favorable pressure gradient*. The increase in pressure in the direction of flow along the rear half of the cylinder is termed an *adverse pressure gradient.*

Consider a fluid particle within the boundary layer indicated in Fig.4.18 . In its attempt to flow from *A* to *F* it experiences the same pressure distribution as the particles in the free stream immediately outside the boundary layer—the inviscid flow field pressure. However, because of the viscous effects involved, the particle in the boundary layer experiences a loss of energy as it flows along. This loss means that the particle does not have enough energy to coast all of the way up the pressure hill (from *C* to *F*) and to reach point *F* at the rear of the cylinder. This kinetic energy deficit is seen in the velocity profile detail at point *C*, shown in Fig. 4.18 *a*. Because of friction, the boundary layer fluid cannot travel from the front to the rear of the cylinder. (This conclusion can also be obtained from the concept that due to viscous effects the particle at *C* does not have enough momentum to allow it to coast up the pressure hill to *F*.)

The situation is similar to a bicyclist coasting down a hill and up the other side of the valley. If there were no friction the rider starting with zero speed could reach the same height from which he or she started. Clearly friction (rolling resistance, aerodynamic drag, etc.) causes a loss of energy (and momentum), making it impossible for the rider to reach the height from which he or she started without supplying additional energy (i.e., peddling). The fluid within the boundary layer does not have such an energy supply. Thus, the fluid flows against the increasing pressure as far as it can, at which point the boundary layer separates from (lifts off) the surface. This *boundary layer separation* is indicated in Fig. 4.18 *a*. Typical velocity profiles at representative locations along the surface are shown in Fig 4.18 *b*. At the separation location (profile *D*), the velocity gradient at the wall and the wall shear stres are zero. Beyond that location (from *D* to *E*) there is reverse flow in the boundary layer.

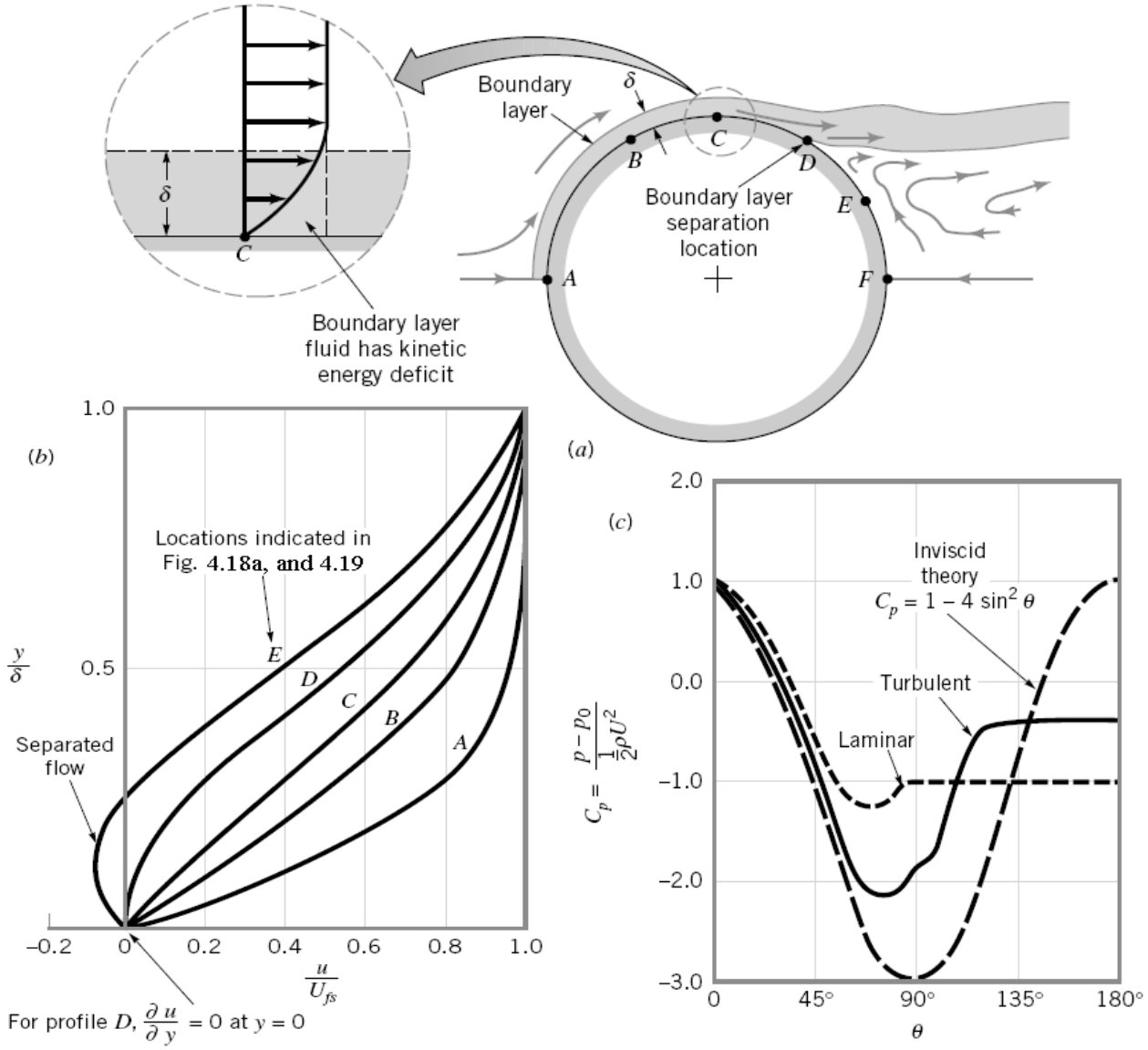

■ **FIGURE** 4.18 **Boundary layer characteristics on a circular cylinder: (*a*) boundary layer separation location, (*b*) typical boundary layer velocity profiles at various locations on the cylinder, (*c*) surface pressure distributions for inviscid flow and boundary layer flow.**

As is indicated in Fig. 4.18 *c*, because of the boundary layer separation, the average pressure on the rear half of the cylinder is considerably less than that on the front half. Thus, a large pressure drag is developed, even though (because of small viscosity) the viscous shear drag may be quite small. D'Alembert's paradox is explained. No matter how small the viscosity, provided it is not zero, there will be a boundary layer that separates from the surface, giving a drag that is, for the most part, independent of the value of μ.

The location of separation, the width of the wake region behind the object, and the pressure distribution on the surface depend on the nature of the boundary layer flow. Compared with a laminar boundary layer, a turbulent boundary layer flow has more kinetic energy and momentum associated with it because: (1) as is indicated in Fig. E4.6, the velocity profile is fuller, more nearly like the ideal uniform profile, and (2) there can be considerable energy associated with the swirling, random components of the velocity that do not appear in the time-averaged x component of velocity. Thus, as is indicated in Fig. 4.18*c*, the turbulent boundary layer can flow farther around the cylinder (farther up the pressure hill) before it separates than can the laminar boundary layer.

The structure of the flow field past a circular cylinder is completely different for a zero viscosity fluid than it is for a viscous fluid, no matter how small the viscosity is, provided it is not zero. This is due to boundary layer separation. Similar concepts hold for other shaped bodies as well. The flow past an airfoil at zero *angle of attack* (the angle between the upstream flow and the axis of the object) is shown in Fig. 4.19 *a*; flow past the same airfoil at a 5° angle of attack is shown in Fig. 4.19 *b*. Over the front portion of the airfoil the pressure decreases in the direction of flow—a favorable pressure gradient. Over the rear portion the pressure increases in the direction of flow—an adverse pressure gradient. The boundary layer velocity profiles at representative locations are similar to those indicated in Fig. 4.18 *b* for flow past a circular cylinder. If the adverse pressure gradient is not too great (because the body is not too "thick" in some sense), the boundary layer fluid can flow into the slightly increasing pressure region (i.e., from *C* to the trailing edge in Fig. 4.19 *a*) without separating from the surface. However, if the pressure gradient is too adverse (because the angle of attack is too large), the boundary layer will separate from the surface as indicated in Fig. 4.19 *b*. Such situations can lead to the catastrophic loss of lift called *stall*, which is discussed in Section 4.4.

Streamlined bodies are generally those designed to eliminate (or at least to reduce) the effects of separation, whereas nonstreamlined bodies generally have relatively large drag due to the low pressure in the separated regions (the wake). Although the boundary layer may be quite thin, it can appreciably alter the entire flow field because of boundary layer separation. These ideas are discussed in Section 4.3.

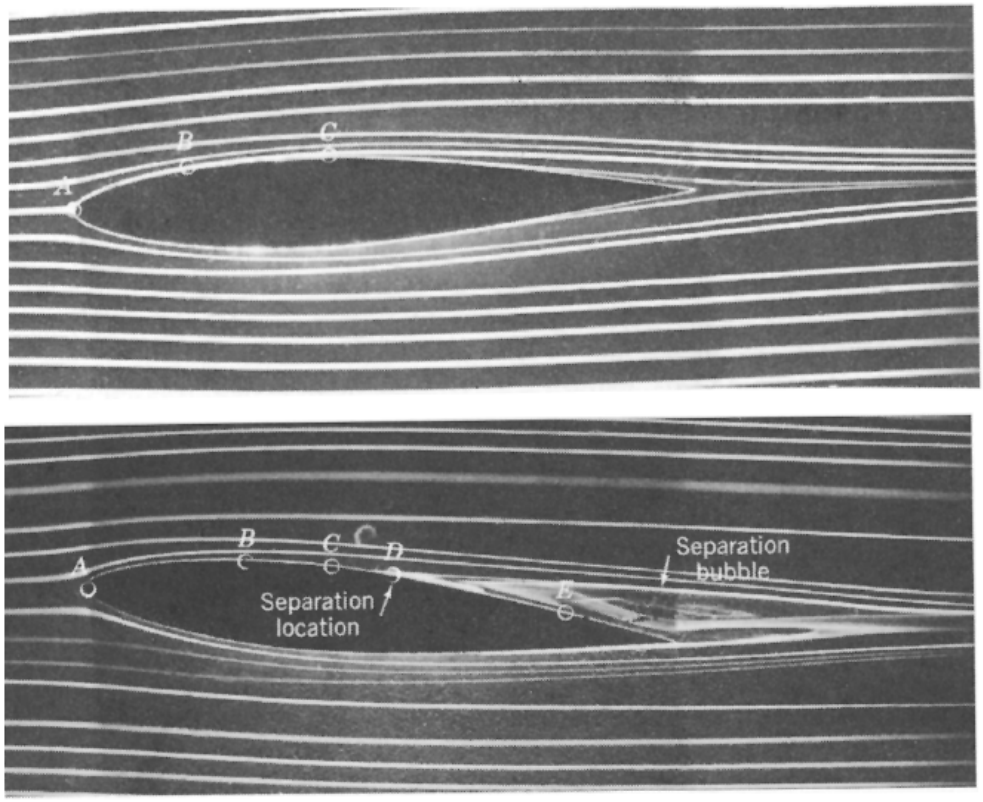

(*a*)

(*b*)

■ FIGURE 4.19 **Flow visualization photographs of flow past an airfoil (the boundary layer velocity profiles for the points indicated are similar to those indicated in Fig. 4.18 *b*): (*a*) zero angle of attack, no separation, (*b*) 5° angle of attack, flow separation. Dye in water. (Photograph courtesy of ONERA, France.)**

4.2.7 Boundary Layers with Non-zero Pressure Gradient:

The flat-plate analysis of the previous section should give us a good feeling for the behavior of both laminar and turbulent boundary layers, except for one important effect: flow separation. Prandtl showed that separation like that in Fig.4.18a is caused by excessive momentum loss near the wall in a boundary layer trying to move downstream against increasing pressure, $dp/dx > 0$, which is called an *adverse pressure gradient*. The opposite case of decreasing pressure, $dp/dx < 0$, is called a *favorable gradient,* where flow separation can never occur. In a typical immersed-body flow, e.g., Fig.4.18a, the favorable gradient is on the front of the body and the adverse gradient is in the rear, as discussed in detail in Part (3) .

We can explain flow separation with a geometric argument about the second derivative of velocity u at the wall. From the momentum equation (4.5) at the wall, where $u = v = 0$, we obtain

$$\left.\frac{\partial \tau}{\partial y}\right|_{\text{wall}} = \mu \left.\frac{\partial^2 u}{\partial y^2}\right|_{\text{wall}} = -\rho U \frac{dU}{dx} = \frac{dp}{dx}$$

or

$$\left.\frac{\partial^2 u}{\partial y^2}\right|_{\text{wall}} = \frac{1}{\mu}\frac{dp}{dx} \qquad (4.51)$$

for either laminar or turbulent flow. Thus in an adverse gradient the second derivative of velocity is positive at the wall; yet it must be negative at the outer layer ($y = \delta$) to merge smoothly with the mainstream flow $U(x)$. It follows that the second derivative must pass through zero somewhere in between, at a point of inflection, and any boundary-layer profile in an adverse gradient must exhibit a characteristic S shape.

Figure 4.20 illustrates the general case. In a favorable gradient (Fig.4.20*a*) the profile

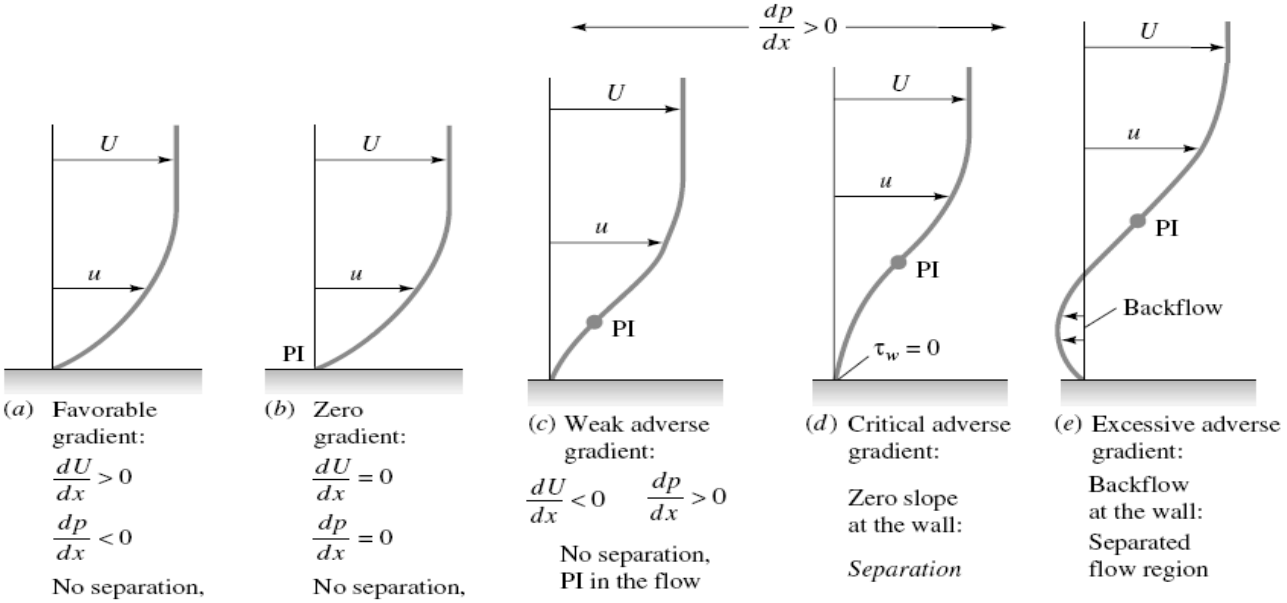

Fig.4.20 Effect of pressure gradient on boundary-layer profiles; PI = point of inflection.

is very rounded, there is no point of inflection, there can be no separation, and laminar profiles of this type are very resistant to a transition to turbulence [1 to 3].

In a zero pressure gradient (Fig.4.20*b*), e.g., flat-plate flow, the point of inflection is at the wall itself. There can be no separation, and the flow will undergo transition at Re_x no greater than about 3×10^6, as discussed earlier.

In an adverse gradient (Fig.4.20*c* to *e*), a point of inflection (PI) occurs in the boundary layer, its distance from the wall increasing with the strength of the adverse gradient. For a weak gradient (Fig.4.20*c*) the flow does not actually separate, but it is vulnerable to transition to turbulence at Re_x as low as 10^5 [1, 2]. At a moderate gradient, a critical condition (Fig.4.20*d*) is reached where the wall shear is exactly zero ($\partial u/\partial y = 0$). This is defined as the *separation point* ($\tau_w = 0$), because any stronger gradient will actually cause backflow at the wall (Fig.4.20*e*): the boundary layer thickens greatly, and the main flow breaks away, or separates, from the wall (Fig.4.17a).

The flow profiles of Fig. 4.20 usually occur in sequence as the boundary layer progresses along the wall of a body. For example, in Fig.4.17*a*, a favorable gradient occurs on the front of the body, zero pressure gradient occurs just upstream of the shoulder, and an adverse gradient occurs successively as we move around the rear of the body.

A second practical example is the flow in a duct consisting of a nozzle, throat, and diffuser, as in Fig.4.21. The nozzle flow is a favorable gradient and never separates, nor

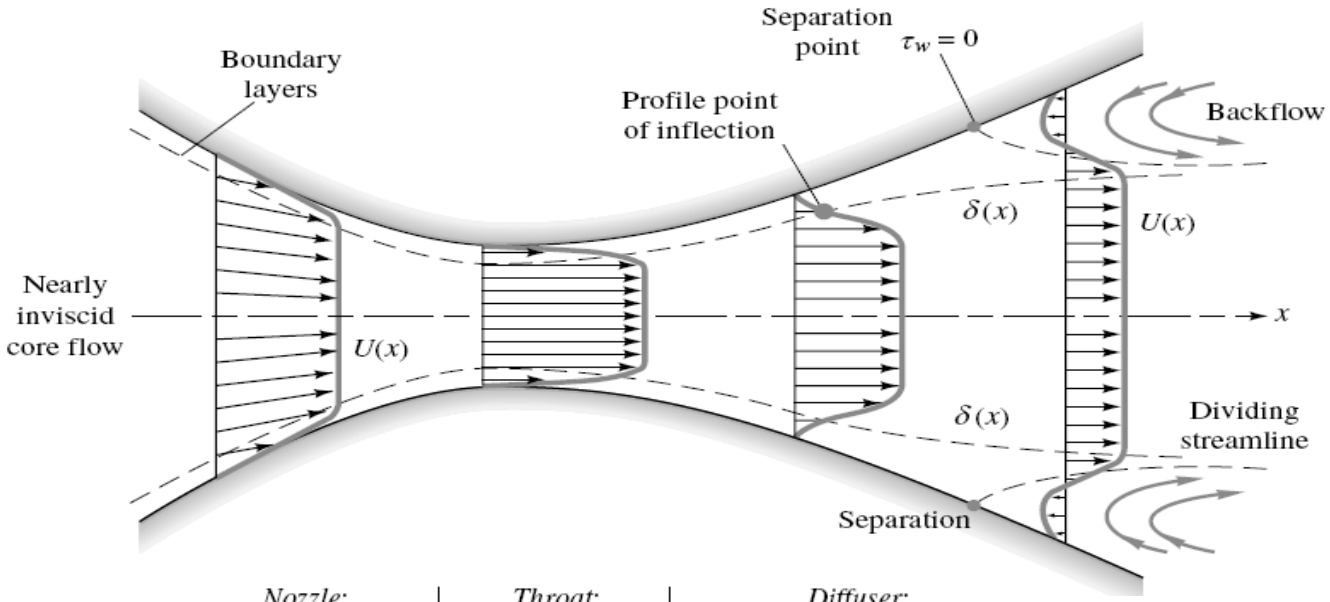

Nozzle:	*Throat*:	*Diffuser*:
Decreasing pressure and area	Constant pressure and area	Increasing pressure and area
Increasing velocity	Velocity constant	Decreasing velocity
Favorable gradient	Zero gradient	Adverse gradient (boundary layer thickens)

Fig.4.21 Boundary-layer growth and separation in a nozzle-diffuser configuration.

does the throat flow where the pressure gradient is approximately zero. But the expanding-area diffuser produces low velocity and increasing pressure, an adverse gradient. If the diffuser angle is too large, the adverse gradient is excessive, and the boundary layer will separate at one or both walls, with backflow, increased losses, and poor pressure recovery. In the diffuser literature [10] this condition is called *diffuser stall,* a term used also in airfoil aerodynamics (Sec. 4.3) to denote airfoil boundary-layer separation. Thus the boundary-layer behavior explains why a large-angle diffuser has heavy flow losses and poor performance .

Presently boundary-layer theory can compute only up to the separation point, after which it is invalid. New techniques are now developed for analyzing the strong interaction effects caused by separated flows [5, 6].

The Laminar Integral Theory:

Both laminar and turbulent theories can be developed from Kármán's general two-dimensional boundary-layer integral relation [7], which extends Eq. (4.34) to variable $U(x)$

$$\frac{\tau_w}{\rho U^2} = \frac{1}{2} c_f = \frac{d\theta}{dx} + (2 + H) \frac{\theta}{U} \frac{dU}{dx} \tag{4.52}$$

where $\theta(x)$ is the momentum thickness and $H(x) = \delta^*(x)/\theta(x)$ is the shape factor. From Eq. (4.51) negative dU/dx is equivalent to positive dp/dx, that is, an adverse gradient.

We can integrate Eq. (4.52) to determine $\theta(x)$ for a given $U(x)$ if we correlate c_f and H with the momentum thickness. This has been done by examining typical velocity profiles of laminar and turbulent boundary-layer flows for various pressure gradients. Some examples are given in Fig.4.22, showing that the shape factor H is a good indicator of the pressure gradient. The higher the H, the stronger the adverse gradient, and separation occurs approximately at

$$H \approx \begin{cases} 3.5 & \text{laminar flow} \\ 2.4 & \text{turbulent flow} \end{cases} \tag{4.53}$$

The laminar profiles (Fig.4.22*a*) clearly exhibit the S shape and a point of inflection with an adverse gradient. But in the turbulent profiles (Fig.4.22*b*) the points of inflection are typically buried deep within the thin viscous sublayer, which can hardly be seen on the scale of the figure.

There are scores of turbulent theories in the literature, but they are all complicated algebraically and will be omitted here. The reader is referred to advanced texts [1, 2, 9].

For laminar flow, a simple and effective method was developed by Thwaites [11], who found that Eq. (4.52) can be correlated by a single dimensionless momentum-thickness variable λ, defined as

$$\lambda = \frac{\theta^2}{\nu} \frac{dU}{dx} \tag{4.54}$$

Using a straight-line fit to his correlation, Thwaites was able to integrate Eq. (4.52) in closed form, with the result

$$\theta^2 = \theta_0^2 \left(\frac{U_0}{U}\right)^6 + \frac{0.45\nu}{U^6} \int_0^x U^5 \, dx \tag{4.55}$$

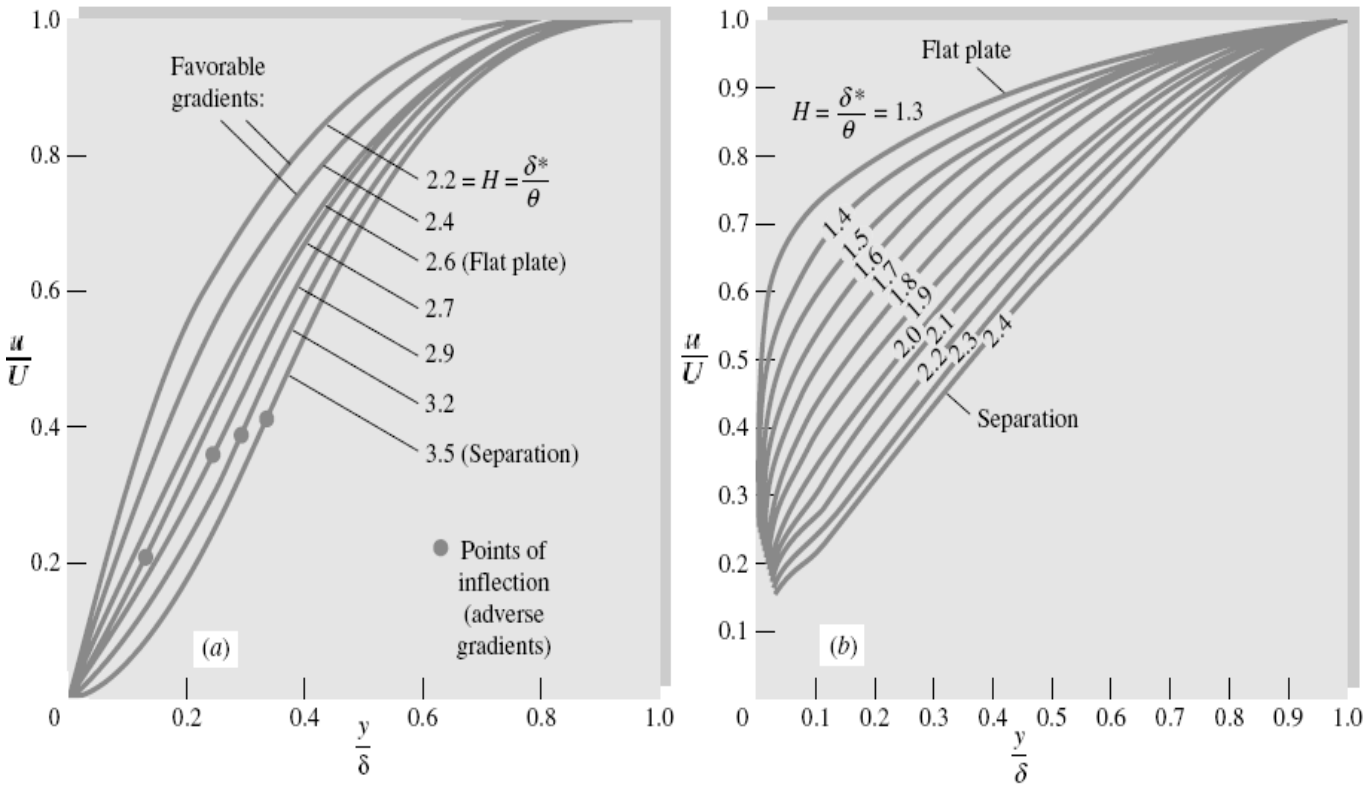

Fig. 4.22 Velocity profiles with pressure gradient: (*a*) laminar flow; (*b*) turbulent flow with adverse gradients.

where θ_0 is the momentum thickness at $x = 0$ (usually taken to be zero). Separation ($c_f = 0$) was found to occur at a particular value of λ

Separation: $$\lambda = -0.09 \tag{4.56}$$

Finally, Thwaites correlated values of the dimensionless shear stress $S = \tau_w\theta/(\mu U)$ with λ, and his graphed result can be curve-fitted as follows:

$$S(\lambda) = \frac{\tau_w\theta}{\mu U} \approx (\lambda + 0.09)^{0.62} \tag{4.57}$$

This parameter is related to the skin friction by the identity

$$S \equiv \tfrac{1}{2}c_f \operatorname{Re}_\theta \tag{4.58}$$

Equations (4.55) to (4.57) constitute a complete theory for the laminar boundary layer with variable $U(x)$, with an accuracy of ± 10 percent compared with exact digital-computer solutions of the laminar-boundary-layer equations. Complete details of Thwaites' and other laminar theories are given in Refs. 2 and 3.

As a demonstration of Thwaites' method, take a flat plate, where U = constant, $\lambda = 0$, and $\theta_0 = 0$. Equation (4.55) integrates to $$\theta^2 = \frac{0.45\nu x}{U}$$

or $$\frac{\theta}{x} = \frac{0.671}{\operatorname{Re}_x^{1/2}} \tag{4.59}$$ 8)

This is within 1 percent of Blasius' exact solution.

With $\lambda = 0$, Eq. (4.57) predicts the flat-plate shear to be

$$\frac{\tau_w\theta}{\mu U} = (0.09)^{0.62} = 0.225$$

or $$c_f = \frac{2\tau_w}{\rho U^2} = \frac{0.671}{\operatorname{Re}_x^{1/2}} \tag{4.60}$$

This is also within 1 percent of the Blasius result, . However, the general accuracy of this method is poorer than 1 percent because Thwaites actually "tuned" his correlation constants to make them agree with exact flat-plate theory.

We shall not compute any more boundary-layer details here, but as we go along, investigating various immersed-body flows, especially in Chap. 8, we shall use Thwaites' method to make qualitative assessments of the boundary-layer behavior.

Example 4.11 :

In 1938 Howarth proposed a linearly decelerating external-velocity distribution

$$U(x) = U_0\left(1 - \frac{x}{L}\right) \tag{1}$$

as a theoretical model for laminar-boundary-layer study. (*a*) Use Thwaites' method to compute the separation point x_{sep} for $\theta_0 = 0$, and compare with the exact digital-computer solution $x_{sep}/L = 0.119863$ given by H. Wipperman in 1966. (*b*) Also compute the value of $c_f = 2\tau_w/(\rho U^2)$ at $x/L = 0.1$.

Solution

Part (a)

First note that $dU/dx = -U_0/L$ = constant: Velocity decreases, pressure increases, and the pressure gradient is adverse throughout. Now integrate Eq. (4.55)

$$\theta^2 = \frac{0.45\nu}{U_0^6(1 - x/L)^6}\int_0^x U_0^5\left(1 - \frac{x}{L}\right)^5 dx = 0.075\,\frac{\nu L}{U_0}\left[\left(1 - \frac{x}{L}\right)^{-6} - 1\right] \tag{2}$$

Then the dimensionless factor λ is given by

$$\lambda = \frac{\theta^2}{\nu}\frac{dU}{dx} = -\frac{\theta^2 U_0}{\nu L} = -0.075\left[\left(1 - \frac{x}{L}\right)^{-6} - 1\right] \tag{3}$$

From Eq. (4.55) we set this equal to -0.09 for separation

$$\lambda_{sep} = -0.09 = -0.075\left[\left(1 - \frac{x_{sep}}{L}\right)^{-6} - 1\right]$$

or $$\frac{x_{sep}}{L} = 1 - (2.2)^{-1/6} = 0.123 \qquad \textit{Ans. (a)}$$

This is less than 3 percent higher than Wipperman's exact solution, and the computational effort is very modest.

Part (b)

To compute c_f at $x/L = 0.1$ (just before separation), we first compute λ at this point, using Eq. (3)

$$\lambda(x = 0.1L) = -0.075[(1 - 0.1)^{-6} - 1] = -0.0661$$

Then from Eq. (4.57) the shear parameter is

$$S(x = 0.1L) = (-0.0661 + 0.09)^{0.62} = 0.099 = \tfrac{1}{2}c_f \,\mathrm{Re}_\theta \qquad (4)$$

We can compute Re_θ in terms of Re_L from Eq. (2) or (3)

$$\frac{\theta^2}{L^2} = \frac{0.0661}{UL/\nu} = \frac{0.0661}{\mathrm{Re}_L}$$

or $$\mathrm{Re}_\theta = 0.257\ \mathrm{Re}_L^{1/2} \qquad \text{at } \frac{x}{L} = 0.1$$

Substitute into Eq. (4): $$0.099 = \tfrac{1}{2}c_f(0.257\ \mathrm{Re}_L^{1/2})$$

or $$c_f = \frac{0.77}{\mathrm{Re}_L^{1/2}} \qquad \mathrm{Re}_L = \frac{UL}{\nu} \qquad \textit{Ans. (b)}$$

We cannot actually compute c_f without the value of, say, U_0L/ν.

4.3 Thermal Boundary Layer on a Flat Plate with Zero Pressure Gradient:

In all previous discussions (Sec. 4.1 & 4.2), any immersed body and any moving fluid around it were both kept at the same temperature, T_∞, of the free stream flow (i.,e., the uniform flow far from the body with a velocity U_∞ parallel to the axis of the body in most cases) For this case we have only one boundary layer generated along the surface of the body because of the no-slip condition and the viscous effects in the wall region. This boundary layer is called the Momentum Boundary Layer (M.B.L) as it is related to the momentum transfer in the viscous region. The analysis given in Sec.4.1 and 4.2 is all related to this M.B.L (Fig. 4.23).

In this section, however, the surface of the body, or the wall temperature, is kept at a constant temperature, T_w, greater than or less than T_∞ of the free stream flow (Fig.4.24). Because of the temperature difference, $T_w - T_\infty$, heat transfer (or forced convection) must take place between the wall and the moving fluid (heat transfer must be from the higher temperature to the lower one according to the 2nd law of thermodynamics). If $T_w > T_\infty$, the heat flux moves from the wall to heat the moving fluid while if $T_w < T_\infty$, the heat flux moves from the moving fluid to heat the wall.

In this section we give an example of the integral method analysis as it is applied to the Thermal Boundary Layer (T.B.L) over a flat plate with zero pressure gradient. Our objective is to calculate the heat flux from or to the plate with specified T_w or to find T_w for a given heat flux. The convective heat transfer coefficient, h, is defined by:

$$q'' = h\,(T_w - T_\infty)$$

where q" is the heat flux in direction normal to the wall, in units of watt/m^2

and h is average heat transfer coefficient over the heated plate,in units of watt/ $K^o.m^2$.

This average value, h, is to be calculated from a local heat transfer coefficient h(x) which is a function of the distance x along the plate. Our task in this section is to find h(x).

Flat Plate

With a fluid flowing parallel to a flat plate, changes in velocity and temperature of the fluid are confined to a thin region adjacent to the solid boundary — the boundary layer. Several cases arise:

1. Flows without or with pressure gradient
2. Laminar or turbulent boundary layer
3. Negligible or significant viscous dissipation (effect of frictional heating)
4. $Pr \geq 0.7$ or $Pr \ll 1$

Flows with Zero Pressure Gradient and Negligible Viscous Dissipation

When the free-stream pressure is uniform, the free-stream velocity is also uniform. Whether the boundary layer is laminar or turbulent depends on the Reynolds number Re_x ($\rho U_\infty x/\mu$) and the shape of the solid at entrance. With a sharp edge at the leading edge (Figure 4.23) the boundary layer is initially laminar but at some distance downstream there is a transition region where the boundary layer is neither totally laminar nor totally turbulent. Farther downstream of the transition region the boundary layer becomes turbulent. For engineering applications the existence of the transition region is usually neglected and it is assumed that the boundary layer becomes turbulent if the Reynolds number, Re_x, is greater than the critical Reynolds number, Re_{cr}. A typical value of 5×10^5 for the critical Reynolds number is generally accepted, but it can be greater if the free-stream turbulence is low and lower if the free-stream turbulence is high, the surface is rough, or the surface does not have a sharp edge at entrance. If the entrance is blunt, the boundary layer may be turbulent from the leading edge.

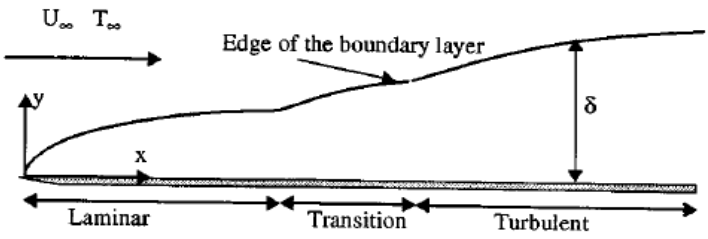

FIGURE 4.23 Flow of a fluid over a flat plate with laminar, transition, and turbulent boundary layers.

Temperature Boundary Layer

Analogous to the velocity boundary layer there is a temperature boundary layer adjacent to a heated (or cooled) plate. The temperature of the fluid changes from the surface temperature at the surface to the free-stream temperature at the edge of the temperature boundary layer (Figure 4.24).

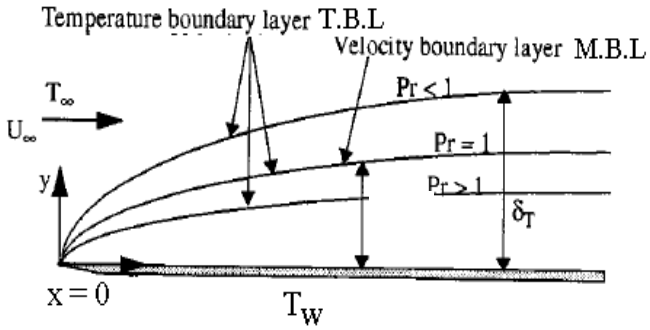

FIGURE 4.24 Temperature boundary layer thickness relative to velocity boundary layer thickness.

The velocity boundary layer thickness δ depends on the Reynolds number Re_x. The thermal boundary layer thickness δ_T depends both on Re_x and Pr

Viscous dissipation and high-speed effects can be neglected if $Pr^{1/2}\, Ec/2 \ll 1$. For heat transfer with significant viscous dissipation see the section on flow over flat plate with zero pressure gradient: Effect of High Speed and Viscous Dissipation. The Eckert number Ec is defined as $Ec = U_\infty^2 / C_p(T_s - T_\infty)$.

4.3.1 Integral Analysis of Thermal Boundary Layer over a Flat Plate:

Consider the flow of a uniform and unbounded stream of viscous fluid over a flat plate (of unit depth normal to the paper, $dz = 1$) as shown in Fig.4.25. The plate is kept at constant temperature T_w, starting at some distance x_o downstream the leading edge (x = 0). The length of the plate between x = 0 and x = x_o is kept at T_∞ as for the free stream which has an enthalpy of , h_∞, and a velocity $U_\infty \neq f(x,y)$ for this zero pressure gradient case. We shall apply the integral form of the energy equation (1^{st} law of thermodynamics) on the shown integral control volume which include both the M.B.L. of thickness, $\delta(x)$, and the T.B.L. of thickness $\delta_T(x)$. Recall from Fig.4.24, that δ_T may be larger than or smaller than δ depending on the value of Pr number of the fluid. The case shown on fig. 4.25 is of $\delta > \delta_T$ which means that Pr # >1 (such as for water).

As shown in Fig.4.25, the M.B.L. starts at x= 0 while the T.B.L. starts at x= x_o. At any point $x > x_o$ along the plate, the axial velocity profile in the M.B.L. is u(y) while the temperature profile is T(y) and the heat flux is dQ/dt as shown. We shall also apply the mass integral equation on the control volume between the cross-section at x, the cross-section at x+Δx and across the T.B.L. edge in order to find the energy crossing these 3 cross-sections.

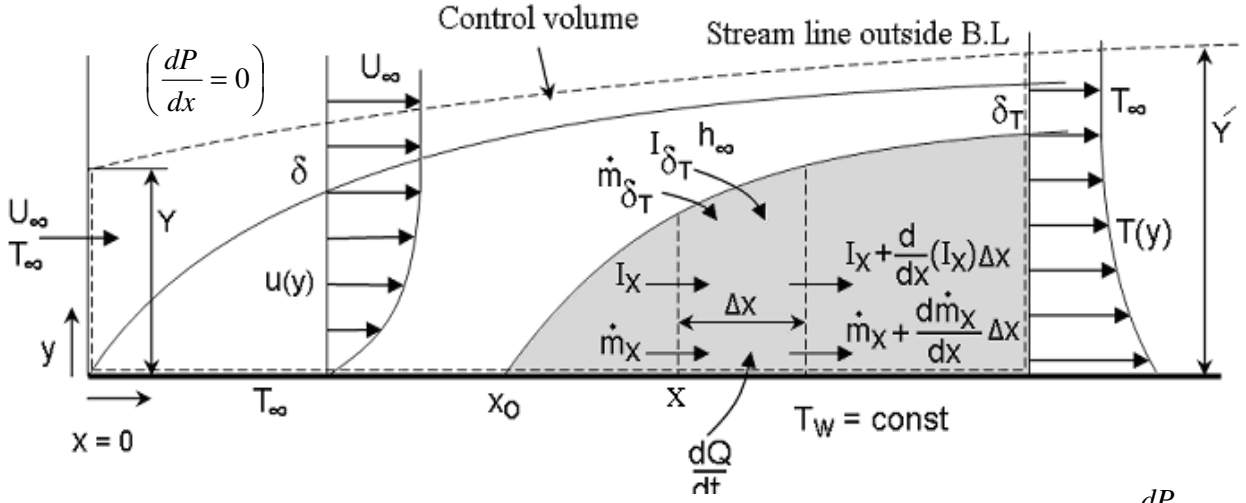

Fig. 4.25 the notations for analysis of T.B.L. over a flat plate with $\frac{dP}{dx}=0$

For the above control volume, the energy equation for a steady, incompressible, 2-D flow, and neglecting body force with no shaft work and is:

$$\frac{dQ}{dt} = \int_{cs}\left(\frac{P}{\rho}+e+g\,y+\frac{1}{2}u^2+\frac{1}{2}v^2\right)\rho\underline{V}\cdot d\underline{A} \qquad (4.61)$$

where $\frac{P}{\rho}+e \equiv h$ (specific enthalpy, j/kg), also $v << u$, $\therefore v^2 << u^2 << h$, the energy eq. is reduced to

$$\frac{dQ}{dt} = \int_{cs}\left(h+\frac{1}{2}u^2\right)\rho\underline{V}\cdot d\underline{A} \qquad (4.62)$$

the R.H.S. is the summation of the energy fluxes crossing the control surface by the flow field. We have to perform this integration at the cross-section at x, the cross-section at x+Δx and across the T.B.L. edge. The mass flux crossing at x is:

$$\dot{m}_x = -\int_0^{\delta_T}\rho u\ dy$$

if we neglect the viscous dissipation because $u^2 << h$, the energy flux at x is: $I_x = -\int_0^{\delta_T}\rho u h\ dy$

Note: the –ve sign because the dot product ($\underline{V}$. $\underline{dA}$) is –ve for the cross-section at x.

The mass flux $\rho(\underline{V}\,.\,\underline{dA})$ at x+Δx must be +ve and is equal to: $\left\{\int_0^{\delta_T}\rho u\ dy+\frac{d}{dx}\left[\int_0^{\delta_T}\rho u\ dy\right]\Delta x\right\}$

This mass flux must be greater than the mass flux entering at x due to increase in δ as x is increased. The increase in mass flux must go across the T.B.L.edge ($\dot{m}_\delta$). This difference must be –ve and is:

$$\dot{m}_\delta = -\frac{d}{dx}\left(\dot{m}_x\right)\Delta x = -\frac{d}{dx}\left(\int_0^{\delta_T} \rho u \; dy\right)\Delta x$$

This mass entering the T.B.L. carrying the enthalpy of the free stream (h_∞ outside T.B.L). The energy flux which goes through the T.B.L. edge is: $I_\delta = \dot{m}_\delta \cdot h_\infty$

If we add all the energy fluxes across the control surface, the energy equation (4.62) becomes:

$$\left(I_x + \frac{d}{dx}\left(I_x\right)\Delta x\right) + I_x + I_\delta = \frac{d\dot{Q}}{dt} = -K_f\left(\frac{\partial T}{\partial y}\right)_0 \Delta x \qquad \text{(per unit width } \Delta z=1)$$

the energy flux that crosses at the cross-section at x+Δx is: $\left\{\int_0^{\delta_T} \rho\, u\, h\, dy + \frac{d}{dx}\left[\int_0^{\delta_T} \rho\, u\, h\, dy\right]\Delta x\right\}$

By substitution and canceling similar terms with different signs, we get:

$$\frac{d}{dx}\left[\int_0^{\delta_T} \rho u h \; dy\right] - h_\infty \frac{d}{dx}\left[\int_0^{\delta_T} \rho u \; dy\right] = -K_f\left(\frac{\partial T}{\partial y}\right)_0 \qquad \text{(we divided by } \Delta x\text{)}$$

where K_f is the thermal conductivity of the fluid. If we put ($dh = C_P\, dT$) and move $\rho\, C_p$ (which are constants) to the R.H.S, the energy equation becomes:

$$\frac{d}{dx}\left[\int_0^{\delta_T} (T_\infty - T) u \; dy\right] = \frac{K_f}{\rho C_P}\left(\frac{\partial T}{\partial y}\right)_0 = \alpha\left(\frac{\partial T}{\partial y}\right)_{y=0} \qquad (4.63)$$

where α = the fluid thermal diffusivity. We note that the integral upper limit must cover all the width δ_T because by definition, outside the T.B.L. $T(y) = T_\infty$ or $(T_\infty - T) = 0.0$.

Equation (4.63) is the Energy Integral Equation (similar to the Momentum Integral Equation 4.26). It may be used for both laminar and turbulent flows and for fluids having any value of the Pr number where $Pr = \nu/\alpha$ (the ratio of the fluid kinematic viscosity to its thermal diffusivity). We must note also that the velocity profile *u(y)* of the M.B.L. is coupled with the temperature profile *T(y)* on the L.H.S. of (4.63) while only the gradient of *T(y)* exists on the R.H.S. of (4.63). In this section, we shall consider only the solution for a Laminar flow Boundary Layer. Other cases are beyond the scope of our study.

4.3.2 Solution of The Energy Integral Equation For Laminar Flow:

By solving the Energy Integral Equation 4.63 (i.e., doing the integration at the cross-section normal to the plate **at the point x** as shown on Fig. 4.25), we should be able from such a solution to get the distribution of the T.B.L. thickness $\delta_T(x)$ and finally the heat transfer coefficient *h(x)* and the heat flux q"(x) as discussed before in the beginning of Sec.4.3.

By analogy to the various methods used to solve the Momentum Integral Equation (4.26), in order to solve the Energy Integral Equation (4.63), we have to assume a velocity distribution *u(y)* inside the M.B.L and also assume another temperature distribution *T(y)* inside the T.B.L region. Many different types of velocity profiles *u(y)* were used before in Sec.4.2, also many different types of temperature profiles may be assumed here for *T(y)* as long as they satisfy the known temperature boundary conditions as discussed here. We do not need to assume *T(y)* to be similar to or to be different than *u(y)* in any way. Just any two profiles *T(y)* and *u(y)* may be assumed to solve the Energy Integral Equation (4.63). It is true that we shall find infinite number of solutions for all types of the assumed profiles *u(y)* and *T(y)*. We must note that the final results shall depend strongly on both the assumed profiles *u(y)* and *T(y)*. The following example shall clarify this point:

4.3.2.1 Example Using 3rd Order profiles for both u(y) and T(y):

Since T_w and T_∞ are constants, we define two temperature differences: ($\theta = T - T_W$, $\theta_\infty = T_\infty - T_W$)

(note: do not mix θ with the boundary layer momentum thickness as it was defined before in Sec.4.1 & 4.2). We shall assume 3rd order polynomial for the dimensionless temperature profile:

Let $\frac{\theta}{\theta_\infty}=\frac{T-T_W}{T_\infty-T_W}=a+b\left(\frac{y}{\delta_T}\right)+c\left(\frac{y}{\delta_T}\right)^2+d\left(\frac{y}{\delta_T}\right)^3$

We need 4 boundary conditions to get the unknown constants a, b, c, and d. We have two known conditions at y=0 and two known conditions at y= δ_T

At $y=0$, $\therefore\ T=T_W$ & $\frac{\partial^2 T}{\partial y^2}=0$ (i.e., the maximum heat flux must be at the wall)

At $y=\delta_T$, $\therefore\ T=T_\infty$ & $\frac{\partial T}{\partial y}=0$ (similar to the patching condition at the edge of M.B.L)

After doing mathematical work, we get $\left(a=c=0\ ,\ b=\frac{3}{2}\ ,\ d=-\frac{1}{2}\right)$, By substitution we have:

$$\frac{\theta}{\theta_\infty}=\frac{T-T_W}{T_\infty-T_W}=\frac{3}{2}\left(\frac{y}{\delta_T}\right)-\frac{1}{2}\left(\frac{y}{\delta_T}\right)^3 \qquad (1)$$

Similarly, assume a 3rd order profile for *u(y)* as:

$$\frac{u}{U_\infty}=a_1+b_1\left(\frac{y}{\delta}\right)+c_1\left(\frac{y}{\delta}\right)^2+d_1\left(\frac{y}{\delta}\right)^3$$

The usual 4 boundary conditions on *u(y)* are:

At y=0, u=0 (no slip-condition) and $\frac{\partial^2 u}{\partial y^2}=0$ (i.e., maximum shear is at the wall)

At y=δ, $u=U_\infty$ & $\frac{\partial u}{\partial y}=0$ (the patching condition at the edge of the M.B.L)

After doing mathematical work, we get: $\frac{u}{U_\infty}=\frac{3}{2}\left(\frac{y}{\delta}\right)-\frac{1}{2}\left(\frac{y}{\delta}\right)^3$ (2)

Interring both equations (1) and (2) into the L.H.S. of the Energy Integral Equation (4.63), we get:

$$\frac{d}{dx}\left[\int_0^Y (T_\infty-T)u\ dy\right]=\frac{d}{dx}\left[\int_0^Y(\theta_\infty-\theta)u\ dy\right]=\theta_\infty U_\infty\frac{d}{dx}\left[\int_0^Y\left(1-\frac{\theta}{\theta_\infty}\right)\left(\frac{u}{U_\infty}\right)\ dy\right]$$

$$=\theta_\infty U_\infty\frac{d}{dx}\left[\int_0^Y\left(1-\frac{3}{2}\left(\frac{y}{\delta_T}\right)+\frac{1}{2}\left(\frac{y}{\delta_T}\right)^3\right)\left(\frac{3}{2}\left(\frac{y}{\delta}\right)-\frac{1}{2}\left(\frac{y}{\delta}\right)^3\right)\ dy\right]=\alpha\left(\frac{\partial T}{\partial y}\right)_W \qquad (3)$$

Using eq.(1) in the R.H.S., we get: $\alpha\left(\frac{\partial T}{\partial y}\right)_W=\alpha\frac{\partial}{\partial y}\left[\theta_\infty\left(\frac{3}{2}\left(\frac{y}{\delta_T}\right)-\frac{1}{2}\left(\frac{y}{\delta_T}\right)^3\right)+T_W\right]_{y=0}=\frac{3\alpha}{2}\left(\frac{\theta_\infty}{\delta_T}\right)$

Note that the constant of (3/2) on the R.H.S depends totally on the shape of the assumed profile $\frac{\theta}{\theta_\infty}$

Note also that the upper limit of the integration must in all cases cover the thickness of the T.B.L. up to Y= δ_T for all types of fluids regardless of the value of δ of the M.B.L as shown on fig. 4.25. We may have two different cases depending on the type of the fluid and the value of *Pr* # where

$$P_r\ number\equiv\frac{\upsilon}{\alpha}=\frac{Kinematic\ \ Viscousity}{thermal\ \ diffusivity}=\frac{\mu C_p}{K_f}=\frac{convective\ \ heat\ transfer}{conductive\ \ heat\ transfer}$$

The convective heat transfer is due to the fluid motion in the M.B.L. while the conductive heat transfer is due to the temperature gradient and effect of thermal diffusivity in the T.B.L. This means that the numerical value of Pr number is proportional to the ratio of (δ / δ_T) which is shown on fig.4.24 and the next figure.

If $P_r<1$, $\therefore\ \delta<\delta_T$ (e.g., for air and gases),

If $P_r>1$, $\therefore\ \delta>\delta_T$ (e.g., for water and liquids)

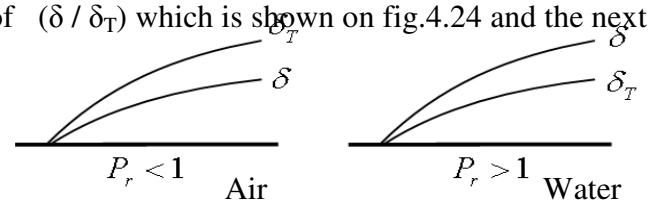

For example: for air: $P_r\approx 0.71$ *up to* 600^oC

While for water: Pr = 4 at 38 ^oC & Pr =2 at 93 ^oC

The P_r number has been found to be the parameter which relates the relative thickness of the hydrodynamic and thermal boundary layers. The momentum diffusivity gives information about the rate at which momentum may diffuse because of molecular motion. Thermal diffusivity gives information about the rate at which heat may diffuse in the fluid. Thus the ratio of the momentum diffusivity / the thermal

diffusivity should express the relative magnitude of diffusion of momentum and heat in the fluid. Large diffusivity means that the viscous or temperature influence is felt farther out in the flow field. For very high P_r number the velocity B.L will be much thicker than the thermal B.L.

For the case of $\delta_T < \delta$ or $Pr > 1$ *(such as water) & for Laminar Flow*

As shown on Fig.4.25, in this case we need only to carry out the integration in the energy eq.(3) $Y = \delta_T$ since the integrand $T_\infty - T$ is zero for $Y > \delta_T$

Then the energy eq is:

$$\theta_\infty U_\infty \frac{d}{dx}\left\{\int_0^{\delta_T}\left[1-\frac{3}{2}\left(\frac{y}{\delta_T}\right)+\frac{1}{2}\left(\frac{y}{\delta_T}\right)^3\right]\left[\frac{3}{2}\left(\frac{y}{\delta}\right)-\frac{1}{2}\left(\frac{y}{\delta}\right)^3\right]dy\right\}=\frac{3\alpha\,\theta_\infty}{2\,\delta_T} \qquad (4)$$

This equation is valid only for the assumed 3rd order $\frac{u}{U_\infty}$ & $\frac{\theta}{\theta_\infty}$. After expansion and doing integration from $y=0$ to $y=\delta_T$, and also we define the ratio ε as: $\varepsilon = \frac{\delta_T}{\delta}$

We get: $$U_\infty \frac{d}{dx}\left[\delta\left(\frac{3}{20}\varepsilon^2-\frac{3}{280}\varepsilon^4\right)\right]=\frac{3\,\alpha}{2\,\delta\,\varepsilon} \qquad (5)$$

Since $\varepsilon < 1$ we may neglect $\frac{3}{280}\varepsilon^4$ as compared to $\frac{3}{20}\varepsilon^2$ and the above eqn. reduces to:

$$\frac{3}{20}U_\infty \frac{d}{dx}\left(\delta\,\varepsilon^2\right)=\frac{3\,\alpha}{2\,\delta\,\varepsilon}$$

Note that $\delta = f_1(x)$ and that $\varepsilon = f_2(x)$. Then after doing the product differentiation on the L.H.S. we get:

$$\frac{1}{10}U_\infty\left(2\delta^2\varepsilon^2\frac{d\varepsilon}{dx}+\varepsilon^3\delta\frac{d\delta}{dx}\right)=\alpha \qquad (6)$$

We can get $(d\delta/dx)$ using the momentum integral equation method (with $\frac{u}{U_\infty}=\frac{3}{2}\left(\frac{y}{\delta}\right)-\frac{1}{2}\left(\frac{y}{\delta}\right)^3$) and for the Laminar Flow case. You can do this part as an exercise to prove the following steps.

Using equations (4.26, 4.28) and the definition of the momentum thickness with the assumed u/U_∞,

we get: $\delta\,d\delta=\frac{140}{13}\frac{\upsilon}{U_\infty}dx$ or $\delta^2=\frac{280}{13}\frac{\upsilon\,x}{U_\infty}+c$

The constant $c = 0$ because $\delta = 0$ at $x = 0$, we get finally $\frac{\delta}{x}=\frac{4.641}{\sqrt{\mathrm{Re}_x}}$ (only for 3rd order u/U_∞)

by substitution of $(d\delta/dx)$ into eqn. (6) it is reduced to: $\frac{1}{10}U_\infty\left(\frac{560}{13}\frac{\upsilon\,x}{U_\infty}\varepsilon^2\frac{d\varepsilon}{dx}+\frac{140}{13}\frac{\upsilon}{U_\infty}\varepsilon^3\right)=\alpha$

which can be written as:

$$\varepsilon^3+4x\varepsilon^2\frac{d\varepsilon}{dx}=\frac{13}{14}\frac{\alpha}{\upsilon} \quad \text{or} \quad \varepsilon^3+\frac{4}{3}x\frac{d\varepsilon^3}{dx}=\frac{13}{14}\frac{\alpha}{\upsilon} \qquad (7)$$

This ordinary differential equation (7) is linear and of the 1st order for the variable (ε^3). Its solution includes a solution of its complementary function added to the source term (*13α/14ν*). The complementary function of (7) is: $\varepsilon^3+\frac{4}{3}x\frac{d\varepsilon^3}{dx}=0$

Which integrates to : $\varepsilon_c^3 = a\,x^{-3/4}$,

where ε_c is the complementary solution of ε and (a) is a constant to be found from the known boundary conditions on ε.

And the final solution is given by : $$\varepsilon^3 = a\,x^{-3/4}+\frac{13}{14}\frac{1}{P_r} \qquad (8)$$

where $P_r=\frac{\upsilon}{\alpha}$

To get (a), from boundary conditions we have: $\varepsilon=\frac{\delta_T}{\delta}=0$ *at* $x = x_0$, After inserting (a) in (8),

the solution for $\varepsilon(x)$ is: $$\frac{\delta_T}{\delta}=\varepsilon=\frac{1}{1.026}P_r^{-1/3}\left[1-\left(\frac{x_0}{x}\right)^{3/4}\right]^{1/3} \qquad (9)$$

which is valid only for 3rd order profiles for $\frac{u}{U_\infty}$ & $\frac{\theta}{\theta_\infty}$

The local heat transfer coefficient is given by: $h_x = -K_f \left(\frac{\partial T}{\partial y}\right)_W / (T_W - T_\infty)$

We use the assumption: $\frac{\theta}{\theta_\infty} = \frac{T-T_W}{T_\infty - T_W} = \frac{3}{2}\left(\frac{y}{\delta_T}\right) - \frac{1}{2}\left(\frac{y}{\delta_T}\right)^3$

Then $h_x = \frac{3}{2}\frac{K_f}{\varepsilon\,\delta}$, where $\delta = \frac{4.641\,x}{\sqrt{\mathrm{Re}_x}}$ for the assumed 3rd order profile: $\frac{u}{U_\infty} = \frac{3}{2}\eta - \frac{1}{2}\eta^3$

Which after substitution for ε & δ becomes:

$$h_x = 0.332\ K_f\ P_r^{1/3}\left(\frac{U_\infty}{\upsilon\ x}\right)^{1/2}\left[1-\left(\frac{x_0}{x}\right)^{3/4}\right]^{-1/3} \qquad (10)$$

The Nusselt number is: $N_{u_x} = \frac{h_x\,x}{K_f}$

$$N_{u_x} = 0.332\ P_r^{1/3}\ \mathrm{Re}_x^{1/2}\left[1-\left(\frac{x_0}{x}\right)^{3/4}\right]^{-1/3} \qquad (11)$$

If the entire plate is heated, $\therefore\ x_0 = 0$

Then $N_{u_x} = 0.332\ P_r^{1/3}\ \mathrm{Re}_x^{1/2}$

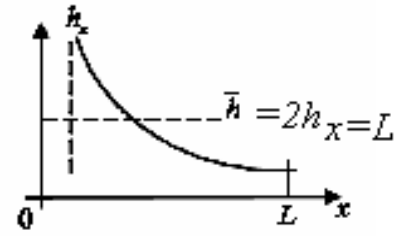

The average H.T coefficient and N_u averaged over $0 \to L$

$\bar{h} = \frac{1}{L}\int_0^L h_x\,dx = 2\,h_x)_{x=L}$,we neglect x_0 (only in doing the integration

$\overline{N_u} = \frac{\bar{h}\,L}{K_f} = 2\,N_u)_{x=L}$

$$\therefore\ \bar{h} \cong 0.664\ K_f\ P_r^{1/3}\left(\frac{U_\infty}{\upsilon\,L}\right)^{1/2}\left[1-\left(\frac{x_0}{L}\right)^{3/4}\right]^{-1/3} \qquad (12)$$

$$\therefore\ \overline{N_u} \cong 0.664\ K_f\ P_r^{1/3}\ \mathrm{Re}_L^{1/2}\left[1-\left(\frac{x_0}{L}\right)^{3/4}\right]^{-1/3} \qquad (13)$$

The previous analysis was based on assumption that fluid properties are constants through out the flow. If there is appreciable variation between wall and free-steam conditions, it is recommended that the properties be evaluated at the mean file temperature defined by: $T_f = (T_w+T_\infty)/2$

For the case of $\delta_T > \delta$ or *Pr < 1 (such as Air) & for Laminar Flow:*

Using the same 3rd order profiles for *u(y)& T(y),*
The integral energy equation (4) is the same:

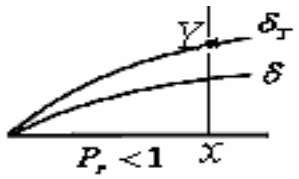

$$U_\infty \frac{d}{dx}\left\{\int_0^{\delta_T}\left[1-\frac{3}{2}\left(\frac{y}{\delta_T}\right)+\frac{1}{2}\left(\frac{y}{\delta_T}\right)^3\right]\left[\frac{3}{2}\left(\frac{y}{\delta}\right)-\frac{1}{2}\left(\frac{y}{\delta}\right)^3\right]dy\right\} = \frac{3\alpha}{2\,\delta_T} \qquad (4)$$

Fig.4.26

The integration upper limit is also $Y = \delta_T$ because *(1-θ/θ∞)* have non-zero values after $y \geq \delta$, but u/U∞=1 in the part $y \geq \delta$

Therefore, the integration in the L.H.S. of (4) is: $\int_0^{\delta_T} = \int_0^{\delta}\left(1-\frac{\theta}{\theta_\infty}\right)\frac{u}{U_\infty} + \int_\delta^{\delta_T}\left(1-\frac{\theta}{\theta_\infty}\right)$ (14)

After expansion and using $\varepsilon = \frac{\delta_T}{\delta}$ and doing all the above integrations with the shown two limits,

we get: $U_\infty \frac{d}{dx}\left[\delta^2\left(\frac{1}{4}\varepsilon^2 - \frac{1}{4}\varepsilon + \frac{1}{10} - \frac{1}{140}\ \frac{1}{\varepsilon^2}\right)\right] = \alpha$

Since $\varepsilon > 1$, we can neglect the last term in (15) as compared to other terms. The final equation is:

$$a_1\,x\,(d\varepsilon^2/dx) + a_2\,x\,(d\varepsilon/dx) + a_3\,\varepsilon^2 + a_4\,\varepsilon = (1/Pr) + a_5 \qquad (15)$$

where the constants are: a_1 =5.3847, a_2 =21.539, a_3= 5.3846, a_4=- 5.3856, and a_5 =2.1538

The exact solution of (15) is very complicated and involves a complex 1st order ordinary differential equation for ε2 and ε with non-zero source term. The exact solution of (15) is beyond the scope of our discussion here. Instead, we try another approximate solution for fluids with Pr # < 1. In Fig.4.26, we should note that the variation in *T(y)* is very small *for y>δ* and in all the region between δ and δ_T which means that

in eq. (14), the integration of the last term on the R.H.S. shall be very small outside the M.B.L. because $(1-\theta/\theta_\infty) \approx 0.0$ as compared to the integration from y=0 to y=δ. Therefore, we neglect last term on R.H.S. of (14) as compared to the 1st term. We get:

(16)

After expansion and doing the integration from $y = 0$ to $y = \delta$, also using the variable $\varepsilon = \frac{\delta_T}{\delta}$, we get: $$U_\infty \frac{d}{dx}\left[\delta\left(\frac{5}{8}-\frac{3}{5}\cdot\frac{1}{\varepsilon}+\frac{4}{35}\cdot\frac{1}{\varepsilon^3}\right)\right]=\frac{3\,\alpha}{2\,\delta_T}$$

because $\varepsilon > 1$, $\therefore \frac{1}{\varepsilon} > \frac{1}{\varepsilon^3}$, we may neglect the last term with $\frac{1}{\varepsilon^3}$ as compared to the term with $\frac{1}{\varepsilon}$

Then $$U_\infty \frac{d}{dx}\left[\delta\left(\frac{5}{8}-\frac{3}{5}\cdot\frac{1}{\varepsilon}\right)\right]=\frac{3\,\alpha}{2\,\delta_T}$$

after doing the product differentiation, we get: $$U_\infty \left\{\frac{3}{5}\left(\frac{\delta}{\varepsilon^2}\right)\frac{d\varepsilon}{dx}+\left(\frac{5}{8}-\frac{3}{5}\cdot\frac{1}{\varepsilon}\right)\frac{d\delta}{dx}\right\}=\frac{3\,\alpha}{2\,\delta\,\varepsilon}$$

or $$U_\infty \left\{\frac{3}{5}\delta^2\left(\frac{1}{\varepsilon}\frac{d\varepsilon}{dx}\right)+\left(\frac{5}{8}\varepsilon-\frac{3}{5}\right)\delta\frac{d\delta}{dx}\right\}=\frac{3}{2}\alpha \qquad (17)$$

We get δ & $(d\delta/dx)$ using the momentum integral equation (with 3rd order profile for $u//U_\infty$) and for the Laminar Flow case we have: $\delta\frac{d\delta}{dx}=\frac{140}{13}\frac{\upsilon}{U_\infty}$ & $\delta^2=\frac{280}{13}\frac{\upsilon\,x}{U_\infty}$

After substitution $$x\frac{1}{\varepsilon}\frac{d\varepsilon}{dx}+0.521\,\varepsilon=0.116\,\frac{\alpha}{\upsilon}+0.5 \qquad (18)$$

This ordinary differential equation is linear and of the 1st order for the variable (ε).For the complementary function, we get $x\frac{1}{\varepsilon}\frac{d\varepsilon}{dx}+0.521\,\varepsilon=0$ which can be integrated to give:

$-1.92\,\varepsilon^{-2}\,d\varepsilon=\frac{1}{x}dx \xrightarrow{\text{by integration}} +1.92\,\varepsilon_c^{-1}=ln\,x+ln\,(a)=ln\,(ax)$, where ln(a) is a constant.

Then $\varepsilon_c=\frac{1.92}{\ln(ax)}$, we must not that $x \geq x_o$

The total solution $$\varepsilon=\frac{\delta_T}{\delta}=\frac{1.92}{\ln\,(ax)}+\left(\frac{0.116}{P_r}+0.5\right) \qquad (19)$$

To get the constant (a), from boundary conditions $\varepsilon=0$ *at* $x=x_0$, then: $\ln(a)=-\left(\ln x_0+\frac{1.92}{\frac{0.116}{P_r}+0.5}\right)$

Local H.T coefficient h(x) at $x \geq x_o$, is given by: $h_x=\frac{-K_f\left(\frac{\partial T}{\partial y}\right)_W}{T_W-T_\infty}=\frac{3\,K_f}{2\,\varepsilon\,\delta}$ where also $\delta=\frac{4.64\,x}{\sqrt{\mathrm{Re}_x}}$

Then $h_x=0.3233\,K_f\left[\frac{1.92}{\ln x+\ln(a)}+\left(\frac{0.116}{P_r}+0.5\right)\right]^{-1}\frac{\sqrt{\mathrm{Re}_x}}{x}$, where *ln(a)* is given above

$$N_{u_x}=h_x\frac{x}{K_f}=0.3233\left[\frac{1.92}{\ln x+\ln(a)}+\left(\frac{0.116}{P_r}+0.5\right)\right]^{-1}\sqrt{\mathrm{Re}_x}\ ,\ \text{only for } x_o > 0.0 \qquad (20)$$

Example:

Air at 25°C and 1.0 atm. Flows over a flat plate at a speed of 2 m/sec. The plate has a unit width and is heated over its entire length, L, to a temperature of 75°C. Use the integral momentum & energy equations with cubic profiles (3rd order) for both the velocity *u(y)* and temperature *T(y)* to:

a) Calculate the M.B.L thickness at distance 10 cm & 20 cm from the leading edge.
b) Calculate the mass flow which enters the M.B.L between x = 10 cm & x = 20 cm.
c) Calculate the rate of H.T in the first 10 cm of the plate and the first 20 cm of the plate.

Solution

The mean film temp.: $T_f=\frac{1}{2}(25+75)=50\ ^oC$, the air properties $\rho=\frac{P}{RT}=1.09\ kg/m^3$, $P_{r\#}=0.7$

$K_f = 0.024\ Kcal/hr.m.^oC = 0.0279\ W/m.^oC,\ \upsilon = 0.086\ m^2/hr = 23.8\times10^{-6}\ m^2/\sec$

a) at x=10cm, $\mathrm{Re}_x = \dfrac{U_\infty\, x}{\upsilon} = \dfrac{2\times0.1}{23.8\times10^{-6}} = 8{,}372$ & at x=20 cm, $\mathrm{Re}_x = 16{,}744$ (Then Laminar Flow),

For 3rd order *u(y)* profile, from (sec 4.3.2.1) the thickness of the M.B.L. is:

$$\delta = \frac{4.64\,x}{\sqrt{\mathrm{Re}_x}},\ \text{at x =10 cm}\quad \delta_{10} = 0.51\ cm \quad \&\quad \text{at x =20 cm}\quad \delta_{20} = 0.72\ cm$$

b) To calculate the mass flow which enters the M.B.L. from the free stream between x=10 cm and x =20 cm , we take the difference between the mass flow in the B.L at these two x-positions. At any x-position the mass flow in the B.L is given by:

Then
$$\dot{m}_x = \int_0^\delta \rho\, u\ dy \qquad , \qquad \frac{u}{U_\infty} = \frac{3}{2}\left(\frac{y}{\delta}\right) - \frac{1}{2}\left(\frac{y}{\delta}\right)^3$$

$$\dot{m}_x = \rho\, U_\infty \int_0^\delta \frac{3}{2}\left(\frac{y}{\delta}\right) - \frac{1}{2}\left(\frac{y}{\delta}\right)^3 dy = \frac{5}{8}\rho\, U_\infty\, \delta$$

$$\dot{m}_{20} - \dot{m}_{10} = \frac{5}{8}x\rho.U_\infty(\delta_{20} - \delta_{10}) = \frac{5}{8}\times1.09\times2\left(\frac{0.72-0.51}{100}\right)\times10^3 = 2.86\ \ gm/\sec$$

c) We can not use equation (19) for Air with Pr # <1, because $x_0 = 0$, As an approximation, we can use equation (11) with x_o=0.0, therefore $N_{u_x} = 0.332\ P_r^{1/3}\ \mathrm{Re}_x^{1/2}$

Then at x= 10 cm:

$N_{u_x} = 0.332\,(0.7)^{1/3}(8372)^{1/2} = 27$, $\quad h_x = N_{u_x}\dfrac{K_f}{x} = \dfrac{27\times0.024}{0.1} = 6.47\ \ Kcal/hr.m^2.^oC = 7.52\ \ W/m^2.^oC$

From x=0 to x=10cm, $\quad \bar{h} = 2h_x = 12.95\ \ Kcal/hr.m^2.^oC = 15.05\ \ W/m^2.^oC$

The average heat flux in 1st 10cm, $q = hA(T_W - T_\infty) = 1295\times0.1(75-25) = 6475\ Kcal/hr.m = 753\ W/m$

Then at x= 20 cm

$$N_{u_x} = 0.332\,(0.7)^{1/3}(16744)^{1/2} = 38.184$$

$$h_x = N_{u_x}\frac{K_f}{x} = \frac{38.184\times0.024}{0.2} = 4.582\ \ Kcal/hr.m^2.^oC = 5.326\ \ W/m^2.^oC$$

From x=0 to x=20cm, $\bar{h} = 2h_x = 9.164\ \ Kcal/hr.m^2.^oC = 10.632\ \ W/m^2.^oC$

The average heat flux in 1st 20cm

$$q = h\,A(T_W - T_\infty) = 9.164\times0.2\,(75-25) = 91.64\ \ Kcal/hr.m = 106.571\ \ W/m$$

4.3.2.2 Example For the case of $\delta_T < \delta$ or Pr > 1 & for Laminar Flow and 2nd Order profiles:

For thermal boundary layer with 2nd order $\dfrac{u}{U_\infty}$ & $\dfrac{\theta}{\theta_\infty}$ profiles:

Prove that the energy equation (4.63) is reduced to: $\quad U_\infty \dfrac{d}{dx}\left[\dfrac{\delta}{6}\varepsilon^2 - \dfrac{1}{30}\delta\,\varepsilon^3\right] = \dfrac{2\,\alpha}{\delta\,\varepsilon}$

Where, $\varepsilon = \dfrac{\delta_T}{\delta}$ and for this 2nd order profile: $\delta = \dfrac{5.48\,x}{\sqrt{\mathrm{Re}_x}}$

we get $\quad \varepsilon^3 + 4x\varepsilon^2\dfrac{d\varepsilon}{dx} = \dfrac{4}{5}P_r^{-1} \quad\Rightarrow\quad \varepsilon^3 + \dfrac{4}{3}x\dfrac{d\varepsilon^3}{dx} = \dfrac{4}{5}P_r^{-1}$

The complementary equation $\quad \varepsilon_c^3 + \dfrac{4}{3}x\dfrac{d\varepsilon_c^3}{dx} = 0$, Which has a solution $\quad \varepsilon_c^3 = a\,x^{-3/4}$

$\varepsilon_{tot}^3 = a\,x^{-3/4} + \dfrac{4}{5}P_r^{-1}$, where $a = -\dfrac{4}{5}P_r^{-1}x_0^{3/4}$ From B.C:($\varepsilon = 0$ at $x = x_0$), then $\quad \varepsilon_{tot}^3 = \dfrac{4}{5}P_r^{-1}\left[1 - \left(\dfrac{x_0}{x}\right)^{3/4}\right]$

or
$$\varepsilon_{tot} = \frac{\delta_T}{\delta} = \frac{1}{1.0772}\,P_r^{-1/3}\left[1 - \left(\frac{x_0}{x}\right)^{3/4}\right]^{1/3}$$

$$h_x = \frac{-K_f\left(\dfrac{\partial T}{\partial y}\right)_{y=0}}{T_W - T_\infty}\ ,\ \text{where}\ \frac{\theta}{\theta_\infty} = \frac{T - T_W}{T_\infty - T_W} = 2\left(\frac{y}{\delta_T}\right) - \left(\frac{y}{\delta_T}\right)^2,\ \text{then}\ h_x = \frac{2\,K_f}{\varepsilon\,\delta} = \frac{2\,K_f}{5.48\,\varepsilon}\left(\frac{U_\infty}{\upsilon\,x}\right)^{1/2}$$

$$h_x = 0.393\ K_f\ P_r \left(\frac{U_\infty}{\upsilon\ x}\right)^{1/2}\left[1-\left(\frac{x_0}{x}\right)^{3/4}\right]^{-1/3}$$

$$N_{u_x} = \frac{h_x\ x}{K_f} \quad \rightarrow \quad N_{u_x} = 0.393\ \ P_r^{1/3}\ \mathrm{R}e_x^{1/2}\left[1-\left(\frac{x_0}{x}\right)^{3/4}\right]^{-1/3}$$

The average heat transfer coeff. $\bar{h} \cong \frac{1}{L}\int_0^L h_x\ dx = 2\ h_x)_{x=L}$ (neglect x_0 in integration), then

$$\bar{h} = 0.786\ \ K_f\ P_r^{1/3}\left(\frac{U_\infty}{\upsilon\ L}\right)^{1/2}\left[1-\left(\frac{x_0}{L}\right)^{3/4}\right]^{-1/3}$$

also

$$\overline{N_u} = 0.786\ \ P_r^{1/3}\ \mathrm{R}e_L^{1/2}\left[1-\left(\frac{x_0}{L}\right)^{3/4}\right]^{-1/3}$$

By calculating the percent of error in case of 3rd order profile, we get:

% error in $\varepsilon_{tot} = \dfrac{1/1.0772 - 1/1.026}{1/1.026} = -4.75\ \%$ w.r.t 3rd order case

% error in $h_x = \dfrac{0.393 - 0.332}{0.332} = +18.37\ \%$ w.r.t 3rd order case

% error in $\bar{h} = \dfrac{0.786 - 0.664}{0.664} = +18.37\ \%$ w.r.t 3rd order case

% error in $\overline{N_u} = \dfrac{0.786 - 0.664}{0.664} = +18.37\ \%$ w.r.t 3rd order case

Oral Exam Questions

Boundary Layer Flow Part(4)

1- Discuss all the differences you know between internal viscous flow and external flow (which can be viscous or non-viscous). What is the role of the no-slip condition and viscous effects in each type? What are the assumptions and equations that may be used in each type? Use sketches to explain your discussion.

2- Define both the physical and mathematical meaning of the following:

I. the boundary layer region and the boundary layer thickness.
II. the stream lines and the stream function inside the boundary layer region.
III. the boundary layer displacement thickness.
IV. the effective body as seen by the real flow.

3- Discuss all the differences you know between the boundary layer over a real flat plate and the boundary layer over a non-real flat plate. Define the critical Rynold's number and the no-slip condition in each type? What are the assumptions of $\partial p/\partial x$ and $\partial p/\partial y$ that may be used in each type? Use sketches to explain your discussion.

4- Define both the physical and mathematical meaning of the following:

I. the boundary layer momentum thickness.
II. the critical Rynold's number in the boundary layer.
III. the pressure distributions: $\partial p/\partial x$ and $\partial p/\partial y$ inside and outside the boundary layer.
IV. the local skin friction coefficient, c_f , and the integrated friction drag coefficient.

5- Discuss both the physical and mathematical relationship between the integrated drag skin friction coefficient , C_f, and the boundary layer momentum thickness, θ.

6- Starting from Navier-Stock's equations, write down and discuss the well known Prandtl's two differential equations for the boundary layer flow. Show all the assumptions used especially for $\partial p/\partial x$ and $\partial p/\partial y$ inside and outside the boundary layer.

7- Using Blasius exact solution for a laminar boundary layer over a flat plate, prove that the boundary layer thickness is: $\delta / x = 5.0 / \sqrt{Re_x}$

8- Using Blasius exact solution for a laminar boundary layer over a flat plate, prove that the boundary layer displacement thickness is: $\delta^* / x = 1.72 / \sqrt{Re_x}$

9- Using Blasius exact solution for a laminar boundary layer over a flat plate, prove that the boundary layer momentum thickness is: $\theta / x = 0.664 / \sqrt{Re_x}$

10- Using Blasius exact solution for a laminar boundary layer over a flat plate, prove that the local skin friction coefficient is: $c_f(x) = 0.664 / \sqrt{Re_x}$

11- Using Blasius exact solution for a laminar boundary layer over a flat plate, prove that the the stream lines must penetrate the boundary layer edge every where.

12- Define and discuss the use of the momentum integral approximate analysis to solve the boundary layer flow over a flat plate.

13- Using the momentum integral method for a laminar B.L and assuming a second order velocity profile, prove that the B.L thickness is: $\delta / x = 5.48 / \sqrt{Re_x}$

14- Using the momentum integral method for a laminar B.L and assuming a second order velocity profile, prove that the B.L displacement thickness is: $\delta^* / x = 1.828 / \sqrt{Re_x}$

15- Using the momentum integral method for a laminar B.L and assuming a second order velocity profile, prove that the B.L momentum thickness is: $\theta / x = 0.731 / \sqrt{Re_x}$

16- Using the momentum integral method for a tripped turbulent B.L and assuming the velocity profile, $u/U_\infty=(y/\delta)^{1/7}$ and the wall shear stress, $\tau_w = 0.0225\ \rho U_\infty^2 (\nu/\delta U_\infty)^{1/4}$, prove that the B.L thickness is: $\delta / x = 0.37 / (Re_x)^{1/5}$

17- Using the momentum integral method for a tripped turbulent B.L and assuming the velocity profile, $u/U_\infty=(y/\delta)^{1/7}$ and the wall shear stress, $\tau_w = 0.0225\ \rho U_\infty^2 (\nu/\delta U_\infty)^{1/4}$, prove that the B.L displacement thickness is: $\delta^* / x = 0.0463 / (Re_x)^{1/5}$

18- Using the momentum integral method for a tripped turbulent B.L and assuming the velocity profile, $u/U_\infty=(y/\delta)^{1/7}$ and the wall shear stress, $\tau_w = 0.0225\ \rho U_\infty^2 (\nu/\delta U_\infty)^{1/4}$, prove that the B.L momentum thickness is: $\theta / x = 0.036 / (Re_x)^{1/5}$

19- Using the momentum integral method for a laminar B.L and assuming a velocity profile as: $u/U_\infty = \sin(\pi y/ 2\delta)$, prove that the B.L thickness is: $\delta / x = 4.8 / \sqrt{Re_x}$

20- Using the momentum integral method for a laminar B.L and assuming a velocity profile as: $u/U_\infty = \sin(\pi y/ 2\delta)$, prove that the B.L displacement thickness is: $\delta^* / x = 1.74 / \sqrt{Re_x}$

21- Using the momentum integral method for a laminar B.L and assuming a velocity profile as: $u/U_\infty = \sin(\pi y/ 2\delta)$, prove that the B.L momentum thickness is: $\theta / x = 0.658 / \sqrt{Re_x}$

22- Using Balsius' soluation for laminar B.L over a flat plate, Compare between the laminar B.L thickness, $\delta_{laminar}$ and the turbulent B.L thickness, $\delta_{turbulent}$ if the laminar B.L is tripped at the leading edge of the plate [use $u/U_\infty=(y/\delta)^{1/7}$and $\tau_w = 0.0225\ \rho U_\infty^2 (\nu/\delta U_\infty)^{1/4}$]

23- Using Balsius' soluation for laminar B.L over a flat plate, Compare between the laminar B.L displacement thickness, $\delta^*_{laminar}$ and the turbulent B.L displacement thickness, $\delta^*_{turbulent}$ if the laminar B.L is tripped at the leading edge of the plate [use $u/U_\infty=(y/\delta)^{1/7}$and $\tau_w = 0.0225\ \rho U_\infty^2 (\nu/\delta U_\infty)^{1/4}$]

24- Using Balsius' soluation for laminar B.L over a flat plate, Compare between the laminar B.L momentum thickness, $\theta_{laminar}$ and the turbulent B.L momentum thickness, $\theta_{turbulent}$ if the laminar B.L is tripped at the leading edge of the plate [use $u/U_\infty=(y/\delta)^{1/7}$and $\tau_w = 0.0225\ \rho U_\infty^2 (\nu/\delta U_\infty)^{1/4}$]

25- Using the momentum integral method for a laminar B.L and assuming (i) a second order velocity profile and (ii) a third order velocity profile, compare the ratios of:
δ(case i) / δ(case ii) , δ^*(case i) / δ^*(case ii) and θ(case I / θ(case ii)

References

1. Schlichting, H., *Boundary Layer Theory*, 7th Ed., McGraw-Hill, New York, 1979.

2. Rosenhead, L., *Laminar Boundary Layers*, Oxford University Press, London, 1963.

3. White, F. M., *Viscous Fluid Flow*, McGraw-Hill, New York, 1974.

4. Currie, I. G., *Fundamental Mechanics of Fluids*, McGraw-Hill, New York, 1974.

5. Blevins, R. D., *Applied Fluid Dynamics Handbook*, Van Nostrand Reinhold, New York, 1984.

6. Hoerner, S. F., *Fluid-Dynamic Drag*, published by the author, Library of Congress No. 64,19666, 1965.

7. Happel, J., *Low Reynolds Number Hydrodynamics*, Prentice Hall, Englewood Cliffs, NJ, 1965.

8. Van Dyke, M., *An Album of Fluid Motion*, Parabolic Press, Stanford, Calif., 1982.

9. Thompson, P. A., *Compressible-Fluid Dynamics*, McGraw-Hill, New York, 1972.

10. Zucrow, M. J., and Hoffman, J. D., *Gas Dynamics*, *Vol. I*, Wiley, New York, 1976.

11. Clayton, B. R., and Bishop, R. E. D., *Mechanics of Marine Vehicles*, Gulf Publishing Co., Houston, 1982.

12. *CRC Handbook of Tables for Applied Engineering Science*, 2nd Ed., CRC Press, 1973.

13. Shevell, R. S., *Fundamentals of Flight*, 2nd Ed., Prentice Hall, Englewood Cliffs, NJ, 1989.

14. Kuethe, A. M. and Chow, C. Y., *Foundations of Aerodynamics*, *Bases of Aerodynamics Design*, 4th Ed., Wiley, 1986.

15. Vogel, J., *Life in Moving Fluids*, 2nd Ed., Willard Grant Press, Boston, 1994.

16. Kreider, J. F., *Principles of Fluid Mechanics*, Allyn and Bacon, Newton, Mass., 1985.

17. Dobrodzicki, G. A., Flow Visualization in the National Aeronautical Establishment's Water Tunnel, National Research Council of Canada, Aeronautical Report LR-557, 1972.

18. White, F. M., *Fluid Mechanics*, McGraw-Hill, New York, 1986.

19. Vennard, J. K., and Street, R. L., *Elementary Fluid Mechanics*, 6th Ed., Wiley, New York, 1982.

20. Gross, A. C., Kyle, C. R., and Malewicki, D. J., The Aerodynamics of Human Powered Land Vehicles, *Scientific American*, Vol. 249, No. 6, 1983.

21. Abbott, I. H., and Von Doenhoff, A. E., *Theory of Wing Sections*, Dover Publications, New York, 1959.

22. MacReady, P. B., "Flight on 0.33 Horsepower: The Gossamer Condor." *Proc. AIAA 14th Annual Meeting* (Paper No. 78-308), Washington, DC, 1978.

23. Goldstein, S., *Modern Developments in Fluid Dynamics*, Oxford Press, London, 1938.

24. Achenbach, E., Distribution of Local Pressure and Skin Friction around a Circular Cylinder in Cross-Flow up to $\mathrm{Re} = 5 \times 10^6$, *Journal of Fluid Mechanics*, Vol. 34, Pt. 4, 1968.

25. Inui, T., Wave-Making Resistance of Ships, *Transactions of the Society of Naval Architects and Marine Engineers*, Vol. 70, 1962.

26. Sovran, G., et al. (ed.), *Aerodynamic Drag Mechanisms of Bluff Bodies and Road Vehicles*, Plenum Press, New York, 1978.

27. Abbott, I. H., von Doenhoff, A. E. and Stivers, L. S., Summary of Airfoil Data, NACA Report No. 824, Langley Field, Va., 1945.

28. Society of Automotive Engineers Report HSJ1566, "Aerodynamic Flow Visualization Techniques and Procedures," 1986.

29. Anderson, J. D., *Fundamentals of Aerodynamics*, 2nd Ed., McGraw-Hill, New York, 1991.

30. Hucho, W. H., *Aerodynamics of Road Vehicles*, Butterworth – Heinemann, 1987.

31. Homsy, G. M., et. al., *Multimedia Fluid Mechanics* CD-ROM, Cambridge University Press, New York, 2000.

Review Problems for Part (4)

1R (Life/drag calculation) Determine the lift and drag coefficients (based on frontal area) for the triangular two-dimensional object shown in Fig. P .1R. Neglect shear forces.

(ANS: 0; 1.70)

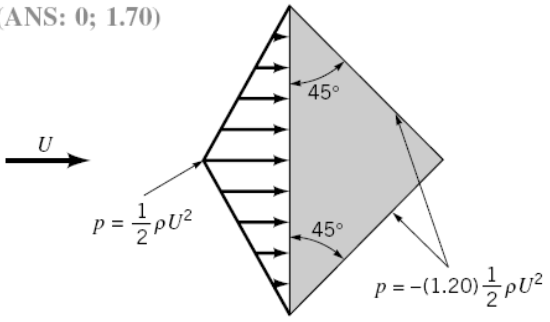

■ FIGURE P .1R

2R (External flow character) A 0.23-m-diameter soccer ball moves through the air with a speed of 10 m/s. Would the flow around the ball be classified as low, moderate, or large Reynolds number flow? Explain.

(ANS: Large Reynolds number flow)

3R (External flow character) A small 15-mm-long fish swims with a speed of 20 mm/s. Would a boundary layer type flow be developed along the sides of the fish? Explain.

(ANS: No)

4R (Boundary layer flow) Air flows over a flat plate of length $\ell = 2$ ft such that the Reynolds number based on the plate length is $\mathrm{Re} = 2 \times 10^5$. Plot the boundary layer thickness, δ, for $0 \le x \le \ell$.

5R (Boundary layer flow) At a given location along a flat plate the boundary layer thickness is $\delta = 45$ mm. At this location, what would be the boundary layer thickness if it were defined as the distance from the plate where the velocity is 97% of the upstream velocity rather than the standard 99%? Assume laminar flow.

(ANS: 38.5 mm)

6R (Friction drag) A laminar boundary layer formed on one side of a plate of length ℓ produces a drag $\mathcal{D}$. How much must the plate be shortened if the drag on the new plate is to be $\mathcal{D}/4$? Assume the upstream velocity remains the same. Explain your answer physically.

(ANS: $\ell_{\text{new}} = \ell/16$)

7R (Momentum integral equation) As is indicated in Table4 .2, the laminar boundary layer results obtained from the momentum integral equation are relatively insensitive to the shape of the assumed velocity profile. Consider the profile given by $u = U$ for $y > \delta$, and $u = U\{1 - [(y - \delta)/\delta]^2\}^{1/2}$ for $y \le \delta$ as shown in Fig. P .7R. Note that this satisfies the conditions $u = 0$ at $y = 0$ and $u = U$ at $y = \delta$. However, show that such a profile produces meaningless results when used with the momentum integral equation. Explain.

(ANS)

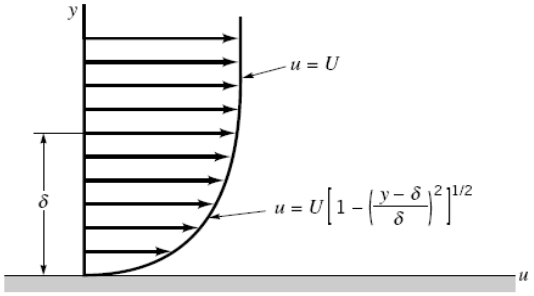

■ FIGURE P .7R

Problems:

.1 Assume that water flowing past the equilateral triangular bar shown in Fig. P .1 produces the pressure distributions indicated. Determine the lift and drag on the bar and the corresponding lift and drag coefficients (based on frontal area). Neglect shear forces.

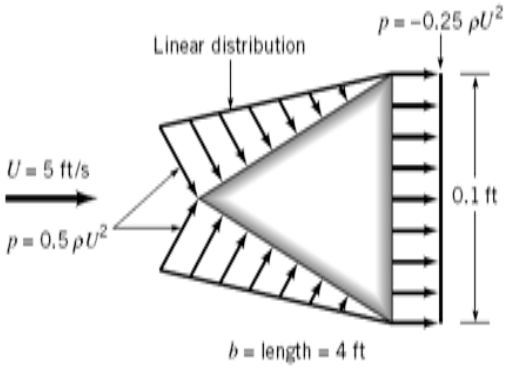

■ FIGURE P .1

.2 Fluid flows past the two-dimensional bar shown in Fig. P .2. The pressures on the ends of the bar are as shown, and the average shear stress on the top and bottom of the bar is τ_{avg}. Assume that the drag due to pressure is equal to the drag due to viscous effects. **(a)** Determine τ_{avg} in terms of the dynamic pressure, $\rho U^2/2$. **(b)** Determine the drag coefficient for this object.

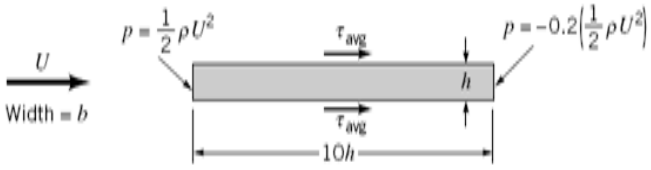

■ FIGURE P .2

.3 The pressure distribution on the 1-m-diameter circular disk in Fig. P .3 is given in the table below. Determine the drag on the disk.

r (m)	p (kN/m^2)
0	4.34
0.05	4.28
0.10	4.06
0.15	3.72
0.20	3.10
0.25	2.78
0.30	2.37
0.35	1.89
0.40	1.41
0.45	0.74
0.50	0.0

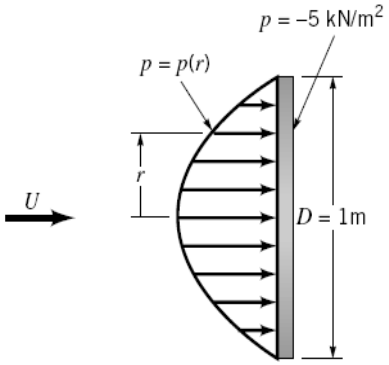

■ FIGURE P .3

.4 The pressure distribution on a cylinder is approximated by the two straight line segments shown in Fig. P .4. Determine the drag coefficient for the cylinder. Neglect shear forces.

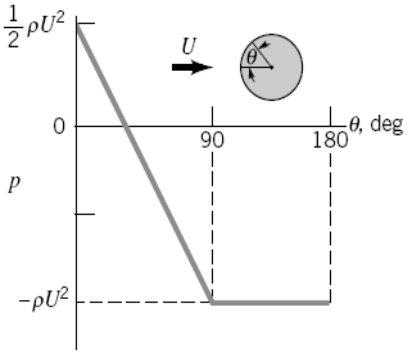

■ FIGURE P .4

.5 Repeat Problem .1 if the object is a cone (made by rotating the equilateral triangle about the horizontal axis through its tip) rather than a triangular bar.

.6 A 17-ft-long kayak moves with a speed of 5 ft/s (see Video V .2). Would a boundary layer type flow be developed along the sides of the boat? Explain.

.7 Typical values of the Reynolds number for various animals moving through air or water are listed below. For which cases is inertia of the fluid important? For which cases do viscous effects dominate? For which cases would the flow be laminar; turbulent? Explain.

Animal	Speed	Re
(a) large whale	10 m/s	300,000,000
(b) flying duck	20 m/s	300,000
(c) large dragonfly	7 m/s	30,000
(d) invertebrate larva	1 mm/s	0.3
(e) bacterium	0.01 mm/s	0.00003

.8 Estimate the Reynolds numbers associated with the following objects moving through air: **(a)** a snow flake settling to the ground, **(b)** a mosquito, **(c)** the space shuttle, **(d)** you walking.

.9 Approximately how fast can the wind blow past a 0.25-in.-diameter twig if viscous effects are to be of importance

throughout the entire flow field (i.e., Re $<$ 1)? Explain. Repeat for a 0.004-in.-diameter hair and a 6-ft-diameter smokestack.

.10 A viscous fluid flows past a flat plate such that the boundary layer thickness at a distance 1.3 m from the leading edge is 12 mm. Determine the boundary layer thickness at distances of 0.20, 2.0, and 20 m from the leading edge. Assume laminar flow.

.11 If the upstream velocity of the flow in Problem .10 is $U = 1.5$ m/s, determine the kinematic viscosity of the fluid.

.12 Water flows past a flat plate with an upstream velocity of $U = 0.02$ m/s. Determine the water velocity a distance of 10 mm from the plate at distances of $x = 1.5$ m and $x = 15$ m from the leading edge.

.13 A Pitot tube connected to a water-filled U-tube manometer is used to measure the total pressure within a boundary layer. Based on the data given in the table below, determine the boundary layer thickness, δ, the displacement thickness, δ^*, and the momentum thickness, Θ.

y (mm), distance above plate	h (mm), manometer reading
0	0
2.1	10.6
4.3	21.1
6.4	25.6
10.7	32.5
15.0	36.9
19.3	39.4
23.6	40.5
26.8	41.0
29.3	41.0
32.7	41.0

.14 Because of the velocity deficit, $U - u$, in the boundary layer, the streamlines for flow past a flat plate are not exactly parallel to the plate. This deviation can be determined by use of the displacement thickness, δ^*. For air blowing past the flat plate shown in Fig. P .14, plot the streamline A–B that passes through the edge of the boundary layer ($y = \delta_B$ at $x = \ell$) at point B. That is, plot $y = y(x)$ for streamline A–B. Assume laminar boundary layer flow.

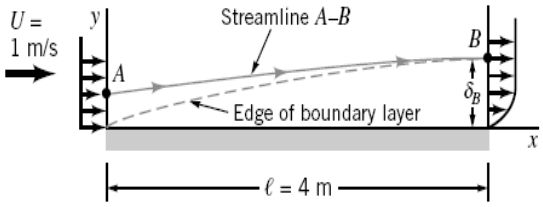

FIGURE P .14

.15 Air enters a square duct through a 1-ft opening as is shown in Fig. P .15. Because the boundary layer displacement thickness increases in the direction of flow, it is necessary to increase the cross-sectional size of the duct if a constant $U = 2$ ft/s velocity is to be maintained outside the boundary layer. Plot a graph of the duct size, d, as a function of x for $0 \le x \le 10$ ft if U is to remain constant. Assume laminar flow.

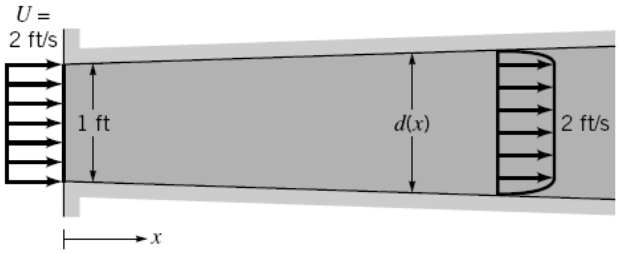

FIGURE P .15

.16 A smooth, flat plate of length $\ell = 6$ m and width $b = 4$ m is placed in water with an upstream velocity of $U = 0.5$ m/s. Determine the boundary layer thickness and the wall shear stress at the center and the trailing edge of the plate. Assume a laminar boundary layer.

.17 An atmospheric boundary layer is formed when the wind blows over the earth's surface. Typically, such velocity profiles can be written as a power law: $u = ay^n$, where the constants a and n depend on the roughness of the terrain. As is indicated in Fig. P .17, typical values are $n = 0.40$ for urban areas, $n = 0.28$ for woodland or suburban areas, and $n = 0.16$ for flat open country (Ref. 23). **(a)** If the velocity is 20 ft/s at the bottom of the sail on your boat ($y = 4$ ft), what is the velocity at the top of the mast ($y = 30$ ft)? **(b)** If the average velocity is 10 mph on the tenth floor of an urban building, what is the average velocity on the sixtieth floor?

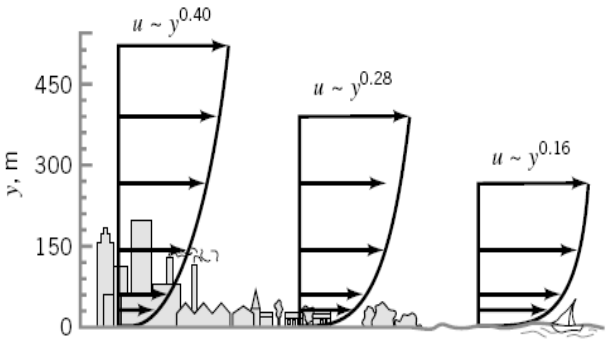

FIGURE P .17

.18 A 30-story office building (each story is 12 ft tall) is built in a suburban industrial park. Plot the dynamic pressure, $\rho u^2/2$, as a function of elevation if the wind blows at hurricane strength (75 mph) at the top of the building. Use the atmospheric boundary layer information of Problem .17.

.19 The typical shape of small cumulus clouds is as indicated in Fig. P .19. Based on boundary layer ideas, explain why it is clear that the wind is blowing from right to left as indicated.

.20 Show that by writing the velocity in terms of the similarity variable η and the function $f(\eta)$, the momentum equation for boundary layer flow on a flat plate (Eq. 4.9) can be written as the ordinary differential equation given by Eq. 4.14.

.21 Integrate the Blasius equation (Eq. 4.14) numerically to determine the boundary layer profile for laminar flow past a flat plate. Compare your results with those of Table 4.1.

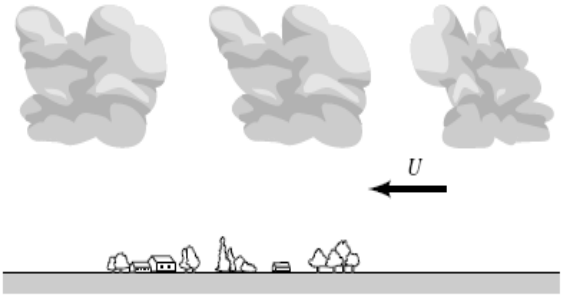

FIGURE P .19

.22 An airplane flies at a speed of 400 mph at an altitude of 10,000 ft. If the boundary layers on the wing surfaces behave as those on a flat plate, estimate the extent of laminar boundary layer flow along the wing. Assume a transitional Reynolds number of $Re_{xcr} = 5 \times 10^5$. If the airplane maintains its 400-mph speed but descends to sea level elevation, will the portion of the wing covered by a laminar boundary layer increase or decrease compared with its value at 10,000 ft? Explain.

.23 If the boundary layer on the hood of your car behaves as one on a flat plate, estimate how far from the front edge of the hood the boundary layer becomes turbulent. How thick is the boundary layer at this location?

.24 A laminar boundary layer velocity profile is approximated by $u/U = [2 - (y/\delta)](y/\delta)$ for $y \le \delta$, and $u = U$ for $y > \delta$. (a) Show that this profile satisfies the appropriate boundary conditions. (b) Use the momentum integral equation to determine the boundary layer thickness, $\delta = \delta(x)$.

.25 A laminar boundary layer velocity profile is approximated by the two straight-line segments indicated in Fig. P .25. Use the momentum integral equation to determine the boundary layer thickness, $\delta = \delta(x)$, and wall shear stress, $\tau_w = \tau_w(x)$. Compare these results with those in Table 4.2.

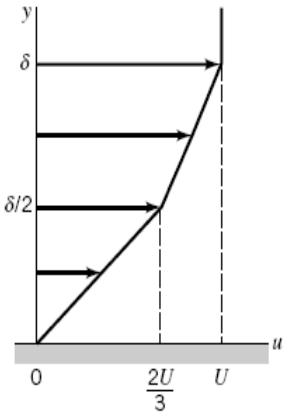

FIGURE P .25

.26 An assumed, dimensionless laminar boundary layer profile for flow past a flat plate is given in the table below. Use the momentum integral equation to determine $\delta = \delta(x)$. Compare your result with the exact Blasius solution result (see Table 4.2).

y/δ	u/U
0	0
0.080	0.133
0.16	0.265
0.24	0.394
0.32	0.517
0.40	0.630
0.48	0.729
0.56	0.811
0.64	0.876
0.72	0.923
0.80	0.956
0.88	0.976
0.96	0.988
1.00	1.000

.27 For a fluid of specific gravity $SG = 0.86$ flowing past a flat plate with an upstream velocity of $U = 5$ m/s, the wall shear stress on a flat plate was determined to be as indicated in the table below. Use the momentum integral equation to determine the boundary layer momentum thickness, $\Theta = \Theta(x)$. Assume $\Theta = 0$ at the leading edge, $x = 0$.

x (m)	τ_w (N/m^2)
0	—
0.2	13.4
0.4	9.25
0.6	7.68
0.8	6.51
1.0	5.89
1.2	6.57
1.4	6.75
1.6	6.23
1.8	5.92
2.0	5.26